Romanian Journal of MINERALOGY

continuation of

DĂRI DE SEAMĂ ALE ŞEDINŢELOR INSTITUTULUI DE GEOLOGIE ŞI GEOFIZICĂ
COMPTES RENDUS DES SÉANCES DE L'INSTITUT DE GÉOLOGIE ET GÉOPHYSIQUE
(1. Mineralogie Petrologie)

Founded 1906 by the Geological Institute of Romania

ISSN 1220-5621

Vol. 77

CONTENTS

SECOND NATIONAL SYMPOSIUM ON MINERALOGY TIMIŞOARA, JULY, 1993

I.G.R. 45 N 24° E

Institutul Geologic al României
Bucureşti – 1995

GEOLOGICAL INSTITUTE OF ROMANIA

The **Geological Institute of Romania** is now publishing the following periodicals:

Romanian Journal of Mineralogy
Romanian Journal of Petrology
Romanian Journal of Mineral Deposits
Romanian Journal of Paleontology
Romanian Journal of Stratigraphy
Romanian Journal of Tectonics and Regional Geology
Romanian Journal of Geophysics

They supersede "Dări de Seamă ale Şedinţelor", "Memorii" and "Studii Tehnice şi Economice", whose apparition goes back to 1910. Beside regular volumes, each series may occasionally contain Supplements (for abstracts and excursion guides to congresses and symposia held in Romania) and Special Issues (for larger papers of special interest). "Anuarul Institutului Geologic al României" will appear also in a new form, containing both the annual activity report and review papers.

Editorial Office:
Geological Institute of Romania
Str. Caransebeş Nr. 1
Tel. (+40) 1 665 66 25, 665 75 30
Fax (+40) 1 312 84 44
e-mail UDUBASA@IGR.RO

The editor has changed the name as follows: Institutul Geologic al României (1910–1952), Comitetul Geologic (1953–1966), Comitetul de Stat al Geologiei (1967–1969), Institutul Geologic (1970–1974), Institutul de Geologie şi Geofizică (1975–1993), Institutul Geologic al României (since 1994).

ROMANIAN JOURNAL OF MINERALOGY supersedes "Dări de Seamă ale Şedinţelor", Series 1/Mineralogie - Petrologie – the last volume with this title being No. 74.

Rom. J. Mineralogy is also the Bulletin of the Mineralogical Society of Romania, a member the EMU and IMA. Thus, this journal follows the rules of the Commission on New Minerals and Mineral Names of the IMA in all the matters concerning mineral names and nomenclature.

The manuscripts should be sent to the scientific editor and/or executive secretary. Correspondence concerning advertisments, announcements and subscriptions should be sent to the Managing Editor.

ISSN 1220-5621
Classification index for libraries 55(058)

Printed by the Geological Institute of Romania
Bucharest

*I*nternational *M*ineralogical *A*ssociation

IMA '98 TORONTO, CANADA

IMA'98: The 17^{th} General Meeting of the International Mineralogical Association, IMA'98, will be held from 9–15 August 1998 at the University of Toronto, Toronto, Canada. The meeting will be preceded and succeeded by field trips across Canada, including important mineral locations, ore deposits, sites of impact craters, and classic petrologic localities. For more information please contact Professor A.J. Naldrett, Department of Geology, University of Toronto, Canada M5S 3B1. Tel. [416] 978 3030, FAX [416] 978 3938. e–mail address: ima98@quartz.geology.utoronto.ca

Rom. J. Mineralogy, 1995, 77, p. 3–10, Bucureşti

MANGANESE OXIDE MINERALS

Rudolf GIOVANOLI

Institute of Inorganic Chemistry, Laboratory of Electron Microscopy,

University of Berne, P.O.B. 140, CH-3000 Berne 9 (Switzerland)

Key words: Manganese oxides. Phyllomanganates. Tunnel manganates. Structure. Ion exchange. Classification.

Abstract: Manganese oxides and Oxidehydroxides generally occur as finely divided and disordered compounds in a variety of phases. There is a series of simple binary oxides: Manganosite MnO. Rocksalt structure. Partridgeite α–Mn_2O_3. Rare Earth C-type structure Hausmannite Mn_3O_4. Structure derived from spinel type. Pyrolusite β–MnO_2. Rutile type. Nsutite γ–MnO_2. Diaspore type with randomly distributed single chains of edge–sharing $[MnO_6]$ octahedra. Another group has a metric similarity to phyllosilicates and is called phyllomanganates. 10 Å phyllomanganate shows exchange properties and collects transition metal ions like Cu^{2+}, Co^{2+}, Ni^{2+} but also Ca^{2+} and Zn^{2+}. Its dehydration product is 7 Åphyllomanganate (birnessite) also with exchange properties, but less pronounced. 10 Å phyllomanganate expands from 10 to 26 Å layer separation by intercalation of dodecylammonium chlorite, precisely as some 10 Å phyllosilicates do. A third group has structural tunnels and may be called tunnel manganates. This group requires large cations to be stable, e.g. Ba^{2+}, K^+, Sr^{2+}, NH_4^+, Pb^{2+}: Hollandite $BaMn_8O_{16}$, Cryptomelane KMn_8O_{16}, Coronadite $PbMn_8O_{16}$. This group has square tunnels along the needle axis. The large cations sit tightly in these tunnels and cannot be exchanged. Another mineral species of the name psilomelane (romanéchite) has similar tunnels, but with a rectangular cross section such that 1 Ba^{2+} and 1 H_2O molecule can be accommodated. While the members of the hollandite tunnel manganate group are very stable mineral species, psilomelane (romanéchite) is less stable and its tunnels collapse, when heated, under water loss to hollandite tunnels. Also frequent intergrowth of hollandite microdomains in a psilomelane (romanéchite) matrix has been observed.

Introduction

Manganese oxide minerals occur in nature frequently as finely divided, nearly amorphous, nonstoichiometric compounds with many admixtures. The usual chemical formula "MnO_2" does not apply very often and some of the more important minerals include OH^- groups and even molecular water in their lattice. In addition to this, we find adsorbed water and adsorbed foreign cations. These cations are sometimes difficult to distinguish from lattice constituents.

We have undertaken, in the past 25 years, efforts to synthesize in the laboratory these phases as crystalline and as stoichiometric as possible. The aim was to study their reaction pathways and their interconversion mechanisms.

Simple Binary Oxides

There exists a range of simple oxides with fairly stoichiometric composition. These will not be the main subject of this article but they may turn up as products in some reactions. The most important minerals species are the following:

- MnO Manganosite. Usually black, may be also green. Rocksalt type structure.
- Mn_3O_4 Hausmannite. Black. Tetragonally distorted spinel structure.
- β–MnO_2 Pyrolusite (= polianite). Black. Rutile type.
- γ–MnO_2. Black. Diaspore type with randomly inserted microdomains of rutile type.

– Mn_5O_8. Black. Produced in laboratory oxidation of Mn_3O_4 under mild conditions. The lattice can be described as a layer structure.
– α–Mn_2O_3. Partridgeite. With Fe^{3+} substituting some of Mn^{3+}: Bixbyite. Black. C type of Rare Earth oxide structures.

Simple Hydroxides and Oxide Hydroxides

– $Mn(OH)_2$. White if pure. Extremely difficult to prepare in the laboratory. Oxidises very fast. Not found in nature. C 6 type.
– γ–MnOOH. Manganite. Most frequent oxide hydroxide. Structure type derived from rutile.
– α–MnOOH. Groutite. Very rare. Diaspore type.
– β–MnOOH. Isostructural with $Mn(OH)_2$. Very rare.

Phyllomanganates: Structure and Ion Exchange

Historically, phyllomanganates have first been found (without being recognized) on the Challenger expedition in 1873 in the form of deep sea manganese nodules (Linklater, 1972). In the laboratory, they first turned up in analytical experiments (Sarkar, Dhar, 1922). Their true nature was independently found out by Feitknecht and Marti (1945) in Berne and by Wadsley (1950) in Australia. The nature of manganese nodules was recognized by Buser and Grütter (1956) again in Berne.

Phyllomanganates consist of a layer lattice (Fig. 1). $[MnO_6]$ octahedra form layers by edge-sharing that are a hexagonal dense packing of O^{2-} and OH^- ions. In this respect they have a close metrical relationship to the layers of phyllosilicates (clay minerals). The distance of 2 neighbouring Mn^{4+} ions is 2,85 Å and the layer separation can have two possible values, namely 10 Å and 7 Å. 10 Å phyllomanganate dehydrates to form the 7 Å phase.

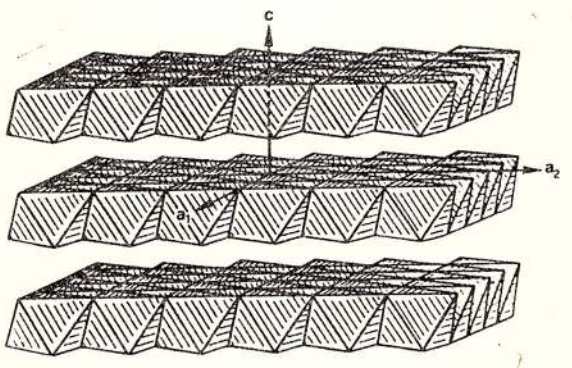

Fig. 1 – Schematic representation of the phyllomanganate structure. $[MnO_6]$ octahedra form the main layers by edge and corner sharing. The c_o distance depends on the interlayer content.

The 7 Å phyllomanganate occurs frequently in nature. It was named birnessite by Jones and Milne (1956) but another variety is much older and is named after the mine of Rancié (Ariège, France). It has been described in another deposit by Bardossy and Brindley (1978). In the laboratory the 10 Å phase can be produced by vigorous oxygenation of freshly precipitated $Mn(OH)_2$ in an alkaline suspension. It consists of platelets of about 1 μ diameter and 200 – 400 Å thickness. The electron diffraction shows the prominent pseudohexagonal spots and the weaker superlattice reflections (Pl. I, Fig. 1).

The proof of the layered structure has unambiguously been given by Paterson (1981) who showed intercalation with the dodecyl ammonium ion in a way similar to certain clay minerals (Pl. I, Fig. 2). The layer separation increases from 10 to 26 Å and many orders of the basal reflection can be observed.

The dehydration of 10 Å phyllomanganate is usually irreversible and the dehydration product (7 Å phyllomanganate) cannot be intercalated with dodecyl ammonium ion. If, however, the initial 10 Å phase has been treated with Ca^{2+} ions (i.e. if the Na^+ content has been totally exchanged against Ca^{2+} ions), then the dehydration is fully reversible.

There exist also disordered varieties. These have order only within the layer (hence the 2,44 Å reflection) but perpendicular to the layer there is random stacking and the basal reflections and pyramidal reflections are missing. This phase has formerly been called "δ–MnO_2" and Arrhenius et al. (1979) have proposed a more appropriate designation: Z disordered manganate or z_d manganate. Such phases may be produced in the laboratory, e.g. from $KMnO_4$, and they are nearly amorphous and have a K^+ content that nucleates very easily the formation of the tunnel manganate KMn_8O_{16} (mineral name cryptomelane; see below) (Fig. 2).

The 10 Å manganate is a selective ion exchanger as pointed out by Wadsley (1950). It scavenges transition metal ions like Co^{2+}, Ni^{2+}, Cu^{2+}, Zn^{2+} and some other ions. We have investigated this reaction and show in Figure 3 exchange curves with Cu^{2+} and 10 Å phyllomanganate. The 7 Å phase has less pronounced ion exchange properties and Figure 3 shows some curves with Zn^{2+} as an example.

While the 10 Å phyllomanganate without transition metal ions dehydrates easily in air, the exchanged products are fairly stable. This is reflected in a slight contraction of the layer separation that occurs within 15 minutes without altering the morphology (Pl. I, Fig. 3).

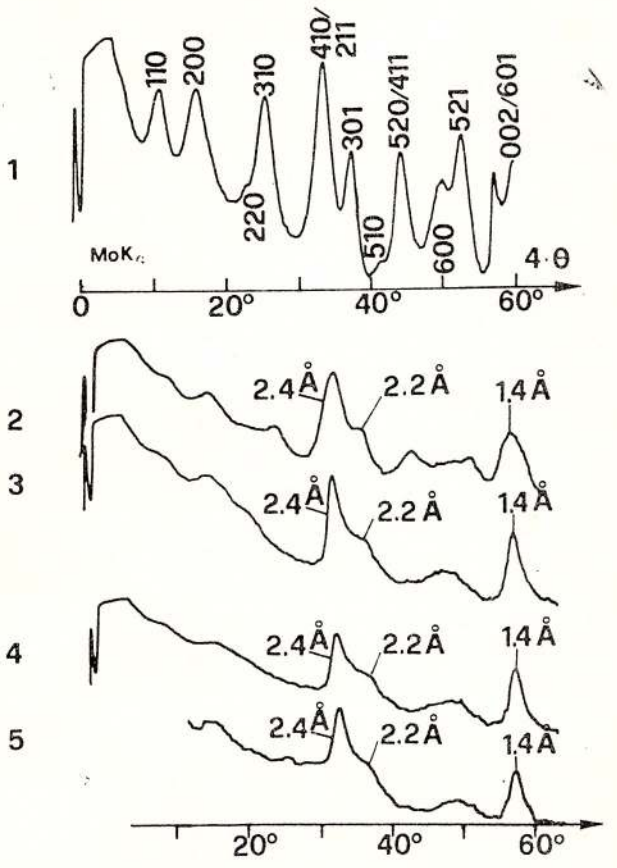

Fig. 2 – Densitometer traces of four X-ray powder patterns of nearly amorphous z_d manganate samples (formerly called "δ–MnO_2"). On top the densitometer trace of poorly crystalline cryptomelane KMn_8O_{16} for comparison. z_d manganate contains frequently K^+ ions and these can nucleate cryptomelane.

The Composition of Phyllomanganates

Depending on the history of the preparations, phyllomanganates can vary widely in composition. The 10 Å phyllomanganate of Figure 2, the most crystalline preparation, cannot be analyzed as the substance dehydrates in air. Its dehydration product, however, can be analyzed and this 7 Å – phyllomanganate gave the analytical composition $Na_4Mn_{14}O_{27}.9H_2O$ (Giovanoli et al., 1970).

If we accept a hexagonal dense oxygen packing, we can accommodate this analysis in the following structural formula:

$$[Mn_5^{4+}(^{Mn^{3+}}_{Mn^{2+}})O_{12}]^+ \cdot [(OH^-)_3 \cdot (H_2O)_9Na_2]^-$$

Main layer Intermediate layer

This formula indicates in the first square bracket the contents of the main layer, where 1 out of 6 Mn^{4+} ions is vacant. Above and below the vacant site there is one Mn^{2+} and Mn^{3+} ion, respectively.

The second square bracket indicates the contents of the intermediate layer, where 3 out of $12H_2O$ molecules are replaced by 3 OH^- ions to balance the charge of the main layer.

The 2 Na^+ ions as well as the Mn^{2+} ion in the intermediate layer can be exchanged against transition metal ions. The 2 Na^+ ions can also be leached by careful treatment in dilute nitric acid and the resulting product shows a higher analytical oxidation state

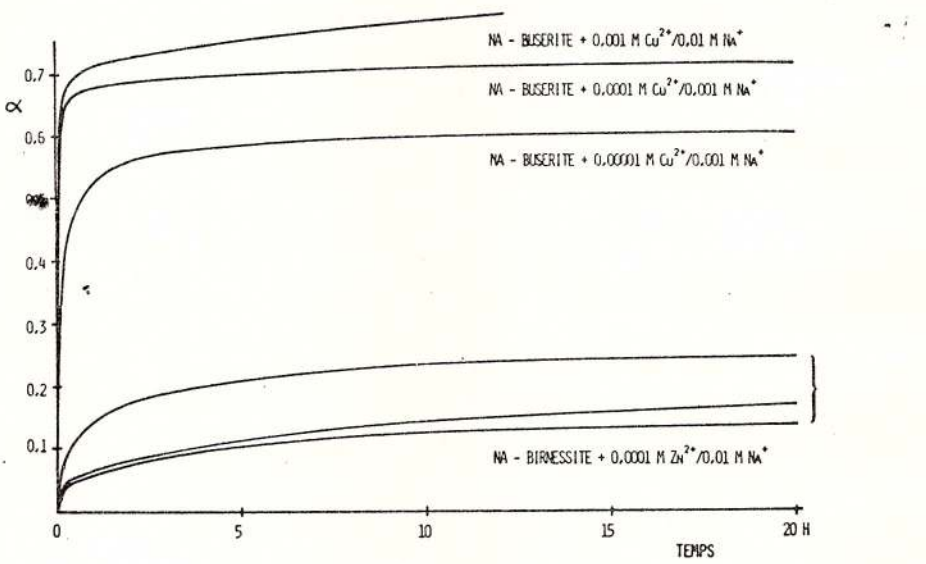

Fig. 3 – Exchange curves for 10 Å – and 7 Å -phyllomanganate samples in suspension with Cu^{2+} and Zn^{2+} ions, respectively. $\alpha = 1$ represents a saturated sample as received after day long standing in a 0.1 – M solution of the salt. Note the fast reaction.

of the Mn ions, i.e. the Mn^{2+} in the intermediate layer is oxidized to Mn^{3+}. The analytical formula of this product is $Mn_7O_{13}.5H_2O$. It is relatively stable and can be stored in air, but within years the water is lost and the product turns finally into a γ–MnO_2 of very poor cristallinity.

Reactions of Phyllomanganates

Na–phyllomanganate reacts with protons. In acid suspension it first releases Na^+, then Mn^{2+}. The product oxidises to an analytical composition $Mn_7O_{13}.5H_2O$. It shows a hexagonal powder pattern without the orthorhombic superstructure of 7 Å - Na - phyllomanganate. This product results in slightly acid conditions both from 10 Å - Na - phyllomanganate and from 7 Å - Na - phyllomanganate. Such a product has been found in nature in the Rancié mine (Ariège, France) (Pl. I, Fig. 4).

If the reaction with protons is prolonged or if higher acid concentrations or higher temperatures are applied, the phyllomanganate structure is destroyed and γ–MnO_2 (nsutite) nucleates. The platelets of the starting product become rafts of γ-MnO_2 needles and finally fall apart (Pl. I, Fig. 5).

Figure 4 shows in a very schematic and simplified manner the structural changes from the layer lattice of the starting product to the goethite type lattice of the γ–MnO_2.

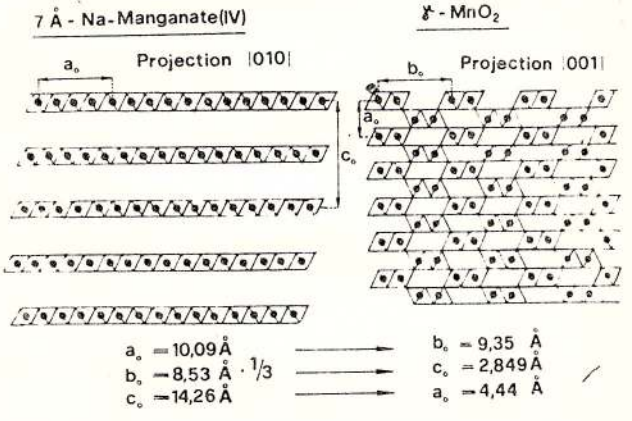

Fig. 4 – Schematic drawing illustrating the decay of the phyllomanganate lattice to γ–MnO_2. The γ–MnO_2 lattice is viewed along the needle axis.

The formation of γ–MnO_2 occurs only in the absence of large cations like K^+, Ba^{2+}, NH_4^+, Pb^{2+} and others. Also there is not one particular compound but γ–MnO_2 forms rather a group of compounds that may differ in crystallinity, disorder and oxidation state of the manganese ion. The highest oxidized product in our experiments was $MnO_{1,96}$. All this variability is shown in 3 examples of γ–MnO_2 with the X–ray powder patterns (Pl. II, Fig. 1).

The reflections are broadened selectively and asymmetrically indicating the particular disorder described by de Wolff (1948). Depending on the way of preparation, reflections may be missing entirely; they are so broad that they disappear in the underground noise.

Refluxing in 2–M HNO_3 at 98° C leads to a rather crystalline γ–MnO_2 in the form of well developed prisms. If the refluxing is extended to several months, β-MnO_2 (pyrolusite) nucleates. This is the thermodynamically stable form of the [MnO_2]. γ–MnO_2 is, however, indefinitely metastable. It is mined in huge quantities, e.g. in Moanda (Gabon) or in various deposits of Brazil. γ–MnO_2 is electrochemically active and is therefore used as oxide cathode in dry batteries of the Leclanché type or the alkaline MnO_2 type.

These valuable properties are due to the goethite type of γ–MnO_2 where there is the possibility of proton diffusion along the crystallographic c axis (Fig. 5).

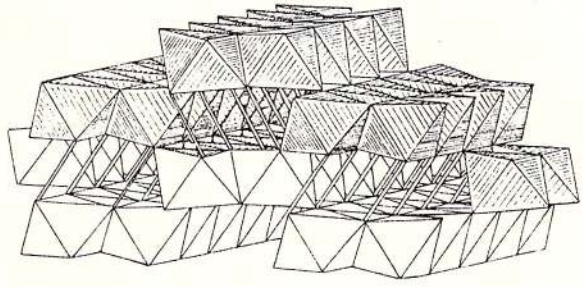

Fig. 5 – Goethite structure. The white diagonal sticks represent the hydrogen bond. These hydrogens can diffuse in and out of γ–MnO_2 as protons.

The cation free 7 Å – phyllomanganate $Mn_7O_{13}.5H_2O$ can also be reduced. A particularly mild reducing agent is cinnamic alcohol which has first been introduced in the field of manganese oxide reduction by Gabano et al. (1965). In a xylene suspension the mild reduction at moderate temperatures leads to γ–MnOOH in the form of very thin needles. Again this reaction is structurally guided: The platelets of the starting product form rafts of γ–MnOOH needles and the selected area electron diffraction shows that these needles are highly oriented. γ–MnOOH (mineral name: manganite) is the thermodynamically stable [MnOOH] and can also be found in natural deposits (Pl. II, Fig. 2).

If γ–MnOOH is oxidized (as a dry powder, under flowing oxygen, or in an acid suspension), the resulting product is β-MnO_2 (pyrolusite). The analogous reduction of γ–MnO_2 with cinnamic alcohol leads to α–MnOOH (mineral name: groutite). If reoxidized

(dry or in suspension), this α–MnOOH produces γ–MnO_2. Both have the diaspore type (Fig. 5) and their interconversion is structurally guided ("topotactic") in that only the diffusion of protons is involved. The matrix lattice is slightly distorted by the reduction of Mn^{4+} to Mn^{3+} due to the Jahn-Teller effect.

Tunnel Manganates

It has been pointed out at various occasions in the above text that large cations like K^+, Ba^+, NH_4^+, Pb^{2+}, Sr^{2+}, Cs^+ play an important role in the reactions of phyllomanganates. Even in the case of aqueous precipitation these ions can direct the reaction in a particular way: they lead to tunnel manganates.

Tunnel manganates have a very stable lattice with the large cation Me^{2+} in a tight fit as shown in Figure 6.

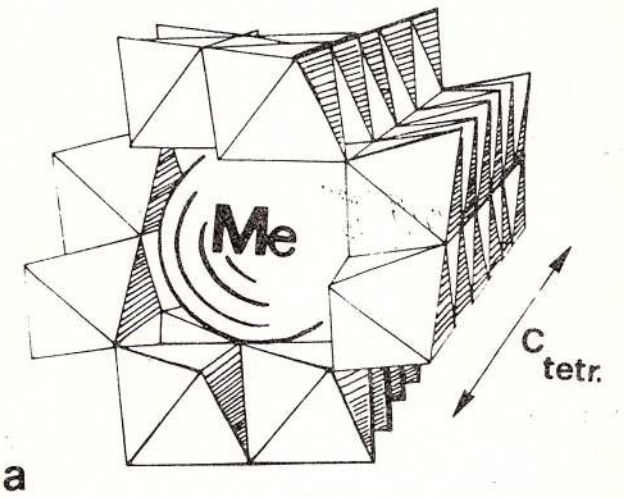

Fig. 6 – Schematic drawing of the structure of 2 x 2 tunnel manganates $MeMn_8O_{16}$. The size of Me is grossly exaggerated to underline the tight fit in the tunnel.

The tunnel manganate with K^+ is called cryptomelane. Needle-like cryptomelane is shown in Fig. 3, pl. II. With Ba^{2+} it is called hollandite and with Pb^{2+} coronadite. All these phases have the composition $Me\ Mn_8O_{16}$. The frequently quoted composition $Me_2Mn_8O_{16}$ could not be confirmed in our laboratory products except for a variety with Na^+ in the tunnels (Giovanoli, Faller, 1989).

Tunnel manganates are frequent in nature since the K^+ ion is an everpresent weathering product of orthoclase. Where lead deposits in the neighbourhood of manganese deposits are remobilized, the formation of coronadite can be observed (Perseil, Giovanoli, 1988).

Tunnel manganates, especially cryptomelane and hollandite, are so stable that they usually stand at the end of a reaction sequence. They cannot transform to other mineral species. Only treatment in very concentrated acid leads to dissolution.

In our synthesis experiments we produced under particular conditions another tunnel manganate, called psilomelane (romanéchite). As shown in Figure 7, this phase has a larger tunnel and can accomodate 1 Ba^{2+} ion and 1 H_2O molecule.

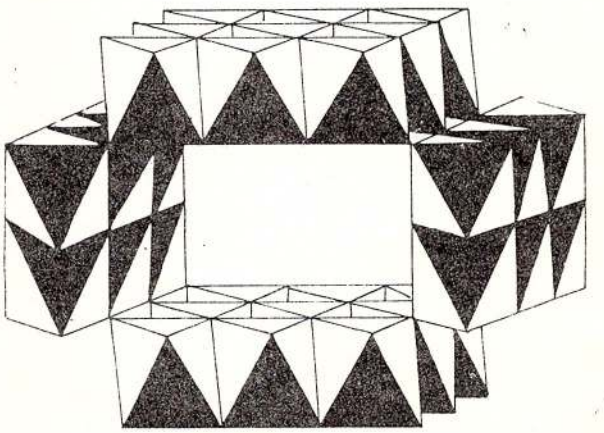

Fig. 7 – Schematic drawing of a 2 x 3 tunnel of the psilomelane (romanéchite) structure. In this tunnel 1 Ba^{2+} and 1 H_2O can be accommodated side by side. Courtesy of Prof. P. Buseck.

Figure 4 in plate II shows how the psilomelane needles grow of a phyllomanganate platelet in the 3 hexagonal directions. At the end of the reaction the platelet disintegrates and the final product consists of needles. An undersirable by–product that we have frequently encountered in this and some other reactions is Mn_3O_4 (hausmannite). It forms bipyramids and is rather stable; i.e. it cannot be easily transformed into other phases. By refluxing in nitric acid it transforms, however, to γ–MnO_2 (nsutite) and eventually to β–MnO_2 (pyrolusite).

Synthetic psilomelane needles are not fully crystalline. They show a type of disorder that can be observed directly in the transmission electron microscope. Figure 5 in plate II shows a hollandite needle with the smaller tunnels and a psilomelane needle with the larger tunnels intergrown with narrower tunnels in a statistical way.

Conclusion

Figure 8 summarizes the reaction pathways in the field of manganese oxides and hydroxides that have

been investigated by the author. It starts on top with the hexaquo manganese (II) ion that is precipitated to form $Mn(OH)_2$. Fast oxygenation leads to hausmannite". Upon further interaction with oxygen this mixture oxidizes to γ–MnOOH (manganite) and at elevated temperature to β–MnO_2 (pyrolusite).

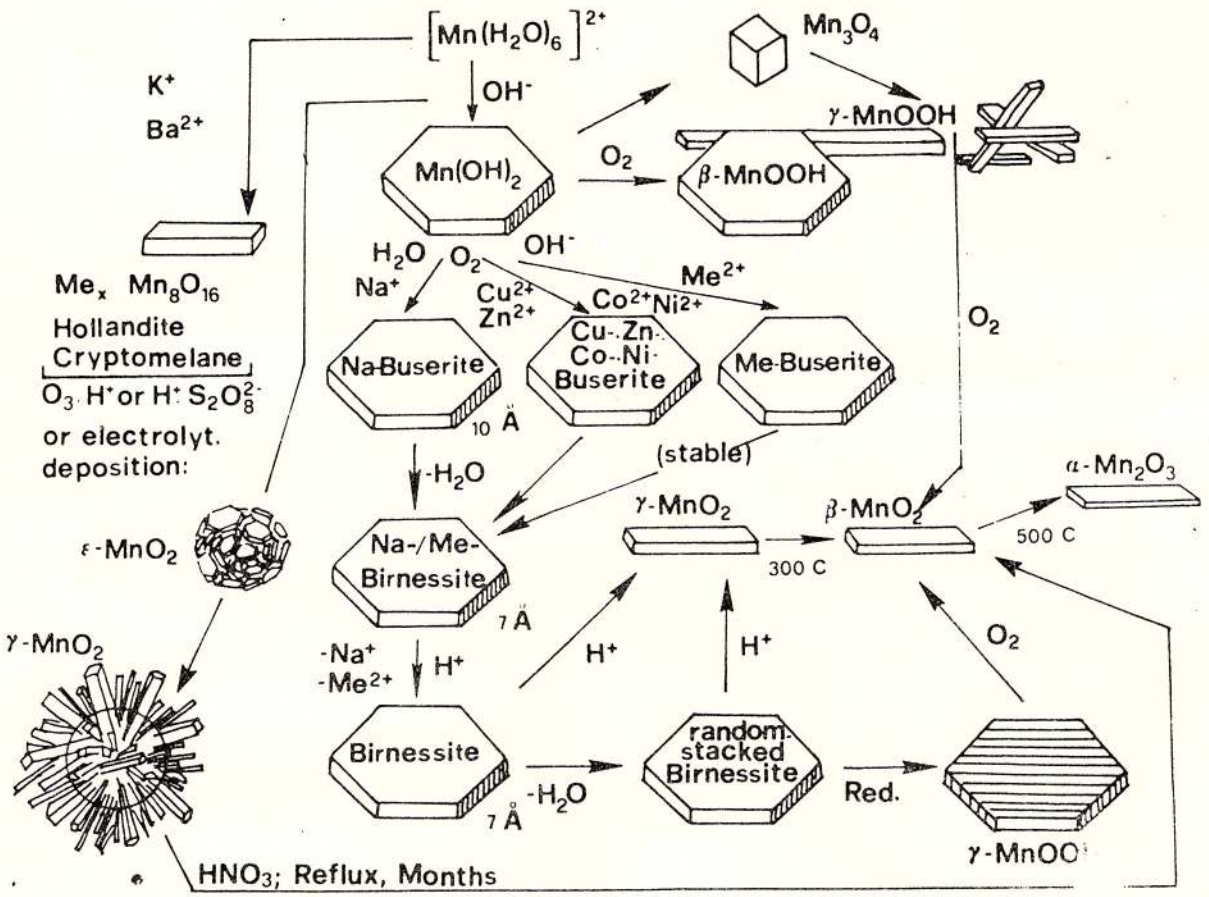

Fig. 8 – Schematic summary of the reaction pathways investigated.

10 Å – phyllomanganate (here called Na–buserite) that can react in various ways down to the bottom of the figure. A sideline reaction (far left) indicates that in the presence of K^+, Ba^{2+}, .. cryptomelane forms from the Mn^{2+} precipitation. This tunnel manganate stays as it is and does not react in any way.

A second side line to the left indicates the industrial production of electrochemically deposited manganese oxide (epsilon–MnO_2) which is used in dry batteries. Upon ageing in acid suspension the spherical aggregations of the tiny platelets of epsilon–MnO_2 turn into spherulites of γ–MnO_2. Extended refluxing leads to β–MnO_2. On the right hand side there is yet another sequence that starts with dry $Mn(OH)_2$ powder in a humid atmosphere. In air the $Mn(OH)_2$ platelets oxidize to a mixture of Mn_3O_4 bipyramids (hausmannite) and platelets of β–MnOOH (feitknechtite). The mixture has initially but wrongly been named "hydro-

References

Bardossy, G., Brindley, T.W. (1978) Rancieite associated with a karstic bauxite deposit. *Am. Mineral.*, 63, p. 762–767, Washington.

Buser, W., Grütter, A. (1956) Ueber die Natur der Manganknollen. *Schweiz. Min.-Petr. Mitteil.*, 36, p. 49–62, Zürich.

Feitknecht, W., Marti, W. (1945) Ueber Manganite und künstlichen Braunstein. *Helv. chim. Acta*, 28, p. 149–156, Zürich.

Gabano, J.P., Morignat, B., Fialdes, E., Emery, B., Laurent, J.F. (1965) Étude de la Réduction Chimique du Bioxyde de Manganèse γ. *Z. physik. Chemie N.F.*, 46, p. 359–372, Berlin.

Giovanoli, R., Stähli, E., Feitknecht, W. (1970) Ueber die Oxidhydroxide des vierwertigen Mangans

mit Schichtengitter. 2. Mitteilung: Mangan (III) manganat (IV). *Helv. chim. Acta*, 53, p. 453–456, Zürich.

– , **Faller, M. (1989)** Oxidhydroxide von Mangan (IV) mit Schichtengitter. 7. Mitteilung: Einbau von Co, Ni, Cu, in Lithiophorit Chimia, 43, p. 54–56, Berna.

Linklater, E. (1972) The Voyage of the Challenger. John Murray, London, p. 1–288.

Paterson, E. (1981) Intercalation of synthetic buserite by dodecylammonium–chloride. *Am. Mineral.*, 66, p. 424–427, Washington.

Sarkar, P.B., Dhar, N.R. (1922) Bestimmung von Mangan durch Permanganat und Untersuchung verschiedener Manganite. *Z. Anorg. Allg. Chemie*, 121, p. 135–155, Berlin.

Wadsley, A.D. (1950) A hydrous manganese oxide with exchange properties. *J. Amer. Chem. Soc.*, 72, p. 1781–1784, New York.

de Wolff, P.M. (1959) Interpretation of some γ-MnO_2 diffraction patterns. *Acta Cryst.*, 12, p. 341–345, Amsterdam.

Received: December 1993
Accepted: February 1994

Plate I

Fig. 1a. – Selected area electron diffraction of a 7 Å – phyllomanganate crystal. The subcell is hexagonal. There are many superstructure reflections indicating that the true symmetry is lower.

Fig. 1b. – Crystals of 7 Å – phyllomanganate.

Fig. 2 – X–ray powder pattern of 10 Å phyllomanganate before (above) and after (below) intercalation with dodecyl ammonium ion.

Fig. 3 – Electron micrographs of exchanged 10 Å – phyllomanganate (a, b), electron diffraction (c) and X–ray powder patterns. The exchanged ion in this experiment was Cu^{2+}. Note that within 15 minutes the slight lattice contraction is completed.

Fig. 4 – Ranciéte from Rancié mine (Ariège, France). Scanning electron micrograph of naturally leached platelets. Courtesy Dr. E.A. Perseil.

Fig. 5 – 7 Å –phyllomanganate before and after treatment in dilute nitric acid. The platelets decompose to prismas of γ–MnO_2.

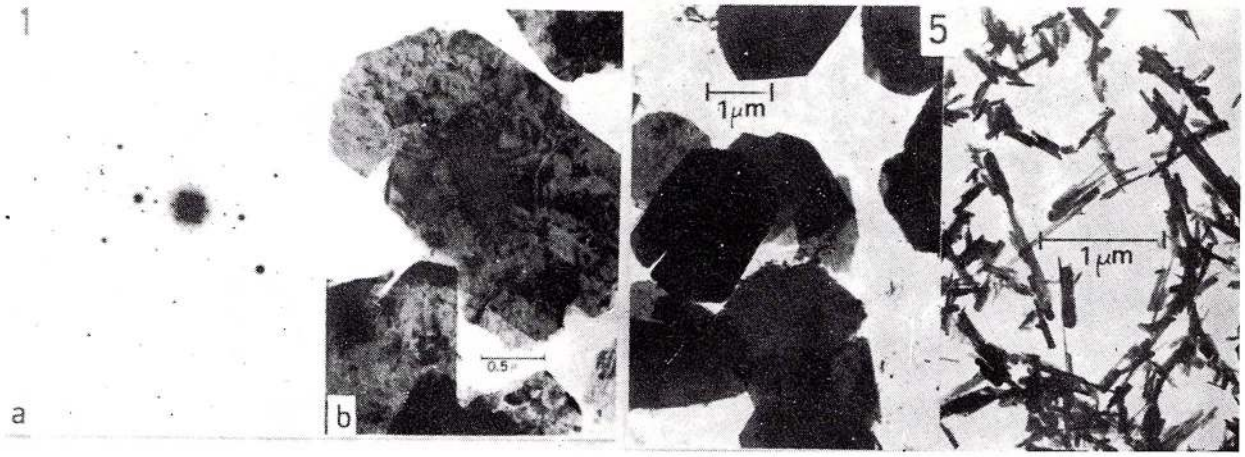

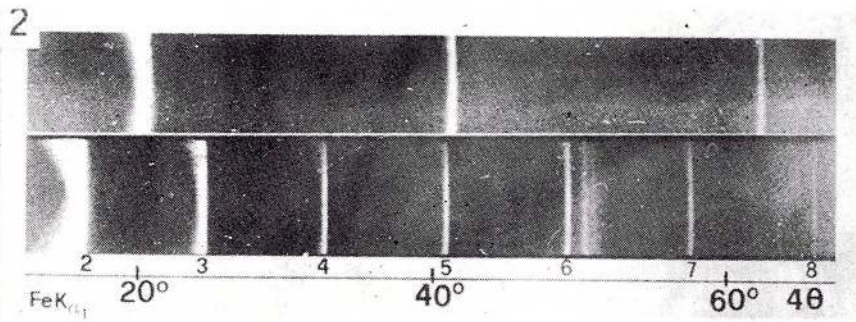

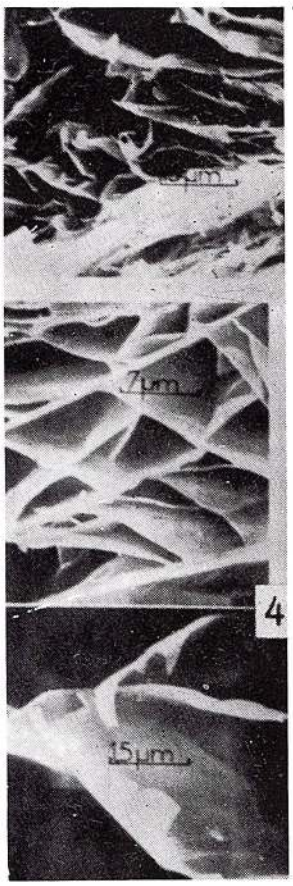

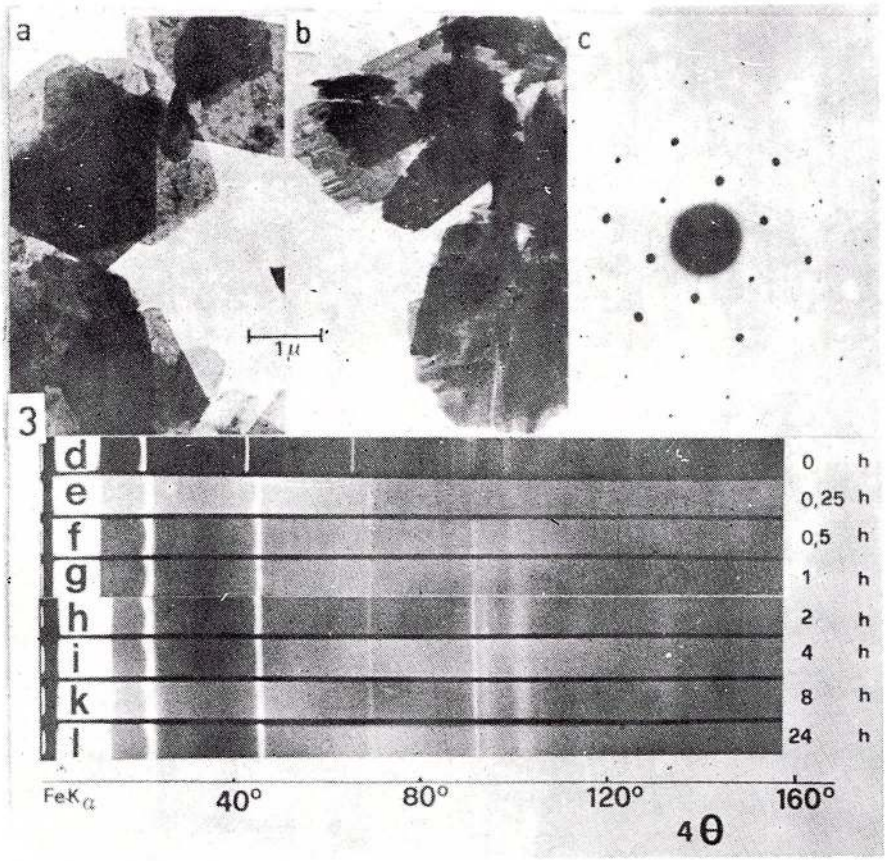

Plate II

Fig. 1 – Three varietes of synthetic γ–MnO_2 (X–ray powder patterns).
From top: – Precipitated by O_3 from an acid $MnSO_4$ solution
– Precipitated by $S_2O_8^{2-}$ from an acid $MnSO_4$
– The same product after refluxing several days in 2 M HNO_2.

Fig. 2 – Electron micrographs (carbon replica technique) of $Mn_7O_{13}.5H_2O$ (leached 7 Å – phyllomanganate) before and after reduction with cinnamic alcohol in wylene suspension under mild conditions. c) and d) are the respective selected area electron diffraction.

Fig. 3 – Needles of hydrothermally grown cryptomelane KMn_8O_{16}.

Fig. 4 – Three stages of the transition of a phyllomanganate platelet into psilomelane (romanechite). The needles grow out of the platelet in the three hexagonal directions. The very small bipyramids in c) are Mn_3O_4, an unwanted side product. – a and b: Direct pictures; c: Replica.

Fig. 5 – Transmission electron micrograph of a hollandite needle and a psilomelane needle. Both are lying flat on the specimen grid and the tunnels can be directly-seen. The psilomelane displays the broader tunnels intergrown with the narrower hollandite tunnels.

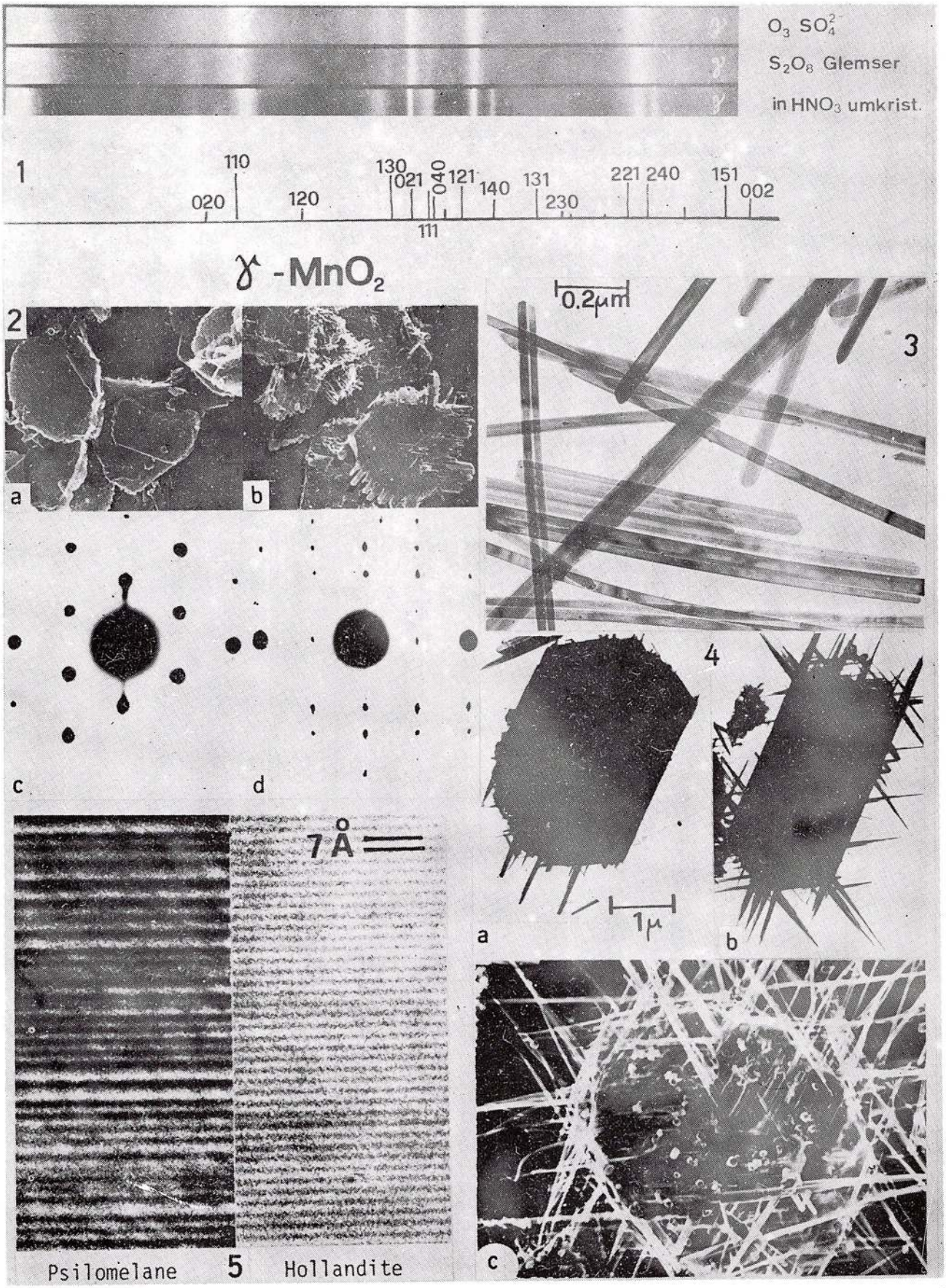

Rom. J. Mineralogy, 1995, 77, p. 11–18, Bucureşti

EVOLUTION MINÉRALOGIQUE DU MANGANÈSE DANS LES CONCENTRATIONS DE OIŢA (MONTS DE BISTRIŢA), CARPATES ORIENTALES - ROUMANIE

Elena Adriana PERSEIL

Laboratoire de Minéralogie du Muséum National d'Histoire de Paris, URA 736 61, Rue de Buffon 75005 Paris France

Rudolf GIOVANOLI

Laboratorium für Elektronenmikroskopie, Universität Bern, Freiestrasse 3, CH-3000 Bern 9, Suisse

Alexandru VODĂ

Institutul Geologic al României. Str. Caransebeş nr. 1, 78344 Bucureşti 32, România

Key words: Manganese Ores. Silicates. Carbonates. Oxides. Pyrophanite. Co-Ni sulpharsenides. East Carpathians. Tulgheş Series (Group). Oiţa Deposit.

Abstract: *Mineralogical evolution of manganese in the Oiţa Concentrations (Bistriţa Mts) East Carpathians - Romania.* The ferromanganese concentrations of the east Carpathians are enclosed in a horizon of black quartzites of the Tulgheş Cambrian series. This series belongs to the metamorphic formations of the alpine sub- bucovinian nappe. The mineralized body of lenticular form consists of alternating ferromanganesian carbonates, silicates and oxides. Most of the oxides are the result of the oxidation of carbonates and silicates, with the exception of garnets which undergo a slight hydrolysis followed by the replacement either by carbonates or by members of the cryptomelane-hollandite group. The ore bodies have a lenticular shape and are intercalated in black quartzite horizons in a concordant manner. They consist of an alternation of carbonates, silicates and oxides; in the Oiţa deposit we have rarely found primary oxides, compared to what is known in other deposits of that group. It consists mainly of pyrophanite and manganesian ilmenite. Both give indications not only on the oxygen fugacity but also on the intensity of metamorphism. The carbonate bands at the base of the body of Oiţa shows numerous inclusions of iron and copper as well as sulpharsenide of cobalt and nickel. Within the ore, however, the content in transition elements is low. The overall analyses of the ore are situated in the region of hydrothermal concentration near the alpine ore bodies in the diagram of Bonatti. Within the various oxidation products an oxide identical to the ε– MnO_2 phase (an industrial product for dry batteries; trade name FARADISER M) has turned up and the paragenetic relations of this phase are discussed.

Introduction

Les concentrations ferro-manganésifères des Carpates Orientales sont contenues dans les formations métamorphiques du socle de la nappe sub-bucovinienne. Au sein des formations métamorphiques, les concentrations ferro-manganésifères auxquelles sont associés des sulfures polymétalliques stratiformes , constituent la série cambrienne de Tulgheş. Les échantillons que nous avons analysés proviennent de la carrière Oiţa, qui appartient au groupe de concentrations de Iacobeni - Şarul Dornei (Ianovici, 1956). De même que tous les autres gisements ferro-manganésifères des Carpates Orientales, le gisement de Oiţa est enfermé dans l'horizon de quartzites noirs, qui est considéré comme un repère (Ianovici, 1956) dans la métallogénie du manganèse. Les corps minéralisés ont une forme lenticulaire - dont les dimensions peuvent varier de quelques centimètres à quelques centaines de mètres; intercalés d'une manière concordante dans l'horizon de quartzites noirs, ils sont constitués d'une alternance de carbonates, silicates et oxydes. La présence de quelques sulfures a été signalée sans que l'on ait pu établir leurs liens avec les paragenèses manganésifères (Bălan, 1976).

Une texture rubannée discrète , à l'intérieur des corps minéralisés, résulte de l'alternance de bandes rose pâle de silicates manganésifères avec des bandes gris-brunâtres de carbonates. Des filons gris-rose de carbonates associés au quartz, traversent la structure rubannée.

Les oxydes primaires - assez rares dans le gisement de Oiţa- sont représentés , soit par des lamelles de pyrophanite associée à la pyroxmangite, soit par des inclusions d'ilménite-manganésifère dans les plages de cummingtonite manganésifère. Pour Craig et al. (1985) la pyrophanite, qui indique un métamorphisme intense, caractérise des milieux riches en manganèse et en titane à fugacité d'oxygène anormalement basse. On peut constater dans le diagramme triangulaire (Fig. 1) que si les lamelles de pyrophanite s'inscrivent dans le domaine classique, par rapport aux données de Craig et al. (1985), les inclusions, par contre, occupent un champ plus large qui correspond au caractère ferro-manganésifère des concentrations. Bălan (1976) considérait aussi la pyrophanite comme un témoignage du chimisme des dépôts initiaux.

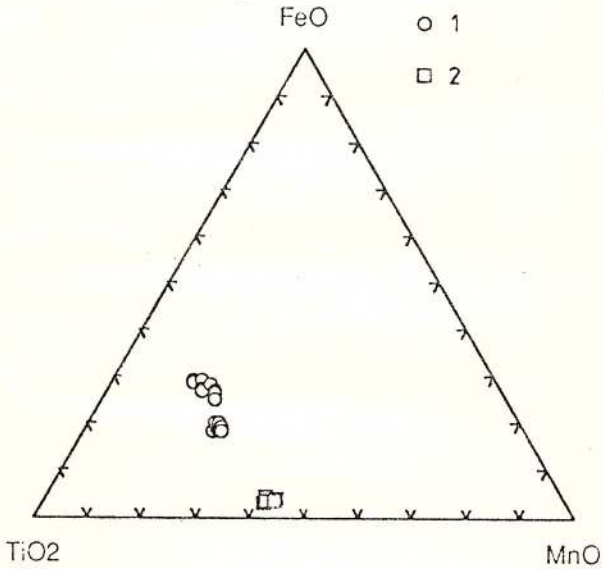

Fig. 1 La position des pyrophanites de Oiţa dans le diagramme triangulaire MnO-TiO_2-FeO. 1, Inclusions de pyrophanite; 2, Pyrophanite en lamelles.

Les sulfures et les sulfoarséniures associées aux carbonates et aux grenats ont été pour la première fois mises en évidence dans les couches de la base de la lentille minéralisée à Oiţa. Les îlots de pyrite transformée en magnétite sont très fréquents dans la masse des carbonates, à la base de la lentille. L'analyse ponctuelle de ces pyrites indique des traces sensibles d'arsenic, qui peuvent atteindre jusqu'à 3%, en concentration, du cobalt ou du nickel qui dépassent souvent 3% en concentration et des traces significatives d'or, d'argent et de bismuth. Des fantomes résiduels de pyrrhotite témoignent de la présence du milieu oxydant.

De nombreuses inclusions, qui prennent parfois l'aspect de nuages opaques, perturbent la transparence des plages de rhodochrosite, que l'oxydation n'a pas entamées . Des inclusions du même type ont été mises en évidence à la périphérie des plages de grenats. L'analyse ponctuelle à la microsonde (sur les plages dépassant 5 μm) a révélé la présence de deux sulfoarséniures de cobalt, la *cobaltite (CoAsS pseudocubique)* et *l'alloclastite (CoAsS-orthorhombique)*. On remarque aussi des termes plus riches en nickel assez proches de la gersdorffite. Nos analyses ponctuelles attestent aussi de la présence du manganèse, qui n'a jamais été signalé dans ces phases (jusqu'à 3 % en atome), aussi bien dans les plages d'alloclastite que dans les plages de cobaltite. La teneur en fer de ces plages est plus importante que dans les échantillons d'alloclastite des Hautes Alpes (France), analysés par Maurel et Picot (1973). Les caractères optiques de l'alloclastite sont assez typiques et diffèrent de ceux de la cobaltite par la couleur blanche, l'anisotropie et la présence des macles polysynthétiques; la détermination de l'alloclastite a aussi été confirmée par un diagramme de poudre.

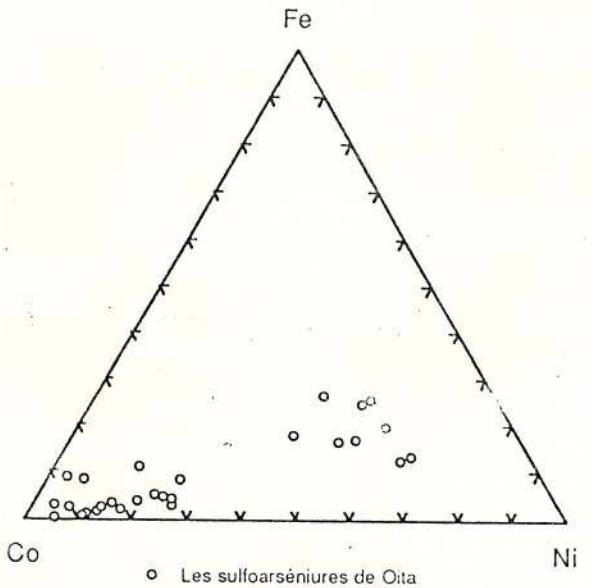

Fig. 2 – Position des inclusions de sulfoarséniures de cobalt et de nickel, dans le diagramme triangulaire Co-Ni-Fe.

On peut constater dans le diagramme triangulaire (Fig. 2), que les analyses ponctuelles de ces inclusions de sulfoarséniures définissent un champ assez large, qui est superposable à celui des cobaltites, alloclastites et gersdorffites analysés par Polushkina et Sidorenko (1963), par Borishanskaya et al. (1965) par Petruk

et al. (1971) ou à celui des cobaltites et alloclastites analysés par Maurel et Picot (1973).

La coexistence de la cobaltite avec l'alloclastite dénote ici des variations rapides dans les conditions de formation qui ont permis la mise en place simultanée des deux variétés dimorphes de CoAsS. L'alloclastite se forme dans un milieu riche en arsenic; le milieu s'enrichit ultérieurement en soufre, ce qui peut expliquer la transformation de l'alloclastite en cobaltite (Maurel et Picot, 1973).

A l'échelle du minerai de Oiţa, la teneur en éléments de transition est cependant faible; plusieurs analyses complètes des échantillons du minerai montrent une composition chimique comparable à celle des gisements alpins (Peters, 1984; Perseil et Latouche, 1989) (Fig. 3). Dans le diagramme de Bonatti et al. (1972), le minerai des concentrations de Oiţa se situe dans le domaine des concentrations hydrothermales à l'intérieur des gisements alpins.

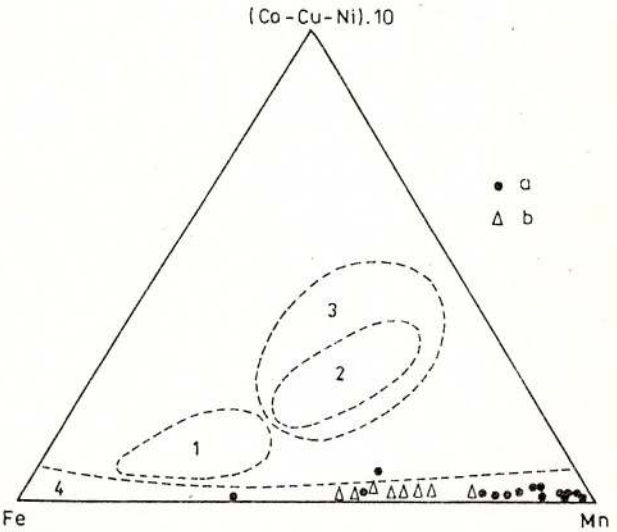

Fig. 3 – La position des échantillons de minerai de Oiţa dans le diagramme de Bonatti et al. 1, Pelliculles ferro-manganésifères à la surface des basaltes; 2, Nodules polymétalliques; 3, Toutes formations à partir de l'eau de mer; 4, Formations liées à l'hydrothermalisme. a, échantillons de minerai de gisements alpins; b, échantillons de minerai de Oiţa.

L'altération des grenats dans les concentrations de Oiţa est moins spectaculaire que dans la plupart des gisements exploitables connus, où le protore est représenté par des quartzites à spessartite: les gisements de Mokta (Côte d'Ivoire), de Tambao (Burkina-Faso), ou ceux de Serra do Navio-Amapa (Brésil). Dans ces grands gisements, le remplacement des grenats par la cryptomélane-hollandite suit l'hydrolyse et le lessivage. Généralement les grenats sont d'abord vidés de leur contenu en manganèse; le calcium et le fer le suivent progressivement; une phase amorphe silico- alumineuse subsiste seule - c'est cette partie qui réagira de diverses manières pour la constitution du minerai (Perseil et Grandin, 1985).

Les grenats des concentrations de Oiţa possèdent des dimensions variables. Ils sont assez riches en fer; leur proportion en spessartite varie entre 70 %– 87% et celle en almandin entre 2 %–20% (Tab. 1).

Assez discrète, *l'hydrolyse* de ces grenats est le plus souvent difficile à mettre en évidence. La partie centrale hydrolysée du grenat (Pl. I, Fig. 1), a été rapidement remplacée par la rhodochrosite qui s'oxyde progressivement en birnessite. L'avance concomitante de l'hydrolyse et du remplacement (du produit de ce processus) par la rhodochrosite est suivie par l'oxydation en birnessite. La birnessite est issue de l'oxydation d'une phase qui épigénise les produits de l'hydrolyse; les îlots restants de grenat hydrolysé ainsi que des carbonates qui ont épigénisé ces produits en témoignent. Le remplacement des produits de l'hydrolyse des grenats par l'apatite, est courante dans le Trias de l'unité du Barrhorn (Alpes du Valais-Suisse).

La plupart des grenats sont affectés par un réseau important de cassures, qui laisse s'infiltrer progressivement à l'intérieur du grenat des oxydes (Pl. I, Fig. 2) qui le remplacent ou l'épigénisent .

Le processus de remplacement ou d'épigénie des silicates dans les concentrations de Oiţa concerne souvent des grenats qui ne présentent aucun signe d'hydrolyse; l'observation microscopique permet cependant de remarquer un réseau important de cassures à l'intérieur de ces grenats, qui se trouvent souvent au voisinage de fines veinules d'oxydes (Pl. I, Fig. 2). L'analyse ponctuelle des oxydes qui remplacent les grenats indique la présence d'une *cryptomélane pure* (Tab. 2). Un enrichissement en potasse peut être lié au réseau de cassures. Des termes intermédiaires de la série isostructurale *cryptomélane-hollandite* ($[Ba, K]_1 - {}_2Mn_8O_{16} \cdot H_2O$), remplissent les fines veinules que l'on retrouve à l'échelle de l'ensemble des concentrations de Oiţa. Nous avons constaté la présence importante de *la stilpnomélane enrichie en potasse et en baryum* au voisinage de ces fines veinules qui traversent la minéralisation.

Dans les lentilles minéralisées, les bandes de carbonates manganésifères sont traversées par des filons de rhodonite associée à la pyroxmangite; il s'agit de deux inosilicates polymorphes pour le pôle $MnSiO_3$, dont le dernier est stable à plus haute pression et plus basse température. Le seul critère de distinction des deux polymorphes est l'angle 2V. Les caractéristiques optiques de cette pyroxmangite sont très proches de celles de la pyroxmangite associée à la rhodonite dans les schistes lustrés de la Haute-Maurienne (Alpes françaises) (Chopin, 1978), le 2V variant autour de 50^0

Tableau 1
Composition ponctuelle des grenats, dans les formations manganésifères de Oiţa

	1	2	3	4	5	6	7
SiO_2	36.37	34.72	36.03	36.69	35.99	36.81	36.12
CaO	2.52	2.32	2.15	2.52	1.99	3.10	3.28
MnO	30.59	31.34	31.43	33.44	34.16	34.01	36.06
MgO	0.17	0.25	0.12	0.35	0.38	0.18	0.28
Cr_2O_3	0.19	0.12	0.07	0.11	0.02	0.24	0.08
FeO	8.26	8.26	7.65	6.38	5.40	3.85	1.15
Fe_2O_3	1.21	1.21	1.16	0.00	0.05	0.30	2.54
Al_2O_3	20.03	19.22	19.27	20.69	20.33	20.08	18.44
TOTAL	99.34	97.44	97.98	100.18	98.32	98.57	97.95
Si	5.99	5.87	6.02	5.97	5.98	6.05	6.03
Ca	0.44	0.42	0.38	0.44	0.35	0.54	0.58
Mn^{2+}	4.27	4.48	4.45	4.61	4.81	4.73	5.10
Mg	0.04	0.06	0.02	0.08	0.09	0.04	0.06
Cr^{3+}	0.02	0.01	0.00	0.01	0.00	0.03	0.03
Fe^{2+}	1.21	1.16	1.07	0.86	0.75	0.52	0.16
Fe^{3+}	0.06	0.15	0.14	0.00	0.00	0.03	0.31
Al	3.89	3.82	3.79	3.97	3.98	3.89	3.63
TOTAL	15.92	15.97	15.87	15.94	15.96	15.83	15.90
Al	0.20	0.19	0.18	0.14	0.12	0.09	0.02
Py	0.01	0.01	0.00	0.01	0.02	0.01	0.01
Sp	0.71	0.73	0.75	0.77	0.80	0.81	0.86
Gr	0.04	0.02	0.02	0.06	0.06	0.07	0.01
Ad	0.02	0.04	0.04	0.00	0.00	0.01	0.08
Ov	0.01	0.00	0.00	0.00	0.00	0.00	0.00

Tableau 2
Composition ponctuelle des cryptomélanes
(Epigénie des grenats)

	1	2	3	4	5	6
MnO_2	88.99	91.12	89.32	88.12	89.83	90.76
Fe_2O_3	0.54	1.29	1.15	1.35	0.85	0.88
K_2O	5.41	5.52	5.59	6.00	6.27	6.36
Na_2O	0.10	0.22	0.08	0.07	0.08	0.10
BaO	0.00	0.00	0.25	0.11	0.18	0.00
CaO	0.37	0.20	0.17	0.32	0.16	0.22
MgO	0.33	0.11	0.81	0.27	0.17	0.11
SiO_2	0.43	0.42	0.29	0.59	0.35	0.96
CoO	0.00	0.04	0.12	0.03	0.13	0.14
NiO	0.09	0.00	0.16	0.00	0.13	0.00
TOTAL	96.26	98.92	98.92	96.86	98.15	99.53
Mn^{4+}	7.62	7.61	7.46	7.53	7.60	7.53
Fe^{3+}	0.05	0.11	0.10	0.12	0.07	0.07
K	0.85	0.85	0.86	0.94	0.98	0.97
Na	0.02	0.05	0.01	0.01	0.01	0.02
Ca	0.04	0.02	0.02	0.04	0.02	0.02
TOTAL	0.91	0.92	0.89	0.99	1.01	1.01

avec une moyenne à 45^0. Dans les concentrations de Oiţa, la pyroxmangite est précoce, correspondant à la brusque mise sous pression au début du métamorphisme régional.

L'oxydation des carbonates et des silicates est le processus principal et responsable de la masse de minerai exploitable dans les concentrations de Oiţa. La plupart des oxydes secondaires sont issus de l'oxydation des carbonates et des silicates. L'analyse microscopique , en section polie, confirmée par l'examen à l'aide des rayon X, des échantillons provenant de la zone la plus oxydée des corps minéralisés, met en évidence l'importance de *la birnessite* $[(Ca, Na, K)(Mg, Mn)Mn_6O_{14} \cdot 5H_2O]$ dans le minerai; elle est ici le résultat de l'oxydation des carbonates et des silicates (il s'agit la plupart du temps de la pyroxmangite et de la rhodonite). La faible réflectance, le pléochröisme intense et la manière forte de réagir entre les nicols croisés sont très caractéristiques de cet oxyde. L'observation au microscope électronique à balayage révèle des agencements de lamelles très caractéristiques de la birnessite (Pl. II, Fig. 1). La birnessite évolue rapidement en *nsutite* ($\gamma - MnO_2$) ; ces deux phases forment ensemble des concrétions (Pl. II, Fig. 2). Nous avons constaté, lorsque la birnessite est issue de l'oxydation d'une rhodochrosite riche en fer et de surcroît associée à des sulfures et sulfoarséniures en voie d'oxydation, que sa composition ponctuelle conserve le trait géochimique du carbonate (Tab. 3) et qu'elle évolue vers une nsutite (γ-MnO_2) particulièrement désordonnée; le diagramme aux rayons X permet d'indexer le produit comme hexagonal, alors que la maille habituelle de la nsutite (γ-MnO_2) est orthorhombique. Les caractéristiques des clichés aux rayons X de cet oxyde sont identiques à celle du $\varepsilon - MnO_2$, (Pl . II, Fig.3) dont la maille est en effet hexagonale (De Wolff et al., 1978). Les différences entre l'agencement structural des deux phases (Fig. 4) ont bien été établies. Dans l'enterprétation des clichés aux rayons X comme dans celle des courbes thermopondérales, nous devons tenir compte des associations intimes entre les oxydes de manganèse et les hydroxydes de fer issues de l'altération des carbonates et silicates, mais aussi de l'altération des sulfures et des sulfoarséniures; pour l'examen aux rayons X, le degré de cristallinité de chaque constituant affecte aussi la qualité du cliché. C'est sur les clichés des produits de synthèse que se manifestent le mieux les différences essentielles entre la phase γ-MnO_2 et ε-MnO_2 (Pl. II, Fig. 3). Les analyses thermopondérales ont été effectuées avec une thermobalance METTLER TA 4000, dans une atmosphère d'oxygène, en utilisant un creuset de corindon (α-Al_2O_3). Les échantillons étaient de l'ordre de 20–50 mg. La vitesse d'échauffement étaient 5^0/min. Chaque

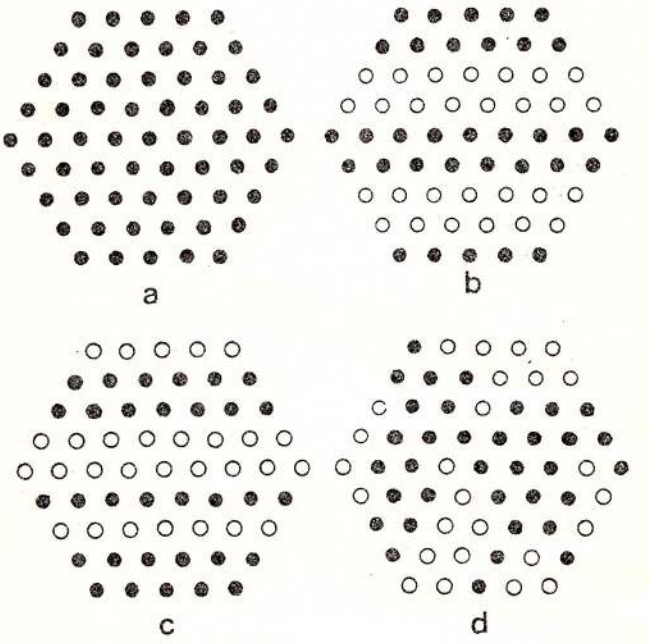

Fig. 4 – Positions octaédriques dans un empilement compact hexagonal. Projection // c, de manière que les deux positions à hauteur z=1/4 et z=3/4 coïncident. ● Position occupée par Mn pour z=1/4, vide pour z=3/4; ○ Position occupée par Mn pour z=3/4, vide pour z=1/4. a) $Mn(OH)_2$, type C6; b) Ramsdellite; c) γ-MnO_2; d) ε-MnO_2

produit final, après l'analyse thermique, a été examiné à l'aide des rayons X. Nous avons tenu compte du fait que le crochet endothermique le plus important pour la phase ε–MnO_2 a lieu vers 538^0. alors que, pour la phase γ-MnO_2 (la nsutite), ce crochet se produit vers 569^0. Le diagramme aux rayons X du produit final indique la présence de la jacobsite $MnFe_2O_4$.

Le ε-MnO_2 est utilisé dans l'industrie des piles sèches sous le nom de FARADISER M, avec le γ-MnO_2, désigné sous le nom de FARADISER WS. L'association de ces deux oxydes ainsi que leur conditions de formation n'avaient encore jamais été signalées.

Conclusion

Les processus de remplacement et d'oxydation des silicates et des carbonates n'apparaissent pas d'une manière très nette dans les concentrations de Oiţa. On notera cependant que, pour chacun de ces deux processus, nous avons pu mettre en évidence la présence d'une phase différente de MnO_2; c'est ainsi qu'une cryptomélane pure caractérise le processus de remplacement des grenats, au voisinage de fines veinules

Tableau 3
Composition ponctuelle des birnessites (1–6); (7–12). Birnessites riches en fer évoluant en ε-MnO_2

	1	2	3	4	5	6
MnO_2	70.90	76.88	79.13	80.09	80.31	80.52
Fe_2O_3	0.49	0.43	0.40	0.45	0.71	0.48
CaO	3.98	4.86	4.78	4.71	4.86	4.84
MgO	1.62	2.15	2.15	2.47	2.23	2.34
Na_2O	0.18	0.10	0.19	0.12	0.13	0.04
SiO_2	10.81	3.62	2.23	0.19	1.53	1.85
CoO	0.03	0.01	0.09	0.07	0.09	0.00
H_2O	10.90	10.51	10.52	10.32	10.32	10.65
TOTAL	98.91	98.56	99.49	98.42	100.18	100.72
Mn^{4+}	5.38	6.05	6.22	6.42	6.27	6.26
Fe^{3+}	0.04	0.03	0.03	0.03	0.06	0.04
Ca	0.46	0.59	0.58	0.58	0.58	0.58
Mg	0.26	0.36	0.36	0.42	0.37	0.39
Na	0.03	0.02	0.04	0.02	0.02	0.01
	7	8	9	10	11	12
MnO_2	69.84	69.70	68.93	67.84	62.79	58.47
Fe_2O_3	7.31	7.70	9.25	10.31	16.78	22.30
CaO	7.40	7.61	7.21	6.94	4.49	4.14
MgO	1.07	1.10	1.04	0.89	0.65	0.25
Na_2O	0.03	0.05	0.05	0.00	0.00	0.00
SiO_2	0.21	0.34	0.28	0.27	1.04	0.83
CoO	0.02	0.00	0.07	0.00	0.12	0.02
H_2O	12.31	12.37	12.41	12.27	12.20	12.05
TOTAL	98.19	98.87	99.24	98.52	98.07	98.06
Mn^{4+}	5.87	5.83	5.74	5.72	5.32	5.02
Fe^{3+}	0.66	0.70	0.83	0.94	1.55	2.08
Ca	0.96	0.98	0.93	0.90	0.59	0.55
Mg	0.19	0.19	0.18	0.16	0.12	0.04
Na	0.01	0.01	0.01	0.00	0.00	0 00

constituées de termes intermédiaires de la série cryptomélane-hollandite. La présence et l'importance des termes de la série de la cryptomélane- hollandite dans le gisement de Oiţa sont liées à la circulation des solutions tardives enrichies, non seulement en manganèse, mais aussi en potasse et en baryum. La birnessite est le produit de l'oxydation des carbonates et des silicates (essentiellement la pyroxmangite et la rhodonite). L'évolution de la birnessite à l'échelle du gisement semble être fonction de la concentration en fer du milieu; la présence de la phase ε-MnO_2 correspond à l'évolution d'un produit d'oxydation des carbonates riches en fer, alors que la prédominance de la nsutite (γ-MnO_2) indique l'évolution d'un produit moins riche.

Bibliographie

Bălan, M. (1976) Zăcămintele manganifere de la Iacobeni. Ed.Acad. R.S.R., 123 p., Bucureşti.

Bonatti, E., Krämer, T., Rydell, H. (1972) Classification and genesis of submarine iron manganese deposits; In: Horn, D.(ed.), Ferromanganese deposits on the ocean floor. Washington, Nat. Sci. Found., p. 149–165.

Borishanskaya, S.S., Krutov, G.A., Makhmudov, A.L. (1965) Alloclastite from south Doshkesan iron-ore (Azerbaydztan) *Doklady Acad. Sci. USSR (A.G.T. Eng Trans) 161*, p. 136–138, Moscova.

Chopin, C. (1978) Les paragenèses réduites ou oxydées de concentrations manganésifères des "schistes lustrés" de Haute Maurienne (Alpes françaises). *Bull. Minéral.*, 101, p. 514–531, Paris.

Craig, J. R., Sandhaus, D. J., Guy, R. E. (1985) Pyrophanite $MnTiO_3$ from Sterling Hill, New Jersey. *Can. Mineral.*, 23, p. 491–494, Ottawa.

De Wolff, P. M., Visser, J. W., Giovanoli, R., Brütsch, R. (1978) Über ε-Mangandioxid. *Chimia*, 32, 7, p. 257–259, Berna.

Ianovici, V. (1956) Informations générales sur les gisements de minerai de manganèse de la Roumanie. Symp. manganeso, XX. Congr. geol. internat., Mexico.

Maurel, C., Picot, P. (1973) Sur le mécanisme de la transformation de l'alloclastite en cobaltite: cas du gisement du Lautaret. *Bull. Soc. fr. Minéral, Cristallogr.*, 96, p. 292– 297, Paris.

Perseil, E.A., Grandin, G. (1985) Altération supergène des protores à grenats manganésifères dans quelques gisements d'Afrique de l'Ouest. *Mineral Deposita*, 20, p. 211–219, Berlin.

— , **Latouche, L. (1989)** Découverte de microstructures de nodules polymétalliques dans les minéralisations manganésifères métamorphiques de Fal otta et de Parsettens (Grisons-Suisse). *Mineral Deposita*, 24, p. 111–116, Berlin.

Peters, Tj. (1984) Geochemie der Oberhalbsteiner und einiger weiterer penninischer Manganvorkommen. *Beitr. geol. Schweiz, geotechn.*, Serie 64, p. 82–90, Zürich.

Petruk, W., Harris, D.C., Stewart, J.M. (1971) Characteristics of the arsenides, sulpharsenides, and antimonides. *Can. Mineral.*, 11, p. 150–186, Ottawa.

Polushkina, A.P., Sidorenko, G.A. (1963) Une variété structurale de cobaltite. *Dokl. Akad. Nauk., SSSR.*, 153, p. 1420, Moscova.

Received: May 1994
Accepted: July 1994

Planche I

Fig. 1 — Grenat hydrolysé. La partie centrale hydrolysée du greanat a été remplacée par de fines concrétions de rhodochrosite (R). On peut constater dans la partie centrale des concrétions (flèche) le début de l'oxydation. Lumière naturelle transmise; le tiret = 10 μm.

Fig. 2 — Remplacement du grenat par la cryptomélane à la faveur des cassures. Lumière naturelle transmise; le tiret = 10 μm.

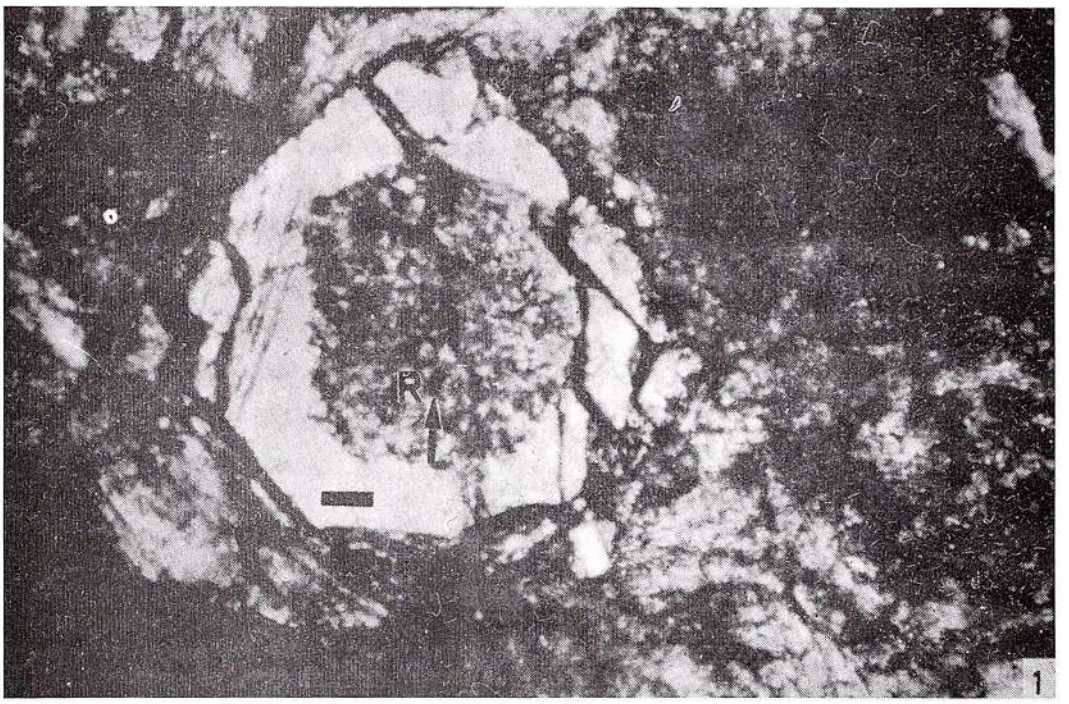

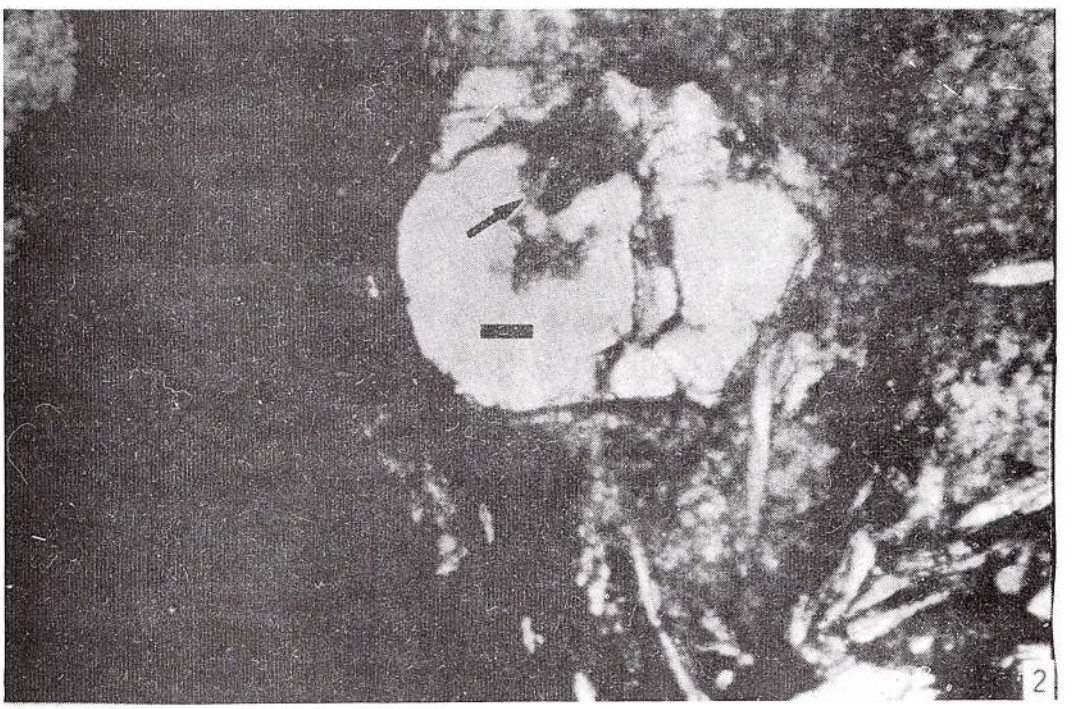

Planche II

Fig. 1 — Faciès caractéristique en lamelles d'une concrétion de birnessite de la zone d'oxydation du gisement Oiţa (Microscope électronique à balayage).

Fig. 2 — Concrétions de birnessite (B) et de nsutite (N). Oxydation de la pyroxmangite (P) en birnessite (B); évolution en nsutite(N). Lumière naturelle réfléchie; le tiret=10μm.

Fig. 3 — Clichés aux rayons X (Chambre Guinier–De Wolff Type IV, $FeK_{\alpha 1}$. 1, γ–MnO_2 (la nsutite); 2, ε–MnO_2 (le produit FARADISER M).

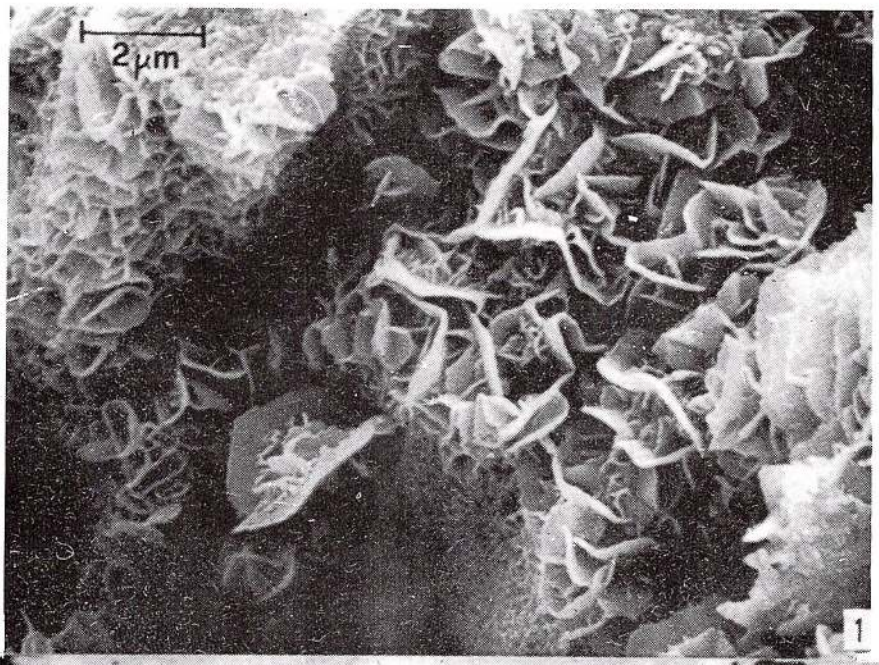

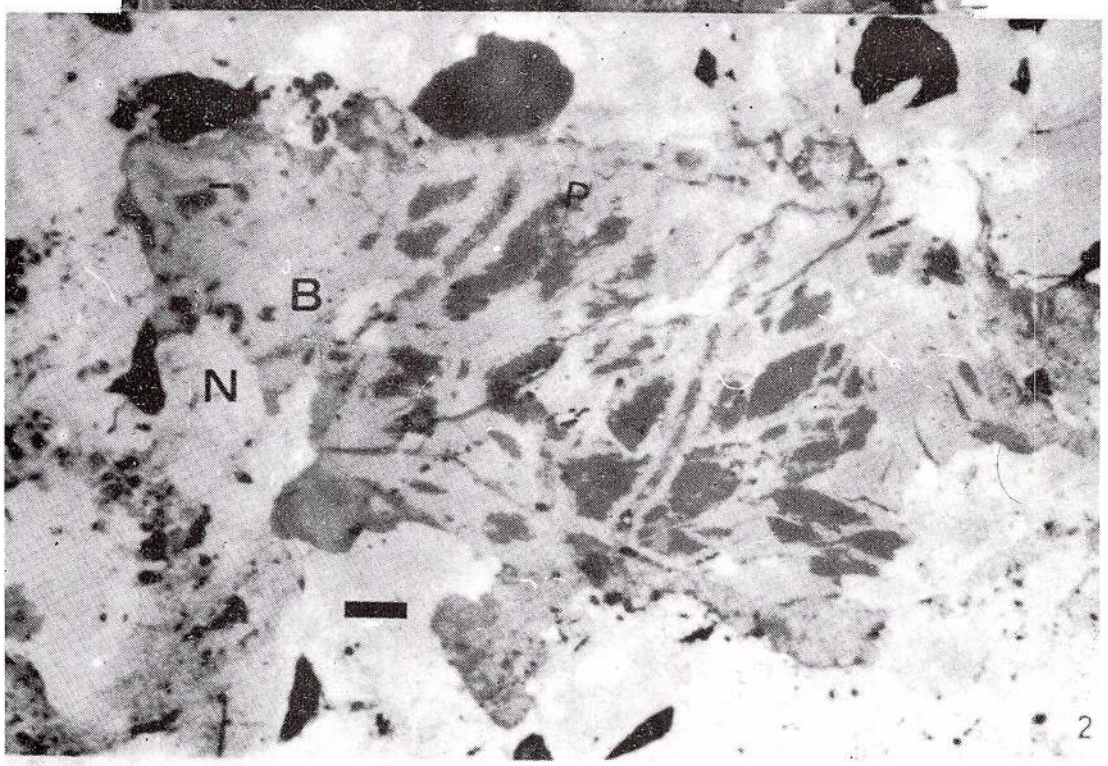

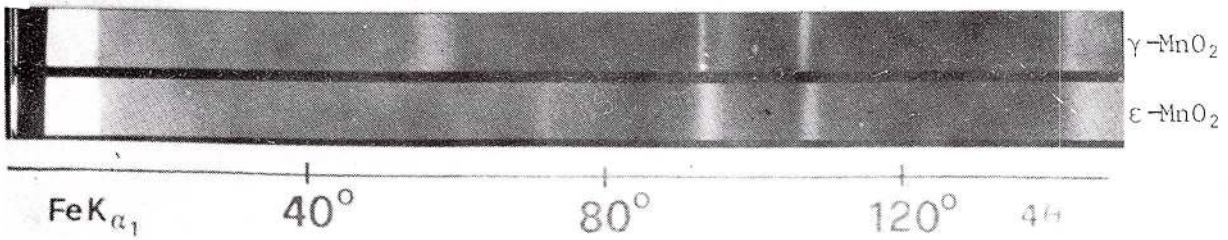

Rom. J. Mineralogy, 1995, 77, p. 19–24, Bucureşti

PYROPHANITE OF DELINEŞTI (SEMENIC MOUNTAINS)

Paulina HÂRTOPANU, Corina CRISTEA, Gabriela STELEA
Institutul Geologic al României. Str. Caransebeş nr.1 78344 Bucureşti, 32

Erna CĂLINESCU
"Prospecţiuni" S.A. Str. Caransebeş nr. 1, 78344 Bucureşti, 32

Key words: Pyrophanite. XDR. IR. Chemical Analyses. Delineşti. Semenic Mts.

Abstract: Pyrophanite is for the first time described in the ores of the Delineşti deposit, where it occurs either as a fine-grained constituent of the spessartine-rich and carbonate-rich ores or as centimetric-sized crystals in veins cutting the spessartine ore. The first type of pyrophanite is closely associated with monazite, whereas the vein pyrophanite is related to quartz, hematite, spessartine-calderite etc. X-ray diffraction data, cell parameters and IR spectra as well as the chemical analyses are presented pointing out differences as against ilmenite and other pyrophanite occurrences.

Introduction

Pyrophanite $MnTiO_3$ or Mn-ilmenite has been mentioned in few occurrences in the world, being first described in the manganese ore in the Harstig mine, Pajsberg, Sweden (Hamburg, Ilink, 1890, cf. Lee, 1955). Pyrophanite occurs in association with garnet, ganophyllite, manganophyllite and calcite. Derby (1901, 1908, cf. Lee, 1955) described pyrophanite from the Piquery mine (Minas Geraes, Brazil) where it is associated with rhodochrosite, tephroite, spessartine, pyrite, ilmenite and more rarely rhodonite. Smith (1947) found this mineral associated with pennantite and he determined it by X-ray analysis (cf. Lee, 1955). Pyrophanite was also mentioned by Lee (1955) in some mines in Japan (Ajiro, Kinko, Kusugi, Noda Tamagawa, Renge and Mine X). Zak (1971) described pyrophanite from the rhodochrosite manganese accumulation at Chvaletice (Bohemia), where it is related to rhodonite, pyrrhotite, pyrite, neotocite, arsenopyrite; in all these associations pyrophanite is an accessory mineral. In Romania, Bălan (1976) described, for the first time in this country, pyrophanite at Iacobeni (Bistriţa Mts), where it is found in association with albite and rhodonite in recent veinlets which cut the manganese ore. He determined the ore by X-ray analysis.

General outlook on the Delineşti ore deposit

The Delineşti Mn-Fe ore deposit constituted the object of many mineralogical researches, the most important ones being those carried out by Savu (1959) and Dimitrescu and Popa (1973). A minute petrographical, mineralogical and genetical study has been recently effectuated by Hârtopanu, Hârtopanu and Cristea (1993) in which the authors quoted 20 new minerals for the ore deposit among which pyrophanite. The complex mineralogy of the ore deposit is the result of its geological evolution: initially regionally metamorphosed, then thermally, metasomatically and hydrothermally altered. The Delineşti ore deposit is situated in the northern part of the Semenic Mts, in the Sebeş-Lotru Series, metamorphosed in the amphibolite almandine facies, penetrated by acid intrusions, veins of granites, locally pegmatoid ones, of pegmatites and by hydrothermal quartz veins. These yielded a contact thermal metamorphism for the primary ore, then a metasomatosis with $^{3+}$Fe, Na, K, B, F, followed by a hydrothermal period. All these processes are materialized by specific minerals (Hârtopanu, Hârtopanu, Cristea, 1993). The petrographic types established on mineralogical and genetical criteria are also the result of the geological evolution of the ore deposit: (1)spessartinic (=gonditic) type, (2)carbonatic (=queluzitic)

and hybrid (=koduritic) type. The hybrid type resulted from the first two types which subsequently underwent the above-mentioned alterations. Pyrophanite is found in the hybrid ore, therefore it is a post-metamorphic mineral. In quantitative respect it is generally an accessory mineral.

Distinguishing features and physico-chemical properties

Pyrophanite in the Delineşti ore deposit occurs either as small crystals (less than 1 mm), frequently in a hybrid ore (both in a primary spessartine ore and in the primary carbonate one), when it shows irregular, rarely hexagonal outlines (probably mistaken for rutile up to now) (Pl.,Figs. 3,4), or as large centimetric up to 1 dm pegmatoid crystals, occurring as veins cutting mostly an old spessartine ore (Pl., Fig. 1). Macroscopically, it resembles ilmenite; under the magnifying glass it differs by the presence of fine, brown irisations on the cleavage planes. It displays cleavages after two directions: perfect after $(02\bar{2}1)$ and good after $(10\bar{1}2)$ as well as triangular striations after (0001). As powder, the ore is brown. In transmitted light pyrophanite is of a yellow-reddish, red-brown or red-orange colour, translucid or transparent and devoid of pleochroism. It is uniaxial negative. Locally, it displays repeated twinning after $(10\bar{1}1)$ similar to the carbonate ones. In reflected light pyrophanite is grey, slightly pleochroic between bright grey and dark grey hues, especially in immersion. Also in immersion, in crossed polarizing prism it displays a strong anisotropy in grey colours and frequent red internal reflexes.

Pyrophanite associations. The small-sized, submillimetric pyrophanite from the hybrid ore-initially gonditic is associated with spessartine-calderite, acmite, monazite; spessartine-calderite, monazite, quartz. It is of note in this type of ore the great affinity of pyrophanite for monazite: large monazite crystals contain pyrophanite grains (Pl., Fig.5), they being contemporaneous. In the hybrid-carbonate ore the same pyrophanite type is associated with rhodonite, pyroxmangite, rhodochrosite, spessartine-calderite, yellow alkaline amphiboles. As regards the pegmatoid pyrophanite, it shows two associations: pegmatoid quartz, pyrophanite and microcline, albite, acmite, phlogopite, spessartine-calderite, hematite (Pl., Fig.6). Pyrophanite is more recent than pyroxmangite, rhodonite, rhodochrosite and it is contemporaneous with acmite, spessartine-calderite, yellow alkaline amphiboles, phlogopite, hematite, monazite, albite, microcline.

X-ray diffraction powder data

X-ray diffraction powder data (Tab. 1) are in good agreement with other published data (Tab. 2). Lattice constants for Japanese and Iacobeni pyrophanite were calculated on the basis of X-ray data given by Lee (1955) and Bălan (1976).

Table 1

X–ray diffraction powder data of pyrophanite from Delineşti

DRON-3 diffractometer. CuK_α radiation

No	D-obs.	D-calc.	h	k	l	I
1	3.768	3.772	0	1	2	25
2	2.780	2.781	1	0	4	100
3	2.564	2.566	1	1	0	45
4	2.257	2.258	1	1	3	25
5	1.886	1.886	0	2	4	37
6	1.744	1.744	1	1	6	55
7	1.654	1.654	0	1	8	15
8	1.520	1.520	2	1	4	30

LATTICE PARAMETERS:

a	b	c	VOL
5.1327 Å	5.1327 Å	14.2601 Å	325.3470 Å^3

ROMBOHEDRAL: a=5.60142 α=54.5372

Table 2

Lattice constants of some pyrophanites

	a	c	V	Chemical Data
DELINEŞTI	5.133	14.260	325.381	MnO 40% TiO_2 52% Fe_2O_3 6% FeO –
CHVALETICE[1]	5.131	14.274	325.447	MnO 32% TiO_2 51.8% Fe_2O_3 – FeO 14.22%
JAPANESE[2]	5.120	14.290	324.416	–
IACOBENI[3]	5.130	14.210	323.862	–

[1] Zak (1971)

[2] Lee (1955)

[3] Bălan (1976)

IR absorption spectra

A pyrophanite sample from Delineşti has been analysed in a spectral interval 4000-200 cm^{-1} in view of pointing out differences from ilmenite, which displays a similar structure. The spectrum obtained in the interval 4000-200 cm^{-1} has been compared with a spectrum of relatively pure ilmenite (collection of Dr. G.Udubaşa) (Fig.1) and with ilmenite diagrams from the literature (Liese, 1967) (Fig.2). The values of the absorption bands for ilmenite and pyrophanite differs as compared with the tolerance admitted by the device, situated between 448, 548 and 690 cm^{-1} (for ilmenite) and 448, 544, 685 cm^{-1} (for pyrophanite). However, there is a difference related to the intensities of the absorption maxima which are higher for pyrophanite as against ilmenite (Fig.1). This is not, however, conclusive because there are ilmenites (Liese, 1967) which show an increase of the bands concomitantly with the increase of the Fe quantity and the decrease of the Ti quantity.

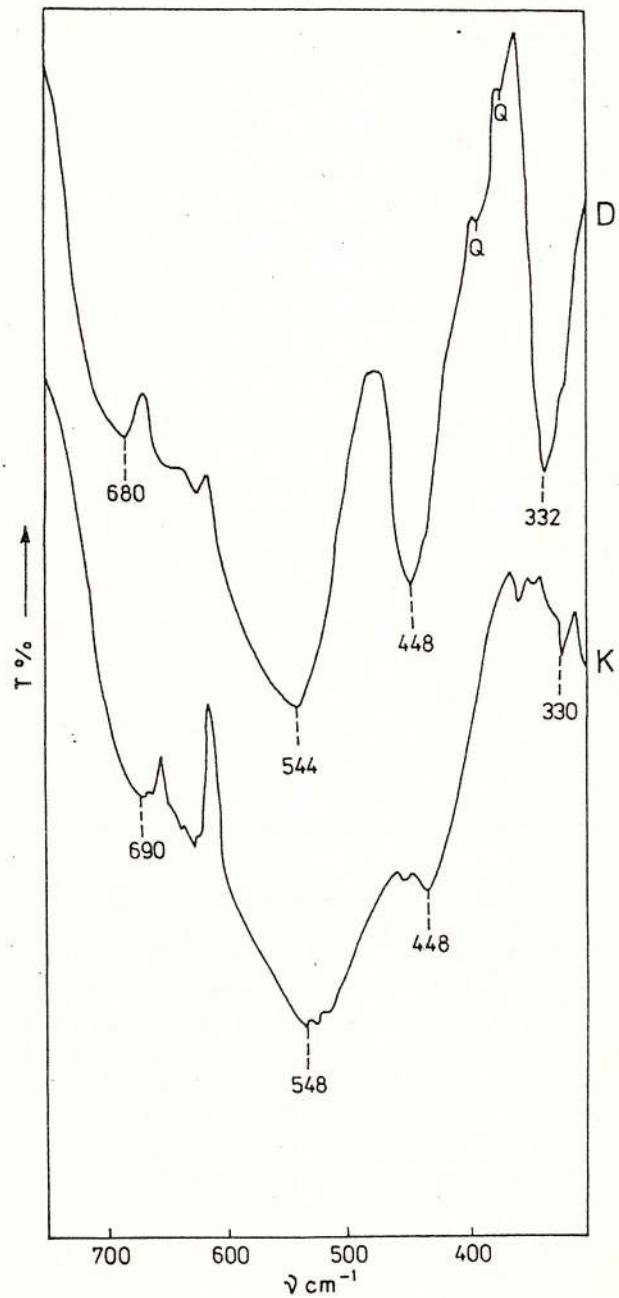

Fig.1- IR spectra of Kragerö ilmenite (K) and of Delineşti pyrophanite (D).

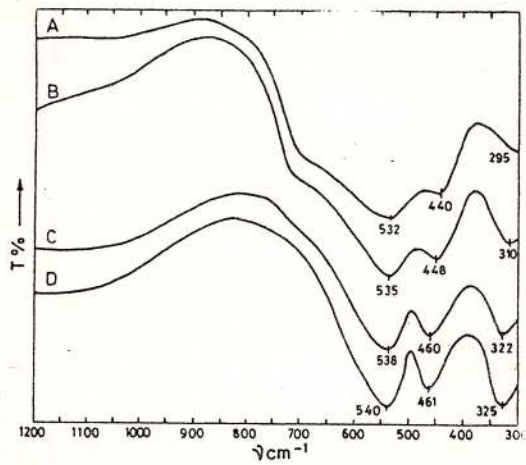

Fig.2- IR spectra for ilmenite of: A - Arendal, Norway; B - Kragerö, Norway; C - Chester, Vermont; D - Waterford - Rhode Island (Liese, 1967).

Table 3
Comparative chemical composition of ilmenite and pyrophanite

ilmenite (K)[1]	ilmenite (W)[2]	pyrophanite (D)[3]	
SiO_2	0.20	0.20	0.46
Al_2O_3	0.20	0.10	0.19
Fe_2O_3	–	–	5.14
FeO	49.90	71.00	0.93
MgO	0.02	0.01	0.27
CaO	0.02	0.01	0.20
Na_2O	0.01	0.02	0.03
K_2O	0.15	0.15	0.05
H_2O^+	0.03	0.03	–
H_2O^-	0.10	0.10	–
TiO_2	47.10	26.50	48.30
CO_2	0.00	0.00	–
MnO	0.03	0.03	43.08
Total	97.8	98.2	98.70

[1](K) = Kragerö Norway (Liese, 1967);
[2](W) = Waterford Rhode Island (Liese, 1967);
[3](D) = Pyrophanite of Delineşti

Table 3 presents the chemical analyses of the ilmenite samples from Kragerö (Norway) -(K), Waterford (Rhode Island) - (W) and the chemical analysis of the Delineşti pyrophanite - (D).

In conclusion, the infrared analysis does not allow the obtaining of exact specifications for pyrophanite identification, the X-ray diffraction powder data and chemical data being fundamental for its recognition.

Chemical composition of pyrophanite

The Delineşti pyrophanite has been analysed chemically in quantitative respect based on the classic and microprobe methods. The results of the classic method analysis are rendered in Table 4. It is to note the absence of FeO and the presence almost only of Fe_2O_3.

The latter may form an isomorphic solution with $MnTiO_3$ (Ishikawa and Akimoto, 1958; cf. Zak, 1971).

Table 4
Comparative chemical composition of pyrophanites (Chv) and (D)

Oxides	Pyrophanite (Chv)*	Pyrophanite (D)
MnO	43.30	39.40
FeO_{total}	3.80	2.00
TiO_2	52.90	57.40
Al_2O_3	0.00	0.04
SiO_2	0.10	0.30

*Zak (1971)

Table 4 shows the chemical composition of the Delineşti (D) and of the Chvaletice pyrophanite (Chv). The higher MnO content for the pyrophanite (D) is to be noticed. In order to establish more precisely the formation medium of the Delineşti pyrophanite a spessartine-calderite sample, a mineral with which pyrophanite is related, has been analysed (sample D 3 s). It shows the following contents: Al_2O_3 = 10.53, SiO_2 = 53.90; CaO = 5.86, TiO_2 = 0.63; MnO = 22.35, Fe_2O_3 = 6.58, FeO = 0.00. The formation medium of this spessartine is oxidating and it occurs also in the pyrophanite formation (which is more recent than spessartine-calderite) because of the Fe presence in its constitution only as Fe_2O_3. The crystallochemical formula of the Delineşti pyrophanites has been calculated on the basis of 1 Mn and of 3 O (for more significant cations and for all the present cations). Si^{4+} presence is due probably to the fine microscopic quartz inclusions in pyrophanite. The calculation of the formula in base 1 Mn is, as follows: $(Mn_{1.0}, MgO_{0.01}, FeO_{0.021})$ $Fe^{3+}_{0.106}Ti_{0.995}O_3$, in base 3 oxigen (with more significant cations): $(Mn_{0.943}Mg_{0.01}Fe^{2+}_{0.02})Fe^{3+}_{0.1}Ti^{4+}_{0.938}O_3$.

Origin of pyrophanite. Pyrophanite has been found in the world in two mineralogical assemblages: (1) in pegmatites, related to eruptive alkaline rocks (Portnov, 1963 cf. Zak, 1971; Newman and Bergatol, 1964, cf. Zak, 1971; Chukhrov and Bonshted-Kupletskaya, 1967) and in the manganese ores (Hamburg, 1980; Campbell, Smith and Claringbull, 1947, cf. Lee, 1955; Zak, 1971; Bălan, 1976). In the manganese ores the origin of pyrophanite was connected with the hydrothermal activity which had been followed by a thermal contact metamorphism, a process which yielded some manganese silicates with which it is associated.

Table 5
Cation calculation from the chemical composition of pyrophanite

Sample D3		
SiO_2	0.460	
TiO_2	48.300	
Al_2O_3	0.190	
Fe_2O_3	5.140	
FeO	0.930	
MnO	43.080	
MgO	0.270	
CaO	0.200	
K_2O	0.050	
Na_2O	0.030	
P_2O_5	0.050	
Total	98.700	
Ti^{4+}	0.995	
Fe^{3+}	0.106	
Fe^{2+}	0.021	
Mn^{2+}	1.000	-calculated in base 1 Mn
Mg^{2+}	0.011	
cations	2.134	
charge	6.364	
Ti^{4+}	0.938	
Fe^{3+}	0.100	
Fe^{2+}	0.020	
Mn^{2+}	0.943	-base 3 oxigen (6 negative charges)
Mg^{2+}	0.010	selected cations
cations	2.012	
charge	6.000	

The two pyrophanite types (pegmatoid and fine granular) at Delineşti seem to have different origins. Thus, the first type is associated with the hydrothermal veins, and the small-sized, submillimetric pyrophanite grains from the hybrid-carbonatic or hybrid-spessartinic ore are probably the result of the titanite alteration. The titanite network was probably distroyed by a thermal contact metamorphism, with the release of calcium and silica, and the manganese rich medium determined the occurrence of pyrophanite not of ilmenite and rutile, the common products of this alteration. The Ti source from pyrophanite may be, therefore, titanite, the more so as its constitution includes sometimes more Ti than Si, replacing it in the SiO_2 group. Considering that initially titanite was rich in Y and Ce (varieties up to 12 % $(Y, Ce)_2O_3$; are also known (Winchell and Winchell, 1961) the monazite occurrence and especially its frequent association with pyrophanite can be explained.

References

Bălan, M. (1976) Mineralogia zăcămintelor manganifere de la Iacobeni. Edit. Acad. RSR., 34 p., Bucureşti.

Chukhrov, F.V., Bonshtedt Kupletskaya, E.M. (1967) Mineralî. 2, 3, p. 275-278, Moscva.

Dimitrescu, R., Popa, Gh. (1973) Asupra minereurilor manganifere din zăcământul Delineşti. *An.Şt.Univ."Al.I.Cuza"*, XIX, p. 1-11, Iaşi.

Hârtopanu, P., Hârtopanu, I., Cristea, C. (1993) Mineralogy and genesis of the Delineşti Mn+Fe ores. (Abs.), *Rom. J. Mineralogy*, 76, part 1, Suppl. 1, p. 19-20, Timişoara.

Lee, D.E. (1955) Mineralogy of some Japanese manganese ores Stanford. *Univ. Publ., University Series, Geol. Sci.*, V, p. 41-43.

Liese, H.C. (1967) An infrared absorption analyses of magnetite. *Am. Min.*, 52, 4, p. 1198-1205.

Savu, H. (1959) Contribuţii la cunoaşterea zăcămintelor manganifere din regiunea Delineşti (Munţii Semenic). *D.S. Inst. Geol.*, XLVI (1958-1959), p. 147-157, Bucureşti.

Winchell, A.N., Winchell, H. (1967) Elements of optical mineralogy. John Wiley and Sons, Inc., 523 p., New York.

Zak, L. (1971) Pyrophanite from Chvaletice (Bohemia) (1971). *Min.Mag.*, 38, 5, p. 312-316.

Received: December 1994
Accepted: February 1995

Plate

Fig.1– Pyrophanite veinlets in spessartine-calderite. Sample D_3 gallery waste 1, N II, x 40.

Fig.2– Acmitic pyroxene (large, with cleavage), pyrophanite (black), spessartine-calderite (small) and quartz (white) assemblage. Sample D 77, gallery waste 1, N II, x 40.

Fig.3– Pyrophanite (black grains) with acmite (large grey grains), spessartine-calderite (small, grey) and quartz (white) assemblage. Sample D 77 a, gallery waste 1, N II, x 40.

Fig.4– Pyrophanite (black) with spessartine-calderite (small, grey grains with a high relief) assemblage. Sample 7113, Tâlva Bobului, N II, x 60.

Fig.5– Large grain of pyrophanite (centre) and other three small satellite grains included in monazite (white, vaguely grey). Monazite is included in spessartine (black). Sample 7(1), gallery waste 1, N+, x 60.

Fig.6– Pyrophanite (black) included in monazite (white, vaguely grey) all included in albite (twins). Sample D_{12}, gallery waste 1, N+, x 60.

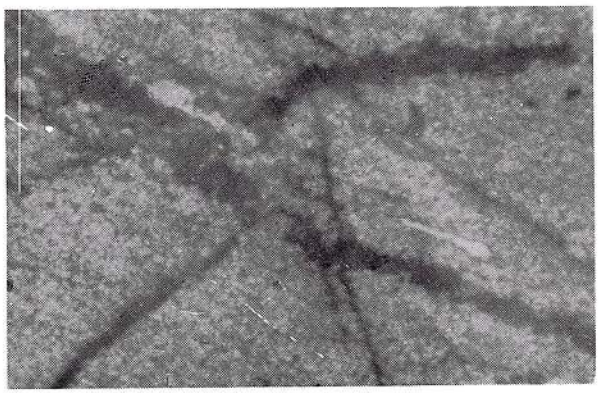

1

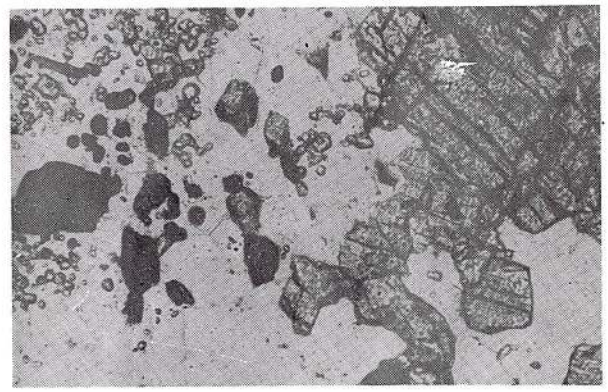

2

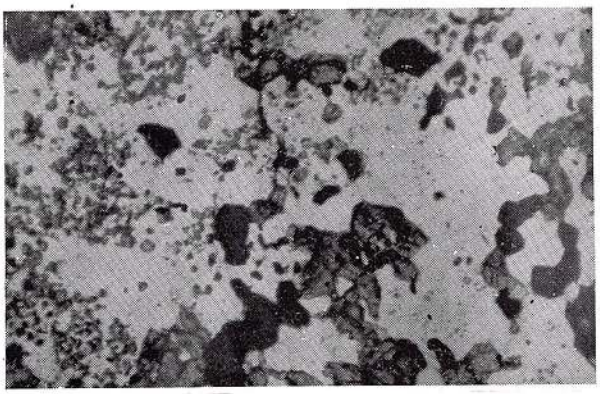

3

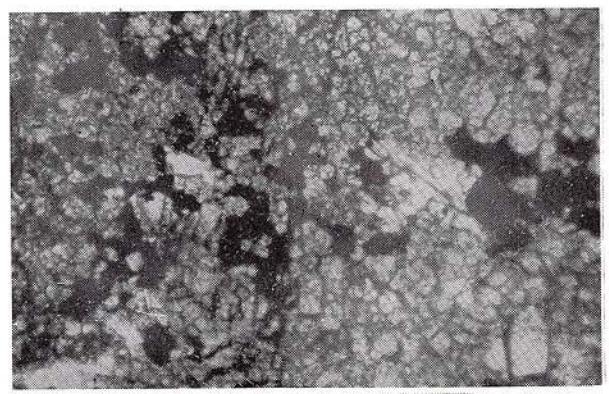

4

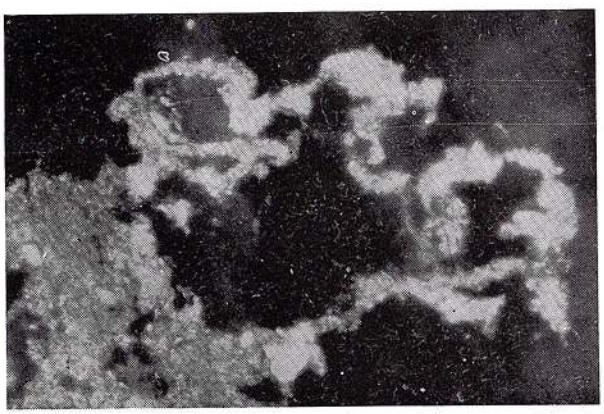

5

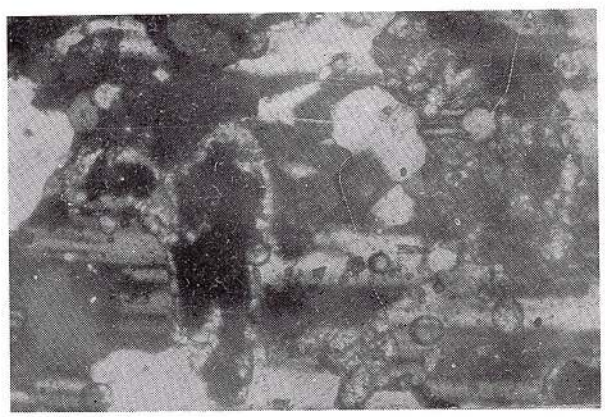

6

Rom. J. Mineralogy, 1995, 77, p. 25–34, Bucureşti

WHITE MINERALS MARKET AND THE EUROPEAN PAPER INDUSTRY

José António L. VELHO, Celso S.F. GOMES
Departamento de Geociências, Universidade de Aveiro, 3800 Aveiro, Portugal.

Key words: Clay minerals. Kaolin. Calcium carbonate. Talc. Paper Industry .

Abstract: Conversion from acid to neutral-alkaline method in many European paper industries resulted in the substitution of kaolin by calcium carbonate with significant price reduction and increase of paper quality. The kaolin producers were thus challenged to obtain new commercial grades of kaolin for very special applications such as delaminated kaolin, mate kaolin, high gloss kaolin, blended kaolin, calcined kaolin, chemically structured kaolin. Consequently kaolin further keeps its dominant role in the mineral raw material industries.

1. Introduction

During the 80's decade many European paper industries processing chemical pulp have converted from the acid to the neutral-alkaline method in order to utilize natural calcium carbonate as filler, much more cheaper than kaolin. For instance, in western Europe, more than 80% of paper industries have adopted the neutral-alkaline method. Besides price, other factors justify the substitution of kaolin by calcium carbonate, such as: the higher brightness of the commercial grades of calcium carbonate, the higher incorporation allowed by calcium carbonate and the higher world-wide availability of calcium carbonate. Allied to the factors that have been mentioned, other mineral raw materials, natural or synthetic, were introduced in the white minerals market as kaolin substitutes and specially directed to solve some particular problems of paper quality.

As a matter of fact, in the last years, kaolin being the traditional white mineral in the paper industry has undergone some erosion in terms of consumption. This results in a challenge for kaolin producers who are trying to keep its dominant role, through the production of new commercial grades for very special applications.

2. White minerals consumption in the European paper market

White minerals consumption in the European paper industry has shown a continuous increase. Figure 1 shows up that consumption evolution in Europe during the period 1970–1989 as well as consumption forecast up to 1994.

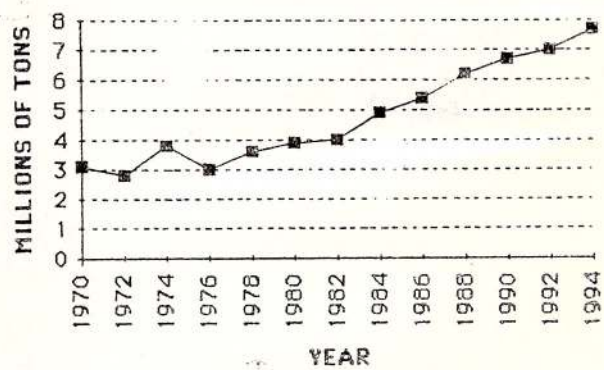

Fig. 1 – White minerals consumption in the European paper industry during the period 1970–1994 (Clark, 1990)

More than 90% of the white minerals used in paper production are incorporated in printing and writing

papers. They confer to them properties, such as: brightness, opacity, gloss and printing quality.

Table 1 contains, relatively to 1989 and to Europe, both quantities and incorporation percentages of white minerals, applied in the principal types of papers.

On the other hand, Figure 2 shows the individual consumptions, relative to 1990, of white minerals used as fillers and pigments in Europe.

the best compromise between price/transport/quality;

2. Continuous demand of new mineral raw materials alternative to kaolin in order to favour national productions;

3. Great complexity of the mineral raw materials market.

Table 2 contains a list of mineral raw materials alternative to kaolin, some natural other synthetic, which

Table 1
Paper production and incorporation percentages of white minerals in Europe (1989)

Paper and Board	Production Millions of Tons (Mt)	Minerals applied Mt	%
Newsprint	8	0,3	0-10
Printing and writing	21	6,0	5-45
Board	4	0,3	3-10
Others	26	-----	-----
Total	59	6,6	-----

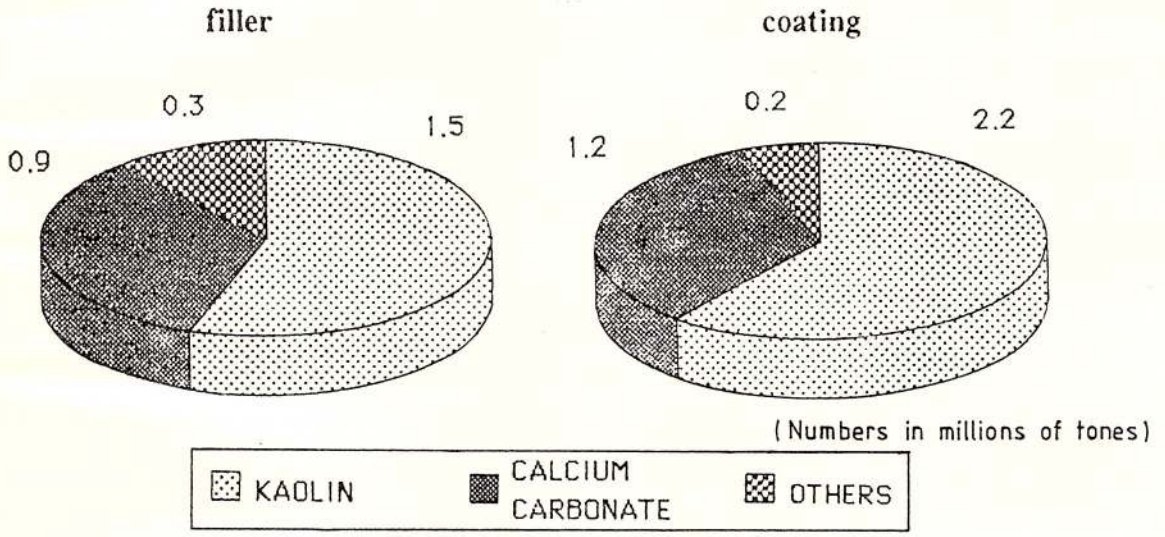

Fig. 2 – Individual consumptions in Europe, relative to 1990, of white minerals applied as fillers and pigments (Seddon, 1991).

In addition to kaolin and calcium carbonate, European paper industries have available a continuously greater number of mineral raw materials alternative to kaolin.

Velho and Gomes (1989) characterize the mineral raw materials market in terms of:

1. Great competition at all levels between producers of the same mineral raw material and between producers of different mineral raw materials in order to offer

appear in the market basically with a two-fold justification: first, as mineral resources beneficiation or as subproducts (i.e. gypsum, mica, dolomite, zeolites); second, as synthetic products directed to the resolution of certain paper problems, as is the case of opacity, where for instance titanium dioxide, BAS (Boliden amorphous silicate), HSPP (hollow spheres polymeric pigment) and synthetic zeolite can preferably substitute kaolin.

Table 2
Mineral raw materials alternative to kaolin

Paper mineral raw materials	Bibliography
Calcium carbonate	Beazley and Bailey (1985), Cahen et Daneault (1990), Coope and Dickison (1984), Fender (1985), Mather (1986)
Titanium dioxide	Coope (1984), Gosset (1990), Loughbrough (1992)
Talc	Ahonen (1985), Huuskonen and Ahonen (1984), Schober (1991)
Natural gypsum	Jané (1981), Jané (1984)
Synthetic gypsum	Klasson and Munter (1990), Svensson (1989)
Mica	Gavelin and Treiber (1982), Gavelin and Treiber (1983)
HSPP (hollow sphere polymeric pigment)	Brown and Latshaw (1990), Brown and Lunde (1987)
BAS (Boliden amorphous silicate)	Holm (1983)
TD (talc + dolomite) pigment	Novak et al. (1991)
Natural zeolites	McVey and Harben (1989)
Synthetic zeolites	Abril et al. (1993)
Diatomite	Harben (1984)
Aluminium hydrate	Canadell (1984), Beazley and Bailey (1985)
Dolomite	Alvarez et al. (1990)

2.1. Calcium carbonate

There are two types of calcium carbonate: natural (CCN) and precipitated (CCP). The first type comprises: chalk, marble as well as lithographic and sublithographic limestone. It is applied as filler to improve paper brightness and ink receptivity.

The most interesting features of CCN are as follows: 1) production and availability of a wide range of grain size (35%– 99% $< 2\ \mu m$) with brightness up to 96; 2) supplies almost illimitable; 3) low price and worldwide distribution; 4) supplies in suspension form containing up to 75% solids; 5) energy savings during paper drying due to its higher retention on paper.

In spite of CCN high brightness, its refractive index is low (1.56). Therefore its opacifying is low, a fact not convenient in paper coating applications. Things can improve using proper flocculants to provide a more massive coating and to allow better compressibility. Nevertheless, the printing quality is still not so good as that obtained with kaolin.

In regard to the comparative advantages and disadvantages of CCN and CCP, the following specificities can be considered: 1) CCP confers better opacity to paper sheets due to its higher light dispersion coefficient; 2) CCP provides less retention and less drainage due to its better particle size classification; 3) CCP affects more paper sheet resistance due to its higher interference with the inter-fibers bonds; 4) CCP is much less abrasive; 5) CCP is whiter.

CCN represents 30% whereas CCP represents 2% of the European consumption of white minerals for paper applications. Altogether EC and Scandinavia produce about 150,000 tons of CCP, applied mainly in cigarette paper, low weight paper and telefax paper.

2.2. Talc

Whenever applied as filler, talc should have grain size $< 20\ \mu m$. The specific properties of talc are as follows: 1) great softness or low abrasivity allowing longer operating durability of the machinery; 2) particle lamellar habit facilitates retention on paper sheets and favours calendering; 3) low particle size classification favours retention and porosity improving paper optical properties.

For paper coating applications talc, according to Finnish specialists, has the following advantages as compared to kaolin: 1) lower gloss; 2) higher opacity; 3) smoother surface; 4) lower abrasivity; 5) better press operationality; 6) particle shape ratio more favourable for calendering.

Despite the advantages reported, talc has the important disavantages of being hydrofobic, oleophylic and

aerophylic. Also, other inconveniencies can be pointed out: 1) higher price; 2) higher difficulty of suspension preparation; 3) greater need of chemicals for paper recycling; 4) rheological problems due to its dilatant behaviour at high shear rates.

As filler supercalendered (SC) paper with mechanical pulp for rotogravure printing talc is highly consumed in Finland. Nevertheless, talc is losing importance relative to calcium carbonate.

As coating, also in Finland, talc is very much used in low weight coating (LWC) paper for rotogravure printing. Future use of talc in this application looks very promising.

Talc great consumption is particularly limited to talc main producing countries (Finland, France and Sweden). Its potentialities in paper applications are very much dependant on costs due both to micronization and suspension preparation technologies.

Figure 3 shows the talc consumption evolution (as filler, coating and pitch control) relative to 1980, 1986 and 1990.

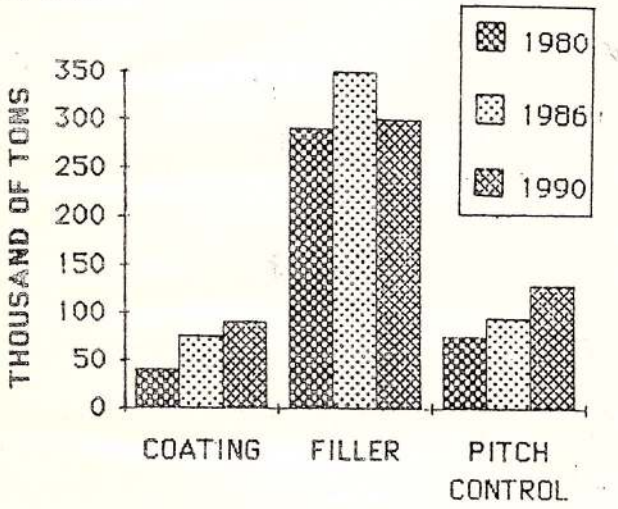

Fig. 3 – Talc consumption in Western Europe in 1980, 1986 and 1990.

3. Consequences of the acid to neutral-alkaline conversion

Conversion of the acid to neutral-alkaline processing method in most European paper industries has allowed, with the incorporation of calcium carbonate as filler, the production of high quality printing and writing papers. Exports of these papers to the Northamerican market did occur favoured by their lower prices. Also, the allowance of higher levels of calcium carbonate incorporation (up to 30%) could be reflected in pulp savings and consequently in reducing paper prices. Table 3 contains, in comparative and short forms, the advantages and disadvantages in terms of paper properties of the acid and neutral- alkaline methods (Wuerl, 1986). Added to the comparative advantages of calcium carbonate there are in Europe numerous and large calcium carbonate deposits which facilitate supplies to paper industries. On the contrary, kaolin deposits in Europe are in smaller number and have much more limited sizes. All the facts reported have produced a global declining in kaolin consumption.

Table 3
Advantages and disadvantages of the acid and neutral-alkaline methods

Properties	Alkaline	Acid
Physical properties	Strong	Weak
Energy consumption	Less	More
Corrosion	Less	More
Filler options	Free	Restricted
Recyclability	More	Less
Permanence	More	Less
Microbiological activity	More	Less
Effluent treatment	Less	More
Water needed for preparation	Less	More

Nevertheless, a growing interest did emerge in what concerns the production of high quality kaolins. From about 16,9 Mt in 1982, world kaolin production attained about 24 Mt in 1989. This corresponds to an average increase of 5% year. In 1993 due to the exploitation of new kaolin deposits it is expected that world kaolin production can attain 27 Mt (Fig. 4).

World kaolin consumption for paper applications was estimated in 1989 at about 10.5 Mt, that is a 45% increase relatively to 1982 consumption. The foreseen production growth of coating grades for use in special papers will promote a kaolin consumption growth rate estimated at 6%/year, up to 1994. Therefore, kaolin consumption for paper applications could attain 12,7 Mt in 1993 and more than 15 Mt in 2ooo, that is a mean growth rate of 4%/year.

Consumption forecast for mineral raw materials in Europe, in the period 1974–1989, is shown in Figure 5. It contains also the consumption forecast up to 1994.

4. Kaolin trends in paper applications

Despite of the competition due to calcium carbonate, particularly in some regions of the world, namely in Europe, kaolin will continue to be, in worldwide terms, the dominating mineral raw material for paper applications. This is due not only to kaolin specific physico-chemical characteristics but also to its varied commercial grades already available. New kaolin

grades, everytime more sophisticated, being the result of new processing technologies, are appearing in the market. The new developments in kaolin treatment have not parallel relative to other mineral raw materials.

Whereas calcium carbonate and talc perform functions with a "generalist" character, kaolin perform functions with a "specialist" character, because it is applied in very specialized types of paper.

In countries characterized by paper monoproduction, as is the case of Portugal where paper made with chemical pulp and without coating is the main production, kaolin consume will be in a weak position and in conditions of being overcomed by calcium carbonate.

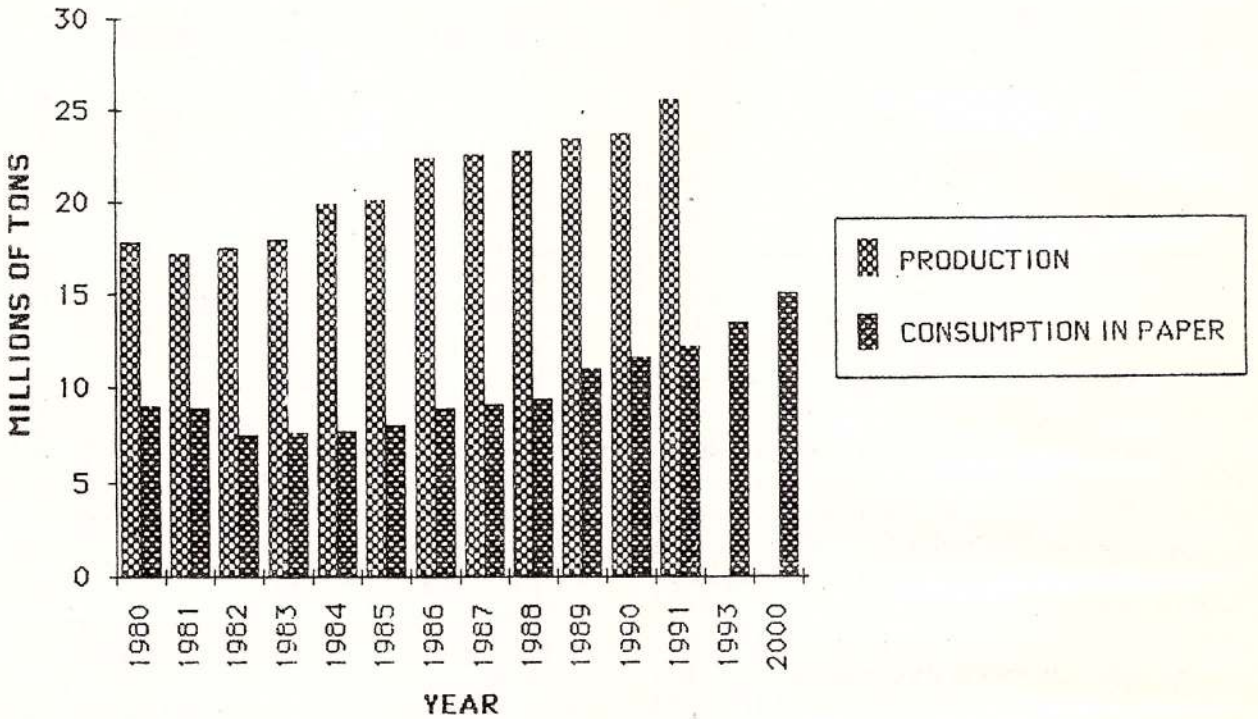

Fig. 4 – World kaolin production and kaolin consumption in paper (Seddon, 1991).

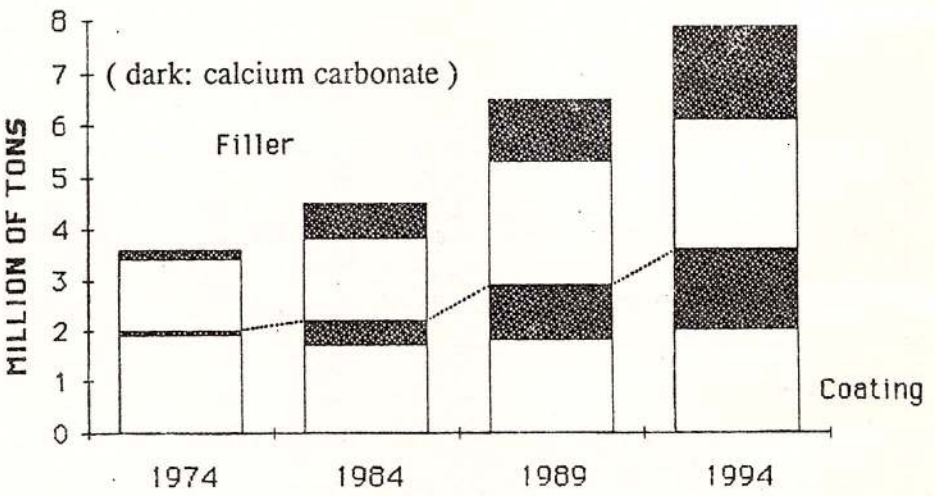

Fig. 5 – Mineral raw materials consumption in Europe, in the period 1974–1989, and consumption forecast up to 1994 (Clark, 1990).

5. Technological development of kaolin grades for paper coating

In what concerns kaolins for fillers and coatings an extraordinary evolution has taken place directed to the development of new commercial grades. From 3–4 kaolin grades that were available, differentiated in terms of brightness and grain size distribution, several very sophisticated grades have been produced in recent years using treatments each time more complex. Table 4 contains five of these treatments.

Table 4
Kaolin beneficiation treatments

Air flotation
Wet separation
Delamination
Calcination
Chemical treatment

The continuous changes taking place in kaolin processing require great investments and are the result of three main factors: 1) accomplishment of paper industries requirements; 2) added value of treated kaolins; 3) need of imports reduction considering the interest of national kaolin resources valuation.

Kaolin production is very competitive in technological terms. New producing processes and new equipments for kaolin treatment are being developed. Also, great competition is taking place in regard to kaolin prices, mainly in the sector of printing and writing papers.

Kaolin properties for applications as filler are not very requiring. Grain size, abrasivity, rheology and other requisites are shown in Table 5.

Table 5
Kaolin requisites for filler

Properties	Requisites
SiO_2	45-55%
Al_2O_3	37-40%
Fe_2O_3	<1%
Loss of ignition	>9%
pH	4,5-7
Brightness (%)	>75
>5 μm	<30%
< 5 μm	>70%
< 2 μm	>40%

For applications as coating kaolin requisites are much more demanding, namely in what concerns grain size distribution, brightness and rheology (Table 6).

In regard to technological developments of kaolin treatment six main trends can be defined (Table 7).

5.1. Delaminated kaolin

Delamination is achieved by the basal cleavage of thick kaolinite crystals (kaolinite books) yielding thinner crystals. New basal surfaces and individual particles are developed and changes in kaolin colour and rheology will take place.

Table 6
Kaolin requisites for coating

Properties	Conditioning
Brightness	Higher as possible(> 83%); high brightness can reduce opacity.
Opacity	Improves whenever crystallinity increases; better for grain size around 0,3μm; improves for high shear rate viscosity.
Abrasivity	Lower as possible;smoothness is quartz and halloysite dependant.
pH	5.5 - 6.
Grain size distribution	Residue on 200 mesh sieve: 0.005%; >5μm:<8%; <5μm: >90%; <2μm : > 70%; particle classification around 2μm; very fine particles (< 0.25 μm) are not convenient.
Retention	Stable suspensions with high solids contents.
Chemical composition	SiO_2: 45-55% ; Al_2O_3: 37-40%; Fe_2O_3: <0.3%; I.L.: >12%.
Rheology	Good rheological characteristics for high shear rates in suspensions with 70% solids. Depends on particle size and particle texture.

Table 7
Main trends in kaolin treatment and grades

Delaminated kaolin
Mate kaolin
High gloss kaolin
Calcined kaolin
Kaolin blending
Chemically structured kaolin

For papers with low weight coating (less than 7–10 g/m^2), the common pigments used impart poor printing capacity related to either the high fluidity of their suspensions or the low packing of their particles. As a consequence, paper surface exhibits numerous and important irregularities which turn difficult the contact between ink and printing paper (Fig. 6).

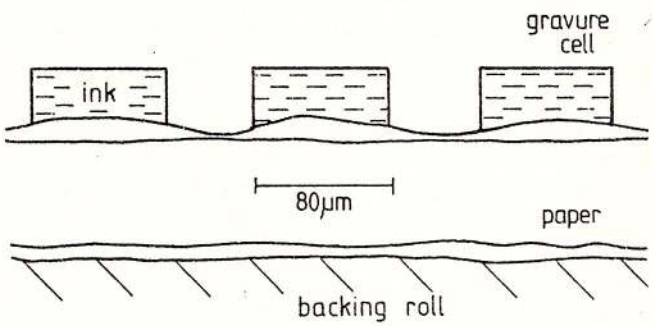

Fig. 6 – Influence of paper surface irregularity upon printing quality (Brociner, 1985).

Pigments characterized by good particle packing provide coatings too compact and yield deficient coatings less compressible during printing than those having not so good particle packing which yield suspensions with higher viscosity.

In order to get a flexible coating, pigments should have the following characteristics: lamellar particles, capacity of forming suspensions with low solids concentration and high specific volume. If such is so, suspensions can be retained at paper surface avoiding rupture through macropores.

5.2. Mate kaolin

Paper mate yields a very low gloss, less than 20%. Its production has increased very much in recent years. Kaolin mate consists of big size particles. No more than 50% are less than 2 μm.

5.3. High gloss kaolin

In the production of high gloss paper ultrafine kaolins, with more than 90% of particles less than 2 μm, have to be used. However, being particles so thin having shape ratio (diameter:thickness) 5:1 they cause some problems, namely water retention and dilatancy. High gloss kaolin production costs are quite high since it implies a very complex kaolin refining.

5.4. Blended kaolin

Many kaolin producers are developing special grades through kaolin blending in order to accomplish specific demands of paper mills. In some cases blending takes place in paper mills. Common kaolins, less expensive, can be mixed with others of higher grade giving place to kaolins with good coating properties.

Frequently some particular kaolin commercial grade is the result of kaolin blending. It is the case, for instance, of CADAM (Brazil) whose kaolin better known, AMAZON 88, corresponds to the blending of three kaolins from the total of eight kaolins occurring in the same deposit.

Blending is a very complex process, requiring previous studies in order to know what should be blended and the blending formulations.

5.5. Calcined kaolin

Calcined kaolin is produced through calcination up to about 1050^{0}C in special kilns of fine grained kaolins. Kaolin becomes fully dehydrated and strong interparticles bonds due to sintering will develop. Particle aggregates formed will favour light dispersion improving opacity.

In general terms, calcination can take place according to two different technologies. In one case, temperature increase is slow and gradual. It is the so called "soak calcination". In the other case, calcination is fast, named "flash calcination". Kaolin with 90% of particles less than 5 μm is heated up very rapidly up to 1050^{0}C. Afterwards is cooled rapidly, in a matter of milliseconds, down to room temperature. In any case the kaolin produced presents different properties.

Naturally, particle aggregates of calcined kaolin show porous structures and despite their vitreous character kaolinite particles mantain the typical lamellar and pseudohexagonal shape. In such conditions kaolin is still able to impart gloss, softness and coating. Figure 7 shows a sketch representing the structure of a kaolin particle aggregate. Light is diffused at the interfaces air - particle improving opacity and brightness.

Due to the pores developed calcined kaolin has lower bulk density. This fact improves its volumetric characteristics. Figure 8 shows that a calcined kaolin has a volume about 45% higher than a not calcined kaolin used for coating.

Table 8 contains the calcined kaolin main properties and requisites.

The great advantage of applying calcined kaolin in low weight (LW) paper is that simultaneously it improves paper optical properties and facilitates ink pen-

etration (see Fig. 9).

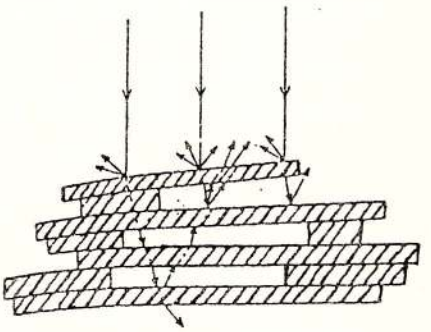

Fig. 7 – Schematic representation of a kaolin particle aggregate (Johns, 1986).

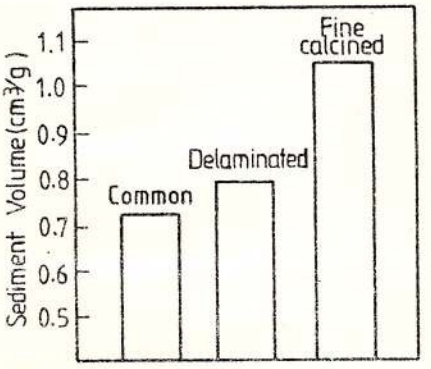

Fig. 8 – Comparison of sediment volume of a calcined and a not calcined kaolin grades (Johns, 1986).

Table 8
Main properties and requisites of a calcined kaolin

Properties	Requisites
Humidity content (%)	0,5
Ignition loss (%)	0
Brightness (%)	90-92,5
Valley abrasivity (mg)	20-40
Specific surface area (m^2/g)	16
Refractive index	1,62
Density	2,70
Light scattering coeffic.(cm^2/g)	220
Oil absorption (g/ 100g)	90
$<2\mu m$ (%)	86-90
+325 mesh residue(%)	0,015

Due to its higher coating capacity properties such as: gloss, opacity, ink receptivity and adhesive migration can be greatly improved. As a consequence of that, printing quality can improve for equivalent coating weight or less coating weight is needed to yield the same printing quality.

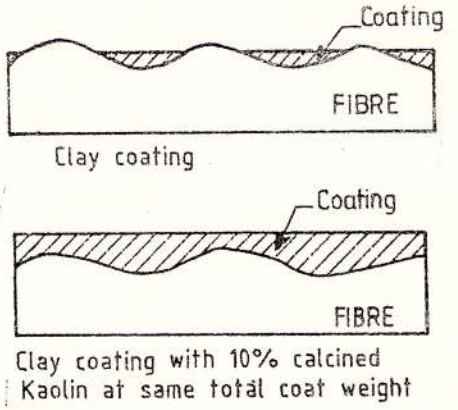

Fig. 9 – Function of calcined kaolin in paper coating (Clark, 1984).

5.6. Chemically structured kaolin

Chemically structured kaolin is a very recent product and is the result of chemical treatment. In comparison with calcined kaolin it is characterized by higher bulk density and more porous structure. For preparation of the chemically structured kaolin particle aggregation results from reaction with adequate flocculant chemicals, generally in hydrothermal conditions. Aggregation state variations are dependant on kaolin nature, reaction conditions and chemicals nature (silicate-metal and silicate-metal/ kaolin ratio).

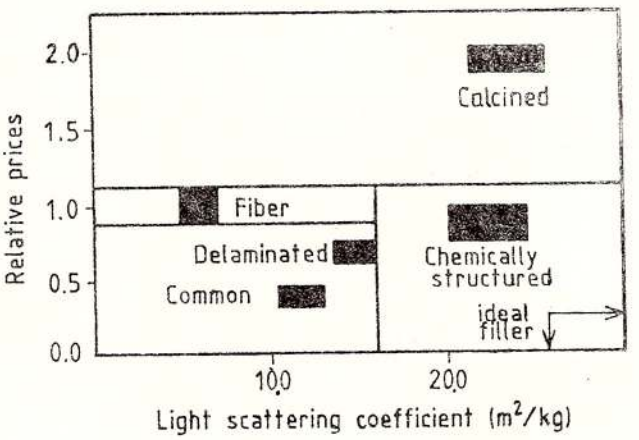

Fig. 10 – Relationship between light scattering coeficient and price for different kaolin commercial grades (Muller and Brink, 1992).

Filler and pigment producers do consider two basic materials properties: high brightness and high $<2\mu m$ particle percentage. Real technological development still pays attention to both properties, however

the actual trend is to conciliate them with a higher efficiency in terms of light dispersion, that is, higher opacity. Obviously, another trend tries to conciliate these characteristics with prices reduction. That is why chemically structured kaolin is taking advantage comparatively to calcined kaolin (Fig. 10).

One problem of chemically structured kaolins is their low brightness, comparable to the brightness of common kaolins. Nevertheless, for coating, they are very efficient. Due to their lower densities, to the same pigment weight corresponds higher volume. Therefore, when dry, final coating layer will be thicker. In consequence of that better fibers coverage, better smoothness and a more open and porous structure can be achieved facilitating ink penetration and improving printability.

Other inconvenience attributed to chemically structured kaolin is its rheology. A solids concentration of 63% should not be overcomed. However, as compared to calcined kaolin, chemically structured kaolin has a solids concentration limit of 50% due to its high dilatancy , making suspensions pumping very difficult.

6. Conclusions

Paper market requires mineral raw materials with the highest quality. This explains the new technologies both on paper processing and minerals beneficiation. New types of paper are entering in the market as a result of research on new kaolin grades and new mineral raw materials.

Despite calcium carbonate competition, particularly in some world regions, kaolin will continue as the dominating mineral raw material, in worldwide terms.

References

Abril, A., Suárez, R., Rodríguez, M. (1993) Empleo de zeolitas sintéticas como cargas en papeles de bajo gramaje. *Inv. y Téc. del Papel*, n^0 115, p. 9–19, Madrid.

Ahonen, P. (1985) Talc as a coating pigment in lightweight coated papers. *Tappi Journal*, November, p. 92–97, Atlanta.

Alvarez, E., Diez, L., Fernández, L., Cayuso, J. (1990) Estudio previo del empleo de dolomitas como pigmento de estucado. *Inv. y Téc. del Papel*, n^0 105, p. 490–498, Madrid.

Andersson, L., Freeman, G., Hardy, R., Schultz, G., Welch, L. (1990) Chemically structured paper coatings. *Proc. 23 rd ABTCP Pulp and Paper Annual Meeting*, p. 609–621, S. Paulo.

Beazley, K., Bailey, D. (1986) Coating pigments improve printability and gloss. *Paper Trade International*, April/May, p. 116–119, San Francisco.

Brociner, R. (1985) China clay for paper filling and coating. *Proc. Pulp and Paper Nordic Symposium*, 17 p., Uppsala.

Brown, J., Latshaw, C. (1990) Computer-assisted reformulation of coatings which utilize a unique "hollow sphere" polymeric pigment. *Proc. 23rd ABTCP Pulp and Paper Annual Meeting*, p. 587–607, S. Paulo.

— **, Lunde, D. (1987)** Developments in hollow sphere pigments for coating. *Tappi Journal*, September, p. 229–231, Atlanta.

Cahen, R., Daneault, C. (1990) Carbonato de cálcio como pigmento em tintas de revestimento de papel. *Proc. 23rd ABTCP Pulp and Paper Annual Meeting*, p. 567–585, S. Paulo.

Canadell, G. (1984) Estucado del Papel. Ed Universidad Politécnica de Barcelona. 87 p., Barcelona.

Clark, D. (1984) Improved printability from new coating pigments. *Proc. The World Pulp and Paper Week*, p. 323–327, Stockholm.

— **(1990)** Feast or famine? The outlook for printing paper - a market perspective. In "Mineral markets in the next decade". *Industrial Minerals*, p. 7–15, Park House, London.

Coope, B. (1984) Titanium minerals - focus on production. In "Raw Materials for the Pulp and Paper Industry". *Industrial Minerals*, p. 14–20, London.

— **, Dickison, T. (1984)** White carbonate fillers. In "Raw Materials for the Pulp and Paper Industry". *Industrial Minerals*, p. 43–48, London.

Fender, J. (1985) Couchage à haute concentration avec du carbonate de calcium naturel. *Revue ATIP*, 39, 2, p. 83–90, Grenoble.

Gavelin, G., Treiber, E. (1982) Mica in paper making. *Svensk Papperstidning*, 10, p. 31–32, Stockholm.

— **, Treiber, E. (1983)** Mica in magazine paper. *Svensk Papperstidning*, p. 8–16, Stockholm.

Gosset, D. (1990) The economic interest of titanium dioxide to get the opacity and the brightness of tomorrow papers. *Inv. y Téc. del Papel*, 105, p. 499–505, Madrid.

Harben, P. (1984) Introduction to paper. In "Raw Materials for the Pulp and Paper Industry", *Industrial Minerals*, p. 4–13, London.

Holm, C. (1983) Fillers as function chemicals, p. 245–247.

Huuskonen, H., Ahonen, I. (1984) Talc as a raw material in the paper industry. In "Raw Materials for the Pulp and Paper Industry", *Industrial Minerals*, p. 65–68, London.

Jané, J. (1981) El sulfato calcico como pigmento para estucado. *Proc. II Congresso Latinoamericano de Celulose e Papel*, p.203–207, Torremolinos.

— **(1984)** El sulfato calcico como carga para el papel. *Inv. y Téc. del Papel*, 79, p. 100–111, Madrid.

Johns, R. (1986) Fine calcined kaolin pigments are superior for many coating uses. *Pulp and Paper*, May, p. 56–60, San Francisco.

— **, Berube, R., Slepetys, R. (1990)** Chemically structured kaolin: a new coating pigment. *Tappi Journal*, February, p. 77–84, Atlanta.

Klasson, C., Munter, L. (1990) Gypsum as a coating pigment - experiences and possibilities. *Proc. 24th EUCEPA Conference*, May, p. 371–378, Stockholm.

Loughbrough, R. (1992) TiO_2 pigment: overcapacity hits again. *Industrial Minerals*, June, p. 37–53, London.

Mather, R. (1986) Recent developments in coating and filler pigments. *T.A.P.P.S.A.*, 12 p.

Muller, K., Brink, H. (1992) A unique kaolin additive for improving the quality of groundwood papers. *Pulp and Paper Canada*, 93, 10, p. 21–24, Montreal.

Novak, G., Malesic, I., Kumar, M. (1991) Posibilidades y limitaciones de un nuevo pigmento, una mezcla de talco y dolomita para el estucado del papel. *Inv. y Téc. del Papel*, 110, p. 702–714, Madrid.

Schober, W. (1991) Talc use in coating formulas gains popularity in European paper mills. *Pulp and Paper* May, p. 117–119, San Francisco.

Seddon, M. (1991) Kaolin consumption increase could mean tight supply in early 1990s. *Pulp and Paper*, May, p. 88–90, San Francisco.

Svensson, G. (1989) Calcium sulphate as coating pigment. *Proc. The World Pulp and Paper Week*, April, p. 319–322, Stockholm.

Turner, R. (1988) Calcined clay can improve the properties of uncoated groundwood papers. *Pulp and Paper Canada*, 89, p. 17–23, Montreal.

Velho, J., Gomes, C. (1989) Matérias primas minerais alternativas do caulino para carga e cobertura do papel. *Geociências*, 4, 2, p. 181–202, Aveiro.

Wuerl, P. (1986) Alkaline papermaking dominates papermaking and coating chemicals scene. *Paper Trade Journal*, July, p. 41–43. New York.

Received: December 1993
Accepted: February 1994

Rom. J. Mineralogy, 1995, 77, p. 35–44, Bucureşti

CLAY MINERALS IN MESOZOIC AND PALEOGENE SEDIMENTARY ROCKS OF HUNGARY

István VICZIÁN

Hungarian Geological Survey. Stefánia út 14, H-1143 Budapest

Key words: Hungary Mecsek Mts. Transdanubian Central Mts. Tertiary Basins. Sedimentary Clay Minerals. Illite. Kaolinite. Smectite (Contents). Illite-Chlorite.

Abstract: The clay mineral associations determined by X-ray methods in Hungarian sedimentary rocks are reviewed. The following types of associations are discussed: 1. Evaporitic facies of the Triassic. Special Mg-rich clay minerals such as corrensite are products of neoformation in a restricted basin environment (Mecsek Mts). 2. Upper Triassic to Lower Cretaceous carbonate rocks. The variation of the kaolinite content is in relation to the paleogeographic situation in the Tethys Basin during the deposition. The main clay mineral is illite (Transdanubian Central Mts, Mecsek Mts). 3. Enrichment of kaolinite in Upper Cretaceous and Paleogene continental sediments ("siderolitic" facies, fire clays in the Transdanubian Central Mts). 4. Tuffaceous and volcanoclastic deposits. Typical minerals are varieties of smectite due to the devitrification of acid to intermediate pyroclastics. 5. Sediments of the Tertiary basins. The detrital clay mineral assemblage is due to high rate of denudation, redeposition and sediment accumulation. In thick sedimentary sequences smectites transform into illite/smectites. In each territory sequences without and with diagenetic transformation are separately discussed.

1. Introduction

Clay mineralogy of Hungarian sedimentary rocks was previously reviewed by Viczián (1976). Valuable data on clay minerals of Hungarian sedimentary formations are found in the books of Nemecz (1981) and Bárdossy (1982). A review on the Neogene clays will be published (Tanács, Viczián, 1994). A short summary was presented at the Timişoara Meeting (Viczián, 1993 c).

The present review is based on the evaluation of approximately 5.000 X-ray patterns taken from Hungarian sedimentary rocks, mainly clays, shales, marls and carbonate rocks in the period 1962 to 1993, as well as on the data published in the literature. These data were discussed in detail in a D.Sc. Thesis by Viczián (1987) where all relevant references are found. In the present review only few more recent publications are cited.

The data are summarized in a stratigraphic sequence. The main tectonic units of Hungary are shown in Figure 1. Typical clay mineral assemblages of stratigraphic formations arranged according to tectonic units are shown in Figures 2 to 6. In each of these figures the stratigraphic schemes of Kázmér (1986) are taken as basis and typical clay mineral associations are shown by letters. For example, the association illite + kaolinite is denoted as IK. Data referring to the <2 μm fraction are given in brackets, e.g. (SI) means smectite + illite in the <2 μm fraction.

Occurrences found in present-day mountainous areas and near the present-day surface are characterized on the right side of the stratigraphic column. On the left side the same formations are shown that lie deep in the basement of the Neogene basins. The difference between the clay content of the near-surface and deep-seated occurrences may be attributed to the diagenesis due to subsidence in Neogene times. On both sides of the stratigraphic column the degree of diagenetic transformation is shown. Rocks affected by diagenesis are most common on the left sides of the diagrams then on the right sides. Rocks are here considered to be affected by diagenesis when expanding, smectite-like phases disappeared and kaolinites are recrystallized.

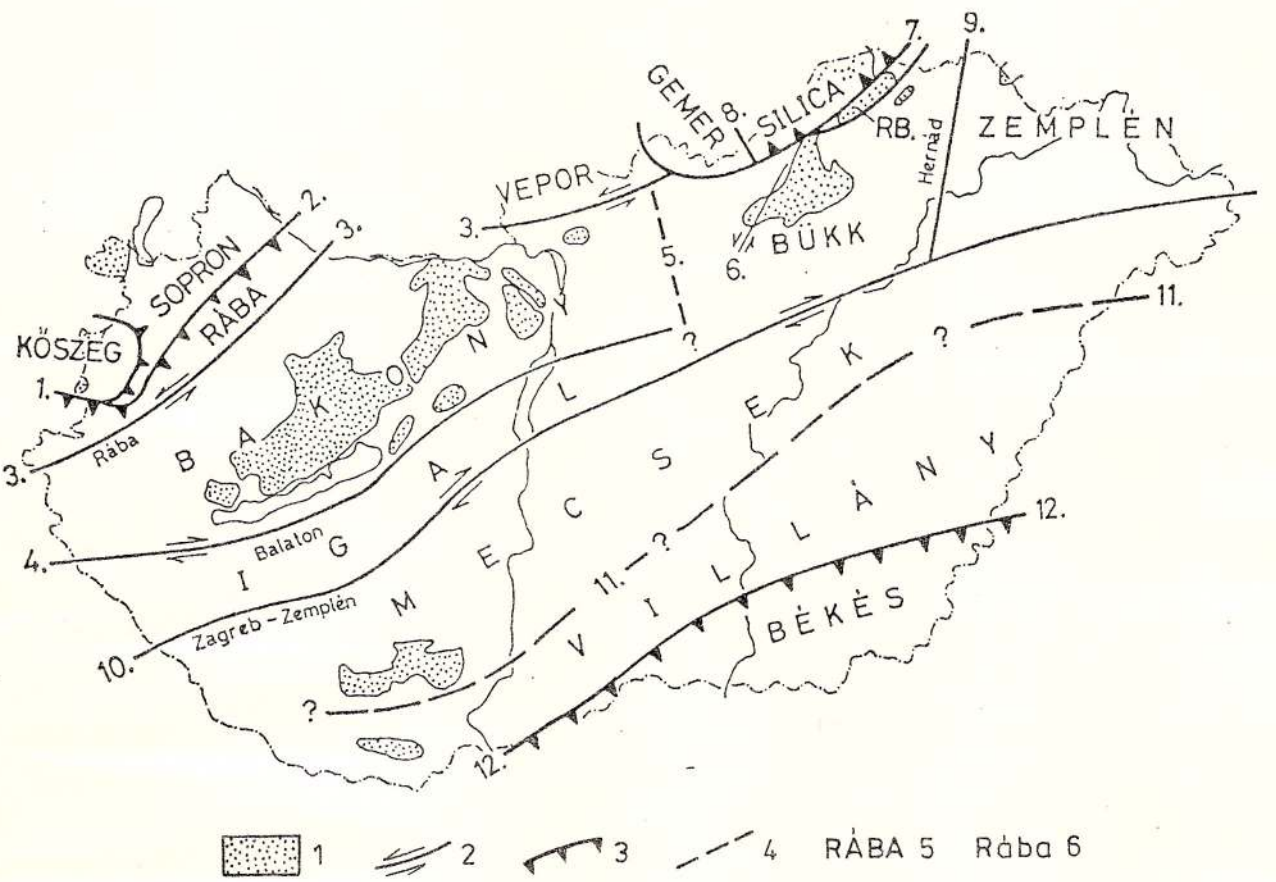

Fig. 1 - Tectonic units of Hungary (after Császár and Haas, 1984, modified by Kázmér, 1986). 1, Pre-Neogene on surface; 2, Strike-slip fault; 3, Nappe; 4, Uncertain boundary; 5, Rába Units; 6, Rába faults.

2. Results

2.1. Upper Permian-Triassic

In the Bakony and in the Mecsek-Villány units alike the Upper Permian-Lower Triassic sandstone complex is characterized by the assemblage of illite + kaolinite (Figs. 2,3,4). Both in the Mecsek Mts and in the basement of the Great Plain, illite-1M of diagenetic origin is present in the pore space of sandstones.

Both in the Bakony and in the Mecsek-Villány tectonic units the Lower and Middle Triassic carbonate rocks deposited in evaporitic, coastal and reef environments are characterized by the predominance of illite which is partly of detrital (2M) and partly of aggradational (1Md) origin. Mixed-layer chlorite/smectite pointing to a restricted basin environment can be also found in the Anisian of the Mecsek Mts (irregular layer sequence and corrensite with regular sequence, see Viczián, 1992 a, b, 1993 a). Ladinian tuffs and overlying limestones contain smectite and illite- 1M with few expandable layers.

In the Bakony unit the Carnian basinal formations are made of marls containing large amounts of terrigenous material. The clay mineral assemblage is polymineralic with the predominance of smectite and illite.

Kaolinite and partly illite are found in the Upper Triassic carbonate platform deposits in the Bakony unit and in the Upper Triassic detrital, terrestrial, lacustrine or lagoonal formations in the Mecsek and Villány units. Berthierine is a typical component of the Keuper sandstone in the Mecsek Mts.

The degree of diagenesis of the Mecsek-Villány-type Lower to Middle Triassic formations encountered in the basement of the SE Great Plain does not differ from that of the similar formations found in the present-day

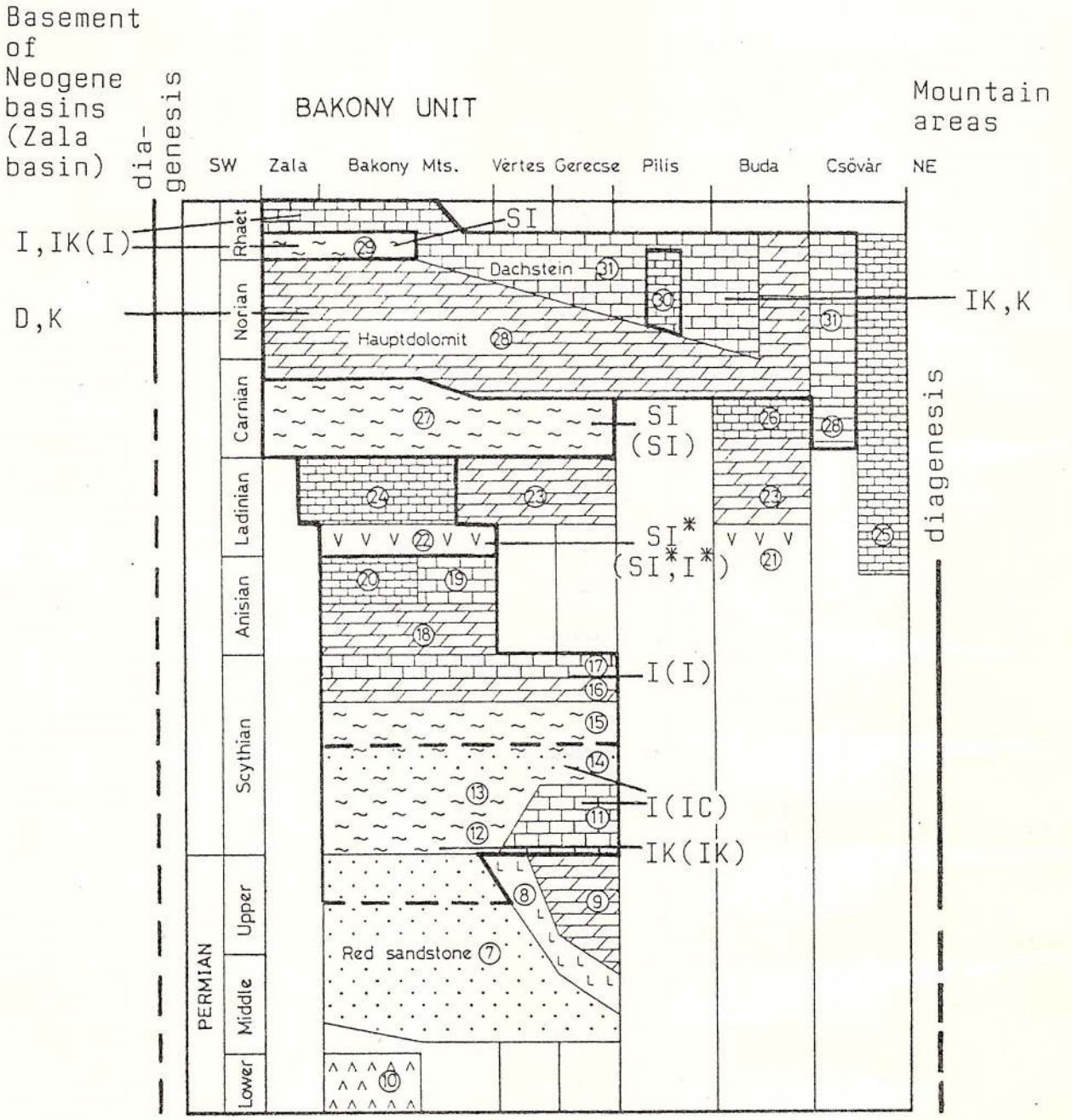

Fig. 2 – Clay minerals in the Upper Permian and Triassic formations of the Bakony unit. Numbers in the stratigraphic column refer to descriptions of the formations in the paper of Kázmér, 1986. The formations contoured by heavy line are considered to contain the clay mineral association indicated on the right and left side of the stratigraphic column (mountain areas and basement of Neogene basins, respectively). Abbreviations of clay minerals: S: smectite and smectite–like illite/smectites, I: illite and illite–like illite/smectites, I*: illite–1M with 5 – 20 % expandable layers, K: kaoline, C, chlorite, D: dickite, B: berthierine, N: nontronite, N/C: nontronite/chlorite, C/S: chlorite/smectite, Corr: corrensite, Su: sudoite, Tosud: tosudite, G: glauconite, Cel: celadonite, Fe–S: iron-rich smectite. Abbreviations of clay minerals in brackets, ( ), refer to clay minerals in the <2 μm fraction.

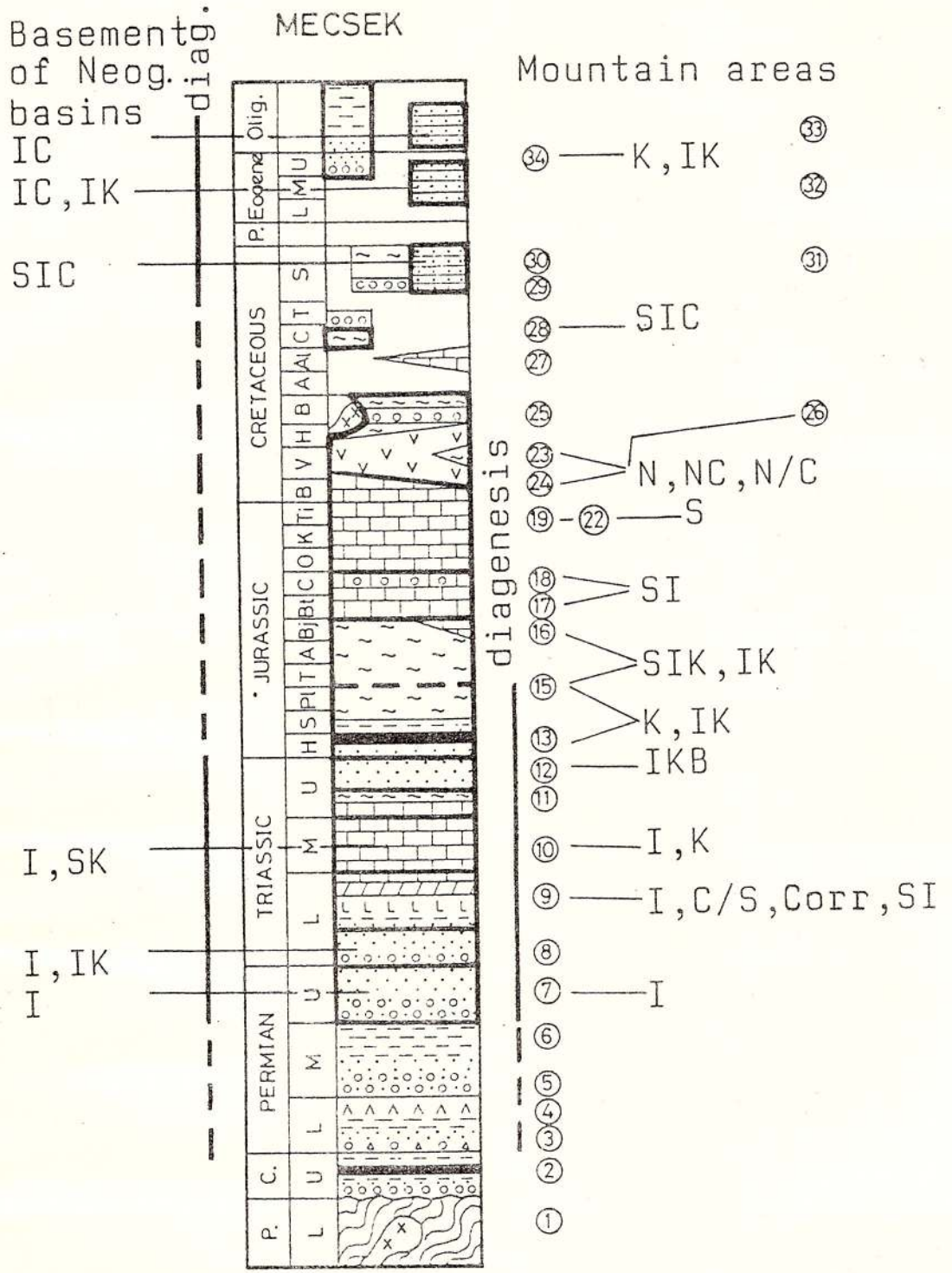

Fig. 3 – Clay minerals in Upper Permian, Mesozoic and Paleogene formations of the Mecsek unit. See for explanations and abbreviations Fig. 2

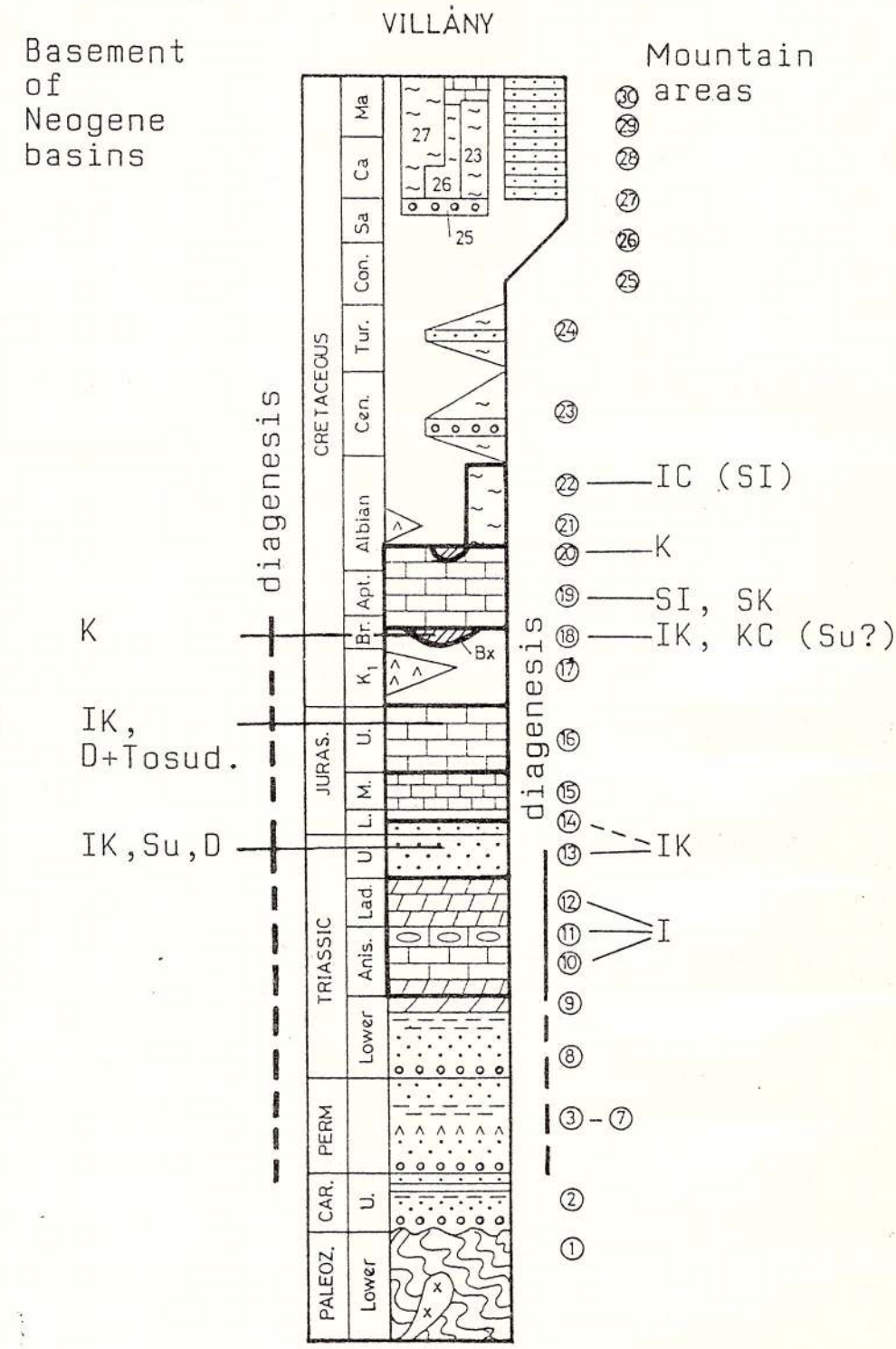

Fig. 4 – Clay minerals in Mesozoic formations of the Villány unit. See for explanations and abbreviations Fig. 2

mountainous areas since both of them are likely to have been developed still during the Mesozoic sedimentary cycle (Figs. 3,4). In the Upper Triassic-Lower Jurassic red terrestrial deposits a mineral association containing dickite, dioctahedral Al- chlorite and their mixed structures shows diagenetic recrystallization presumably due to subsidence of the basement in the Neogene (Fig.4).

In the Upper Triassic, there is a higher degree of diagenesis in the basement of the Zala Basin than in the Bakony Mts (Fig.2). Here and S of Lake Balaton, well- crystallized kaolinite and dickite were formed due to deep diagenetic and hydrothermal effects, active in Triassic carbonate rocks along main structural lines.

2.2. Jurassic

In the Jurassic sequence of the Transdanubian Central Range (Fig.5) and the Mecsek Mts (Fig.3), stratigraphically upwards, kaolinite is replaced by illite (in the Liassic) and by smectite (from the middle of the Dogger), as attested by the insoluble residue of marls and limestones (Viczián, 1994). Kaolinite is more frequent in the Mecsek Mts than in the Bakony unit, the sedimentary environment of which was more distant from the ancient shores. Liassic manganese ores in the Bakony Mts are accompanied by clays of exceptionally high smectite content and containing iron-rich phases such as Fe-smectite and celadonite (Kaeding et al., 1983).

There is no diagenetic transformation in the Jurassic of the Bakony Mts. In the basement of the Zala Basin isochronous formations which had subsided to a greater depth were more strongly affected by diagenesis (see Fig.5). In the insoluble residue of these carbonate rocks the clay mineral assemblage is uniformly reduced to illite. The composition of the mixed-layer illite/smectite and the degree of crystallinity of illite correlate with the depth of burial.

2.3. Cretaceous

In the Transdanubian Central Range the smectite-rich assemblage characterizing the upper part of the Jurassic continues with no change, as far as the Aptian limestone, in the Lower Cretaceous carbonate formations (Fig. 5). Smectite is likely to be a neoformation associated with a more distant basic submarine volcanism. The detrital reworking of basic volcanic material is also suggested by the mineralogical and geochemical composition of the Albian siltstones of Tata in which a rather rare chlorite + smectite clay mineral association has been found (Földvári et al., 1973).

Both in the limnic part and the underlying formations of the Senonian coal complex of Ajka the associations rich in smectite and kaolinite are prevailing (Fig. 5). Mixed- layer kaolinite/smectite represents transition from smectite to kaolinite. In the coal measures complex, in minor intervals an illite + chlorite association identical with that of the overlying terrestrial-detrital formation is encountered. In the overlying Upper Cretaceous marine beds a smectite + illite association prevails (Góczán et al., 1986).

Remains of a smectite-rich weathering crust and of a kaolinite-rich one pointing to warm and humid climate can be distinguished in the Middle and Late Cretaceous terrestrial and nearshore formations (Fig. 5). Bauxite is related to the kaolinite-rich weathering crust. It is still uncertain to which extent the smectite-bearing weathering crust has been formed from volcanic tuffs.

In the Mecsek Mts, volcanic glass produced by early Cretaceous volcanic activity was halmyrolitically altered (Fig. 3). The product is a smectite of nontronite-saponite composition which forms either mixed structure or a mixture with chlorite. The exchangeable cation of smectite is in part Na^+, and the peperite breccia is frequently cemented by analcime-bearing matrix (Viczián, 1966).

The Middle and Upper Cretaceous marls of Vékény, Mecsek Mts, and of Villány Mts, contain terrigenous, detrital, polymineralic clay minerals and exhibit only slight diagenetic transformation (Figs. 3,4).

Upper Cretaceous carbonate rocks sampled from the basement of the Zala Basin contain less smectite than the corresponding stratigraphic horizons in the Bakony Mts (Fig. 5).

In the basement of the SE Great Plain (borehole Doboz I. see Viczián, 1992 a) illite + kaolinite association was found in the insoluble residue of a limestone corresponding to the Malm-Lower Cretaceous limestone in the Villány Mts (Fig. 4). In materials collected from fault surface and tectonic breccia tosudite and dickite have been identified. The latter was developed due to the diagenetic recrystallization of the deposit originating from a kaolin-bearing weathering crust. This occurrence represents a link between the underlying formations of the Villány and the Pădurea Craiului (Királyerdö) bauxites, in the basement of the Great Hungarian Plain.

2.4. Paleogene

Clay minerals in the shallow Tertiary basins have only slightly been modified by diagenesis. Three major associations can be distinguished: 1. kaolinite-rich, 2. illite + chlorite-rich and 3. smectite-rich associations.

2.4.1. Kaolinite-rich associations. The main component of Paleogene terrestrial clays is disordered kaolinite frequently accompanied by halloysite, sometimes by few gibbsite and few inherited illite. Such a mineral composition was identified in the following profiles:

–in the Bakony unit, at the bottom of the Eocene coal and Oligocene sandstone formations (Fig. 6),

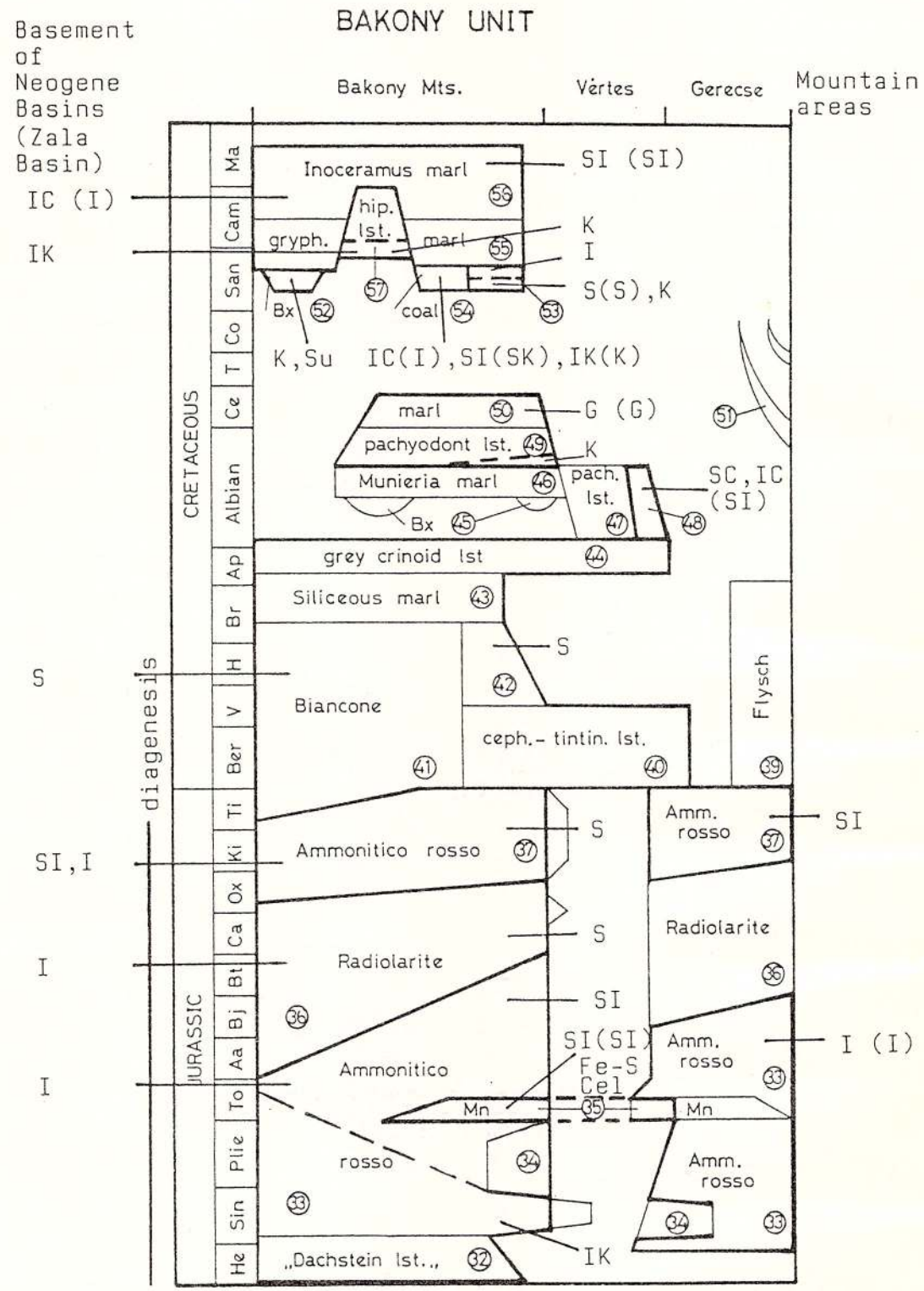

Fig. 5 – Clay minerals in Jurassic and Cretaceous formations of the Bakony unit. See for explanations and abbreviations Fig. 2

– the early Miocene (?) Cserszegtomaj fireclay deposited on karstic surface developed on carbonate rocks (Bárdossy, 1961),

– in N Hungary, at the bottom of the Oligocene sandstone formation and in the intercalated clay beds (Felsöpetény refractory clay deposit),

– on the surface of weathered crystalline basement rocks of the Vepor Massif cut in the base of Oligocene in the borehole Balassagyarmat 5 and

– in the Paleogene and Lower Miocene terrestrial deposits of the Mecsek Mts (Fig. 3).

Of the detrital, fluvial, littoral, shallow-water - shallow-lacustrine coarse-grained formations, kaolinite is the main clay mineral in the Middle Eocene, Lower and Middle Oligocene sandstone formations except perhaps some basal layers of the Csatka Sandstone Formation (Fig. 6).

rite are well- crystallized, and illite is of 2 M polytype. In the clay fraction mixed-layer illite/smectite is enriched, and the smectite proportion ranges from 80 to 100 per cent. In untreated state d(001/001) varies between 12 and 15 Å. Formations of this kind are:

- the non-tuffaceous part of the Eocene siltstones (Mór Fm.),
- the Lower Oligocene clays (Tard, Kiscell Fm.) and
- the Upper Oligocene Eger Formation (Fig. 6).

2.4.3. Smectite-rich associations. Smectite is the most frequent product of hydrothermal and halmyrolitic alteration of acid pyroclastics. Kaolinite and illite are much less frequent. The smectite (+ illite + kaolinite) clay mineral association predominates also in the volcanogenic sediment transported into the sedimentary basin by pyroclastic fallout and by erosional transport of volcanic rocks. The proportion of smectite-rich volcanogenic sediments is high in the Upper Eocene Halimba Tuff Formation. In deep buried position corrensite may develop from these volcanogenic sediments (borehole Zebecke 2, Zala Basin,

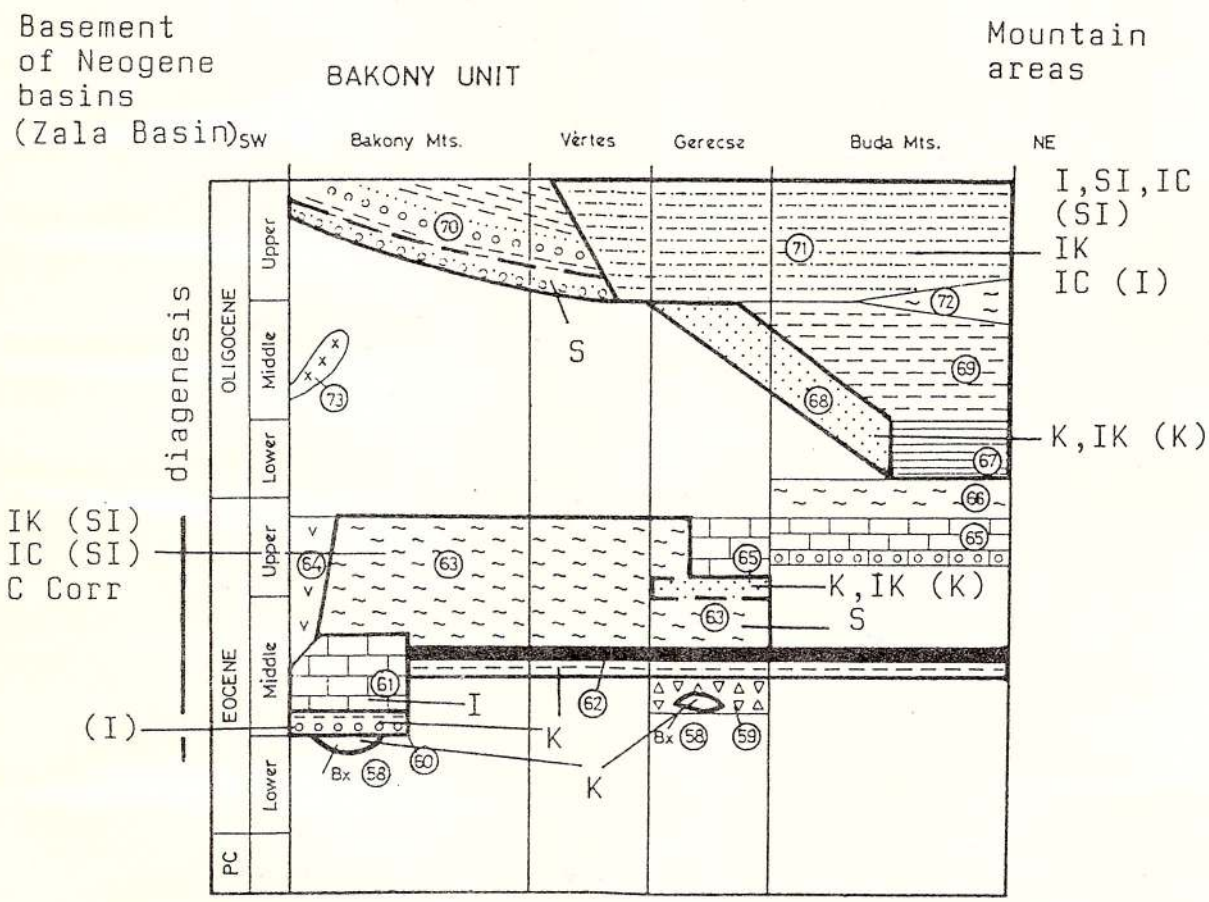

Fig. 6 – Clay minerals in Paleogene formations of the Bakony unit. See for explanations and abbreviations Fig. 2

2.4.2. Illite + chlorite-rich associations. In fine-grained, detrital formations found well inside the Paleogene basins an averaged, uniform, polymineralic clay mineral association prevails, in which illite and chlo-

see Fig. 6). Volcanogenic intercalations in the North Hungarian Oligocene are not yet really investigated.

The transformation of smectite into illite in deeply buried sediments of the Neogene of the Pannonian Basin is well known and well documented (Tanács, Viczián, 1994). The same process continues also in the underlying Paleogene series in the central zones of the North Hungarian Paleogene Basin (e.g. Zagyva Graben, Viczián, 1993 b).

3. Conclusions

The clay mineral associations that occur in the Mesozoic and Paleogene formations of Hungary can be grouped into several genetic types that have their counterparts in other classical areas of the European clay research:

3.1. **Evaporitic facies of the Triassic** of Germany, France and Spain. Special Mg-rich clay minerals such as corrensite are products of neoformation in a restricted basin environment. Such deposits are known in the Anisian of the Mecsek Mts.

3.2. Upper Triassic to Lower Cretaceous carbonate rocks of the Alps and adjacent platform areas. One important feature is the variation of kaolinite content in relation to paleogeographic situation in the Tethys basin during deposition. Occurrences of this type can be found in the unmetamorphosed Mesozoic of the Transdanubian Central Mts and Mecsek areas.

3.3. Enrichment of kaolinite in Upper Cretaceous and Paleogene continental and shallow marine sediments and siderolite facies of France. Abundance of kaolinite is due to climatic and environmental conditions during this period. Most examples can be found in near-shore and continental deposits of the Transdanubian Central Mts.

3.4. Tuffaceous and volcanoclastic deposits. Typical minerals are varieties of smectite formed by devitrification of acid to intermediate pyroclastics in the Upper Eocene. Submarine alteration of Lower Cretaceous basalts in the Mecsek Mts resulted in the formation of iron- and magnesium- rich varieties.

3.5. Sediments of Tertiary basins such as Rhine Graben, Molasse and Vienna Basins, southern Poland, Transylvanian and Pannonian Basins. The pellitic sediments of the North Hungarian Paleogene Basin fit into this type. A detrital clay mineral assemblage is typical here due to high rate of denudation, redeposition and sediments accumulation. High geothermal gradients and thick sedimentary sequences result in typical diagenetic transformation of smectite into mixed-layer illite/smectites and illite.

References

Bárdossy, Gy. (1961) Contribution to the knowledge of the kaolinitic refractory clay deposits of Cserszegtomaj. *Ann. Inst. Geol. Publ. Hung.*, 49, 4, p. 1029-1052, Budapest.

— **(1982)** Karst bauxites. Bauxite deposits on carbonate rocks. (Developments in Economic Geology 14), Elsevier, Amsterdam etc. and Akadémiai Kiadó, Budapest.

Földvári, M., Lelkes, Gy., Vető, I., Viczián, I. (1973) Joint application of petrographical, mineralogical and geochemical methods to the study of Lower Cretaceous borehole samples from Tatabánya (in Hungarian). *Földt. Közl.*, 103. 3-4, p. 364-371, Budapest.

Góczán, F., Siegl-Farkas, Á., Móra-Czabalay, L., Rimanóczy, Á., Viczián, I., Rákosi, L., Csalagovits, I., Parténvi, Z. (1986) Ajka Coal Formation: biostratigraphy and geohistory. *Acta Geol. Hung.*, 29, 3-4, p. 221-231, Budapest.

Kaeding, L., Brockamp, O., Harder, H. (1983) Submarin-hydrothermale Entstehung der sedimentären Mangan-Lagerstätte Úrkút/Ungarn. *Chem. Geol.*, 40, 3-4, p. 251-268, Amsterdam.

Kázmér, M. (1986) Tectonic units of Hungary: their boundaries and stratigraphy (a bibliographic guide). *Ann. Univ. Sci. Budapest. R. Eötvös Nom., Sect. Geol.*, 26, p. 45-120, Budapest.

Nemecz, E. (1981) Clay minerals. Akadémiai Kiadó, Budapest.

Tanács, J., Viczián, I. (1994) Smectite proportions in mixed- layer illite/smectites and types of clay sedimentation in Neogene of the Pannonian Basin, Hungary. *Geol. Carpathica, Ser. Clays* (in prep.), Bratislava.

Viczián, I. (1966) Submarine Ausbruch- und Gesteinszersetzungserscheinungen im unterkretazischen Diabaskomplex der Bohrung Kisbattyán Nr. 1 (in Hungarian with German and Russian abstracts). *Annual Rept. of Hung. Geol. Inst. on 1964*, p. 75-92, Budapest.

— **(1976)** A review of the clay mineralogy of Hungarian sedimentary rocks (with special regard to the distribution of diagenetic zones). *Acta Geol. Hung.*, 19 (1975), 3-4, p. 243-256, Budapest.

— **(1987)** Clay minerals in sedimentary rocks of Hungary. D. Sc. Thesis (in Hungarian), 205+139 p., Budapest.

— **(1992 a)** Clay minerals of a thick sedimentary sequence in SE part of the Pannonian Basin (Hungary). *Geol. Carpathica, Ser. Clays, 1*, p. 27-30, Bratislava.

— **(1992 b)** Diagenetic neoformations in Middle Triassic evaporitic and carbonate rocks, Mecsek Mts (S Hungary) (abstract). *Beih. z. Eur. J. Min.*, 4, 1, 286 p., Stuttgart (DMG-Tagung, Tübingen, 1992).

— **(1992 c)** Diagenetic neoformations in Middle Triassic evaporitic and carbonate rocks, Mecsek Mts (S Hungary). *Acta Min. Petr.*, 33, p. 13-24, Szeged.

— **(1993 a)** Clay mineralogy of Middle Triassic evaporitic and carbonate rocks, Mecsek Mts (southern Hungary). 11th Conf. Clay Min. Petr., Č.Budějovice, 1990 (ed. by J. Konta), p. 135-144, Univerzita Karlova, Praha.

— **(1993 b)** Mineralogy and diagenesis in the North Hungarian Paleogene Basin (abstract). 8th Meeting of the Ass. European Geol. Soc., Budapest, 1993. Abstracts of Papers 53, Hungarian Geological Society, Budapest.

— **(1993 c)** Typical clay mineral associations in Hungarian sedimentary rocks (abstract). Second Symp. on Min., Timişoara, 1993. Abstracts Volume, *Romanian J. Min.*, 76, Suppl. 1, 52, Bucureşti.

— **(1994)** Clay mineralogy of Jurassic carbonate rocks, Central Transdanubia, Hungary. Ann. Rept. of Hung. Geol. Inst. on 1992 (in prep.), Budapest.

Received: June 1994
Accepted: September 1994

Rom. J. Mineralogy, 1995, 77, p. 45–50, Bucureşti

CONSIDÉRATIONS GÉOCHIMIQUES SUR LA MUSCOVITE DES PEGMATITES À ALBITE ET SPODUMÈNE DE CONŢU (MONTS CIBIN)

Titus MURARIU

Universitatea "Al.I.Cuza", Departamentul de Mineralogie–Geochimie.

Bulevardul Copou, 6600 Iaşi

Key words: Lithian Pegmatites. Muscovite. Chemical and Normative Composition. South Carpathians-Cibin Mts.

Abstract: *Geochemical Considerations on the Muscovite from the Albite–Spodumene Pegmatite at Conţu (Cibin Mts).* In the lithian pegmatites in the Conţu area, Cibin Mountains, muscovite occurs as large crystals and fine lamellae, forming two characteristic mineralogical assemblages: quartz-muscovite and albite-spodumene. The chemical analyses of muscovite show constant and high contents of SiO_2 and Al_2O_3 and low values of MnO and CaO. The prevalence of Fe^{2+} over Fe^{3+} and of K over Na is also obvious. The content in titanium is characteristic of muscovite in metamorphic pegmatites. Muscovite associated with spodumene has the lowest Mg content. In the analyzed muscovites the correlations between Na and K and Fe and Ti are positive. The normative composition and the degree of substitution of Si^{4+} for Al^{3+} in tetrahedral sites differentiate muscovites from pegmatites over those from paragneisses. Crystallochemical formulae suggest that Al is both four-fold and six-fold coordinated and also a wide participation of the alkaline elements in the X sites.

1. Contexte géologique. Les formations cristallines du champ pegmatitique de Conţu–Monts Cibin, où sont localisées les occurrences des pegmatites à albite et spodumène, se rattachent à la série de Sebeş–Lotru de la nappe gétique. Elles ont subi un métamorphisme au faciès des amphibolites à almandin, la zone à staurotide et la zone à disthène (Savu, 1970). Ces roches ont été encadrées en trois complexes: les complexes inférieurs (le complexe des paragneiss et le complexe des amphibolites et des gneiss quartzo-feldspathiques) et le complexe supérieur (des micaschistes). Les roches du complexe des paragneiss représentent les formations les plus anciennes du champ pegmatitique de Conţu. Les pegmatites à albite et spodumène connues forment des filons et des corps lenticulaires qui sont disposés d'une manière concordante dans le complexe des paragneiss. Rarement, on rencontre aussi des corps pegmatitiques situés dans les roches du complexe des micaschistes.

La structure zonale des certains corps pegmatitiques correspond au type symétrique (Maieru et al., 1968), en comportant trois zones (marginale, intermédiaire, centrale) nettement contourées; d'autres zones appartiennent au type structural avec zonation partielle.

2. Données minéralogiques. Dans la composition minéralogique des pegmatites à albite et spodumène de Conţu on rencontre du quartz, des feldspaths, de la spodumène, de la muscovite, de la biotite, de la tourmaline, des grenats, de l'apatite, de l'ambligonite, de la montébrasite, de la triphylline-lithiophyllite, de la purpurite, de la cassitérite, de la tavorite, de l'huréaulite, de la manganocolumbite, de la sphalérite(?), de la topaze (Pomârleanu et al., 1967; Maieru et al., 1968; Movileanu, Pomârleanu, 1972; Hann, 1987; Săbău et al., 1987; Murariu, 1992). La composition minéralogique quantitative est: 25–30 % quartz; 30–43 % albite; 15–20 % spodumène; 0–5 % feldspaths potassiques; 3–10 % muscovite; 0–1 % biotite. D'après la composition minéralogique, les occurrences pegmatitiques appartiennent au type albite-spoduménique (Solodov et al., 1980). Dans les pegmatites à albite et spodumène de Conţu, la muscovite est présente soit sous forme des cristaux largement développés, soit en lames fines, incolores (dans le complexe quartzo-muscovitique) et à teintes verdâtres (dans le complexe albite-spoduménique).

3. Données géochimiques. Dans les muscovites des pegmatites à albite et spodumène de Conţu on a déterminé des teneurs constantes en silice (45,33–46,63 % SiO_2), ainsi que des valeurs élevées pour la teneur en aluminium (36,39–36,86 % Al_2O_3). La présence dans les muscovites analysées des éléments tels que Fe et Mg est soit le résultat de la présence des traces de la muscovitisation de la biotite, soit le résultat de la substitution diffusive de l'Al des positions octaédriques (Al_{VI}). Les analyses chimiques (Tab. 1) on mis en évidence des teneurs réduites en Mn (0,06 % MnO), Ca (0,01–0,03 % CaO) et la prédominance du Fe^{2+} sur le Fe^{3+}. La teneur en Na est généralement constante (0,60–0,66 % Na_2O) et s'accorde bien avec les données expérimentales (Eugster, Yoder, 1955), d'après lesquelles la limite maximale de la solubilité de la paragonite dans la muscovite est d'environ 24 mol. %, ce qui correspond à un pourcentage de 2 % Na_2O). La teneur en Ti(0,15–0,19 % TiO_2) est caractéristique pour la muscovite des pegmatites métamorphiques. La moindre valeur de la teneur en magnésium a été enregistrée pour la muscovite du complexe albite-spodumènique: 0,05 % MgO. La valeur obtenue se trouve entre les limites présentées récemment par Zakorski et Kuznetsova (1990) pour la muscovite des pegmatites à albite et spodumène du champ "Glavnii" de Sibérie (0,01–0,07 % MgO).

Dans les muscovites étudiées les corrélations Na_2O: K_2O et TiO_2: ($FeO+Fe_2O_3$) ont un caractère positif (Fig. 1).

Le degré de la substitution du Si^{4+} par Al^{3+} en position tétraédrique (a_{si}) est plus élevé dans la muscovite des pegmatites (Tab. 1).

L'examen des formules cristallochimiques permet de constater la double position de l'Al(Al_{IV}; Al_{VI}) (Fig. 2), ainsi que d'observer la participation plus large des éléments alcalins dans la position "X" (Tab. 1).

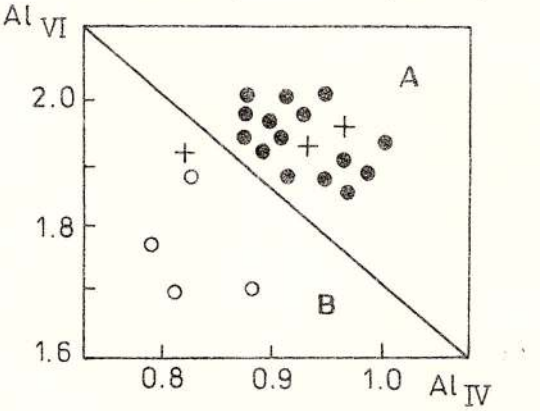

Fig. 2 – La corrélation Al_{IV}:Al_{VI} dans les muscovites des pegmatites de la Province Carpatique (A) et des métamorphites encaissantes (B); (+) les muscovites des pegmatites et des paragneiss de Conţu.

La composition normative de la muscovite des pegmatites lithinifères de Conţu montre des teneurs réduites en ferrimuscovite, ferromuscovite et phengite. Des résultats similaires ont été obtenus pour la muscovite d'autres champs pegmatitiques de la Province Carpatique (Tab. 2).

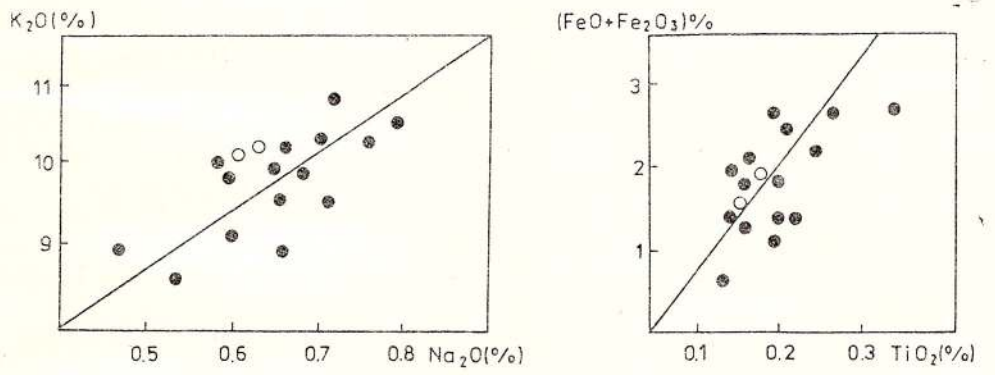

Fig. 1 – Les corrélations K_2O:Na_2O et TiO_2:($FeO+Fe_2O_3$) dans la muscovite des pegmatites de la Province Carpatique; o les teneurs dans les muscovites des pegmatites à albite et spodumène de Conţu; • les teneurs dans les muscovites des autres pegmatites.

Dans la composition de la muscovite des paragneiss encaissants on remarque une augmentation de la teneur en Si, Ti, Fe, Ca, Mg et la diminution accusée de la valeur d'Al (Tab. 1). La teneur en Ti de la muscovite des paragneiss est située entre les valeurs qui caractérisent la muscovite du faciès amphibolitique.

Dans la muscovite des paragneiss encaissants on a mis en évidence la participation plus large de la ferrimuscovite, de la ferromuscovite et de la phengite et la diminution du composant "muscovite" (Tab. 2).

Tableau 1
La composition chimique et les formules cristallochimiques des muscovites

(%)	Ms-17	Ms-18	Ms-16
SiO_2	46,63	45,33	46,51
TiO_2	0,15	0,19	1,01
Al_2O_3	36,86	36,39	33,98
Fe_2O_3	0,51	0,59	0,96
FeO	1,26	1,30	1,72
MnO	0,06	0,06	0,03
MgO	0,05	1,06	1,02
CaO	0,01	0,03	0,09
Na_2O	0,60	0,66	1,16
K_2O	9,84	10,11	9,61
H_2O^+	3,67	3,81	3,01
H_2O^-	0,51	0,63	0,36
Somme	100,15	100,16	99,46
a_{si}	22	23	20
(ppm)			
Li	684	70	Al_{IV}
Be	20	2	$a_{si}=\frac{}{Al_{IV}+Al_{VI}}\cdot 100$
Sn	200	100	
B	300	65	

Les formules cristallochimiques:

Ms-17 (la muscovite du complexe albite-spoduménique):

$(K_{0,83}Na_{0,08})_{0,91}(Al_{2,01}Fe^{2+}_{0,06}Fe^{3+}_{0,02})_{2,09}$
$(Si_{3,12}Al_{0,88})_4O_{10}(OH_{1,63}O_{0,37})_2$

Ms-18 (la muscovite du complexe quartz-muscovitique):

$(K_{0,86}Na_{0,08})_{0,94}(Al_{1,93}Fe^{2+}_{0,07}Fe^{3+}_{0,02}Mg_{0,10})_{2,12}$
$(Si_{3,05}Al_{0,95})_4O_{10}(OH_{1,71}O_{0,29})_2$

Ms-16 (la muscovite des paragneiss encaissants):

$(K_{0,83}Na_{0,15})_{0,98}(Al_{1,90}Fe^{2+}_{0,09}Fe^{3+}_{0,04}Mg_{0,10}Ti_{0,05})_{2,18}$
$(Si_{3,17}Al_{0,83})_4O_{10}(OH_{1,36}O_{0,64})_2$

La variation de la composition normative pour la muscovite des pegmatites et des paragneiss de la zone Conţu–Monts Cibin est présentée dans les diagrammes d'addition des composants (Fig. 3).

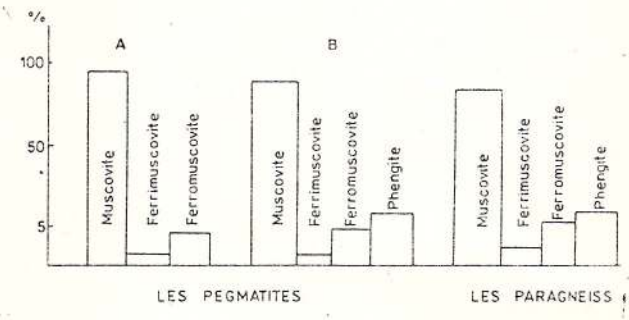

Fig. 3 – Le diagramme d'addition des composants normatifs de la muscovite des pegmatites et des paragneiss de Conţu. A = le complexe albite-spoduménique; B = le complexe quartz–muscovitique.

Dans la muscovite des pegmatites à albite et spodumène de Conţu on a determiné les suivants éléments en trace: Li, Be, Sn, B (Tab. 1). Les résultats obtenus montrent que la muscovite du complexe albite-spoduménique présente les teneurs les plus élevées en ces éléments.

La teneur en Li des muscovites est déterminée par des substitutions du type:
$Al^{3+}_{IV}2Al^{3+}_{VI} \leftarrow Li^+2Si^{4+}_{IV}$; $2Al^{3+}_{IV}3Al^{3+}_{IV} \leftarrow 3Li^+3Si^{4+}_{IV}$ et influencée par les particularités géochimiques des pegmatites lithinifères. La possibilité que l'aluminium octaédrique soit substitué par le Li dans la muscovite des pegmatites de la Province Carpatique est argumentée par la corrélation inverse établie dans le diagramme Li:Al_{VI} (Fig. 4).

Tableau 2
La composition normative des muscovites (%)

Echantillon	Muscovite	Ferrimuscovite	Ferromuscovite	Phengite
Ms–17	96,2	0,9	2,8	0,01
Ms–18	91,0	0,9	3,3	4,6
Ms–16	86,2	1,8	4,2	4,7
Les données comparative: (Murariu, 1979; 1988):				
La muscovite des pegmatites de la série de Rebra (Monts Rodna)				
Ms–144	94,7	1,5	1,9	1,9
La muscovite pegmatites de la série de Răzoare (Monts Preluca)				
Ms–423	94,2	1,2	2,4	2,2
La muscovite des pegmatites de la série de Someş (Monts Gilău)				
	93,0	2,5	1,5	3,0

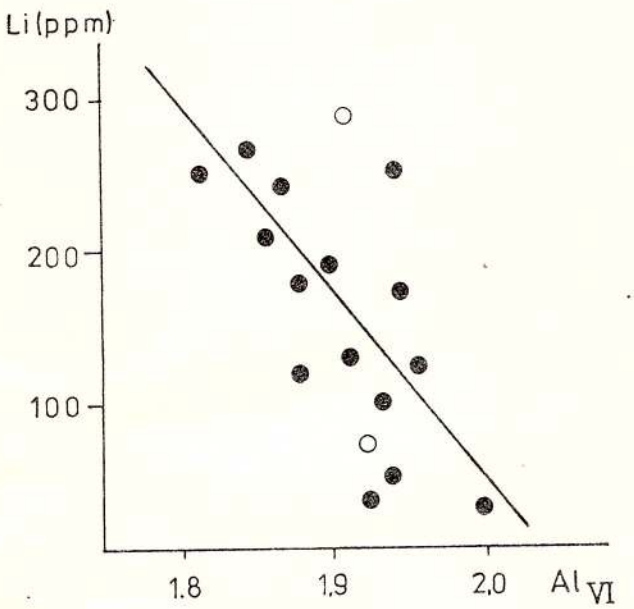

Fig. 4 – La corrélation Li:Al$_{VI}$ dans la muscovite des pegmatites de la Province Carpatique; ○ la muscovite des pegmatites à albite et spodumène de Conţu; • des autres muscovites.

La moyenne de 377 ppm Li trouvée pour la muscovite des pegmatites lithinifères de Conţu se rapproche de la moyenne calculée par Solodov et al. (1980) pour la muscovite des pegmatites à albite et spodumène (400 ppm) et elle est plus élevée que les teneurs déterminées dans les muscovites des pegmatites à mica et des pegmatites feldspathiques de la Province Carpatique (Murariu, Zămărcă, 1979; Hann, 1987; Murariu, Gandrabura, 1992).

Le beryllium est un élément caractéristique pour les pegmatites granitiques. Dans les pegmatites lithinifères de Conţu, la muscovite du complexe albite-spoduménique montre une teneur plus élevée en Be: 20 ppm. Cette valeur est presque la même que la moyenne calculée par Manuilova et al. (1966) pour la muscovite des pegmatites à terres rares: 28,9 ppm.

La teneur réduite en Be déterminée dans la muscovite du complexe quartz-muscovitique est en accord avec les données présentées dans la littérature (Shmakin, 1971; Liahovici, 1972; Hann, 1987) qui révèlent l'abondance réduite de cet élément dans la muscovite des pegmatites à mica et des pegmatites feldspathiques. Dans la muscovite, la présence du Be est due à des substitutions du type: $2Al^{3+}_{IV} \leftarrow Be^{2+}Si^{4+}_{IV}$; $[SiO_4]^{4-} \leftarrow [BeO_2(F,OH)]^{4-}$.

La muscovite des pegmatites étudiées est caractérisée par des teneurs bien diminuée en Sn par rapport à la muscovite des aplites: 320 ppm et des granites: 339 ppm (Liahovici, 1972). Les valeurs obtenues (100–200 ppm Sn) sont plus élevées que dans la muscovite des pegmatites feldspathiques ou des pegmatites à mica de la Province Carpatique (Murariu, 1979; Hann, 1987) et que dans les muscovites d'autres champs pegmatitiques: Mamsk-Siberie (Shmakin, 1971), Baikal (Manuilova et al., 1966) etc. Dans la muscovite, la présence du Sn est déterminée par l'affinité de cet élément pour l'aluminium.

Les déterminations du B montrent des teneurs plus élevées dans la muscovite du complex albite-spoduménique. La valeur de 65–300 ppm B incorporé dans les muscovites des pegmatites étudiées s'explique par la capacité de cet élément d'occuper la place de l'Al, suite à un isomorphisme du type: $Al^{3+} \leftarrow B^{3+}$.

L'ordre des concentrations des éléments en trace dans la muscovite des pegmatites à albite et spodumène de Conţu est: Li>B>Sn>Be.

Les données géochimiques obtenues montrent que la teneur en Li, Be, Sn, B de la muscovite des pegmatites lithinifères peut être utilisée comme un indice de leur minéralisation.

Bibliographie

Eugster, H.P., Yoder, H.S. jr. (1955) The join muscovite-paragonite. *Carnegie Inst.*, 1248, p. 124–126, Washington.

Hann, H.P. (1987) Pegmatitele din Carpaţii Meridionali. Ed. Acad., 141 p., Bucureşti.

Liahovici, V.V. (1972) Redkie elementi v porodoobrazuiuschih mineralah granitoidov. Izd. Nedra, 199 p., Moskva.

Maieru, O., Superceanu, C., Apostoloiu, A.(1968) Neue Spodumen und Beryllpegmatite im mitleren südkarpatischen Schiefergebirge (Romänien). *Geologie*, 17(4), p. 388–397, Akademie Verlag, Berlin.

Manuilova, M.M., Petrov, L.L., Ribakova, M.M., Sokolov, Iu.M., Shmakin, B.M. (1966) Zakonomernosti raspredeleniia tchcelocinih elementov i berilliia v mineralah pegmatitov Severo-Baikaliskogo poiasa. *Gheohimia*, 4, p. 410–422, Moskva.

Movileanu, A., Pomârleanu, V. (1972) Contributions to the geochemistry of pegmatites with spodumene of the Sadu Valley (Southern Carpathians, Romania). *Rev. roum. Géol., Géophys., Géogr., (Géologie)*, 16, p. 11–16, Bucureşti.

Murariu, T. (1979) Studiul mineralogic, geochimic şi structural al pegmatitelor din munţii Rodnei. Inst. Geol., Geofiz., *St. tehnice şi economice, seria I, Miner.-Petrogr.*, 15, 264 p., Bucureşti.

— **(1988)** La composition de la muscovite dans certains pegmatites de Roumanie. *Anal. şt. Univ. "Al.I.Cuza" s.II b*, XXXIV, Geologie–Geografie, p. 17–19, Iaşi.

— **(in press)** Contributions à l'étude chimique du spodumène des pegmatites de la zone Conţu–Negovanu (Monts Cibin). *Anal. şt. Univ. "Al.I.Cuza", Geologie*, XXXVIII, Iaşi.

— **, Zămârcă, A. (1979)** Litiul în pegmatitele din Munţii Apuseni. *Anal. şt. Univ. "Al.I.Cuza"*, XXV, s.IIb, Iaşi.

– **, Gandrabura, E. (in press)** Litiul în muscovitul pegmatitelor din România. *Anal. şt. Univ. "Al.I.Cuza", Geologie*, XXXVIII, Iaşi.

Pomârleanu, V., Barbu, A., Apostoloiu, A., Prunescu, Şt. (1967) Contribuţii asupra genezei spodumenului în unele pegmatite din munţii Lotru–Cibin. *Anal. şt. Univ. "Al.I.Cuza"*, s.II, XIII, p. 1–6, Iaşi.

Savu, H. (1970) Stratigrafia şi izogradele de metamorfism din provincia metamorfică prebaikaliană din munţii Semenic. *An. Inst. Geol.*, XXXVIII, p. 223–311, Bucureşti.

Săbău, G., Apostoloiu, A., Urcan, T. (1987) Mineral asemblages within the lithian pegmatites at Conţu, Lotru Mts. (Central South Carpathians) and their genetical bearing. *D.S. Inst. Geol.*, 74, 1, p. 251–262, Bucureşti.

Shmakin, B.M. (1971) Tipohimiceskie osobennosti glavnih mineralov muscovitovih pegmatitov Vostocinoi Sibiri. Izd. Nedra, p. 72–101, Moskva.

Solodov, N.A., Balashov, L.C., Kremenetski, A.A. (1980) Gheohimiia litiia, rubidiia i tseziia. Izd. Nedra, 233 p., Moskva.

Zagorski, V.E., Kuznetsova, A.G. (1990) Gheohimiia spodumenovih pegmatitov i shtchelocino redkometallinih metasomatitov. Izd. Nauka, 139 p., Novosibirsk.

Received: January 1994
Accepted in revised form: June 1994

Rom. J. Mineralogy, 1995, 77, p. 51–56, Bucureşti

EVOLUTION OF ZONING AT THE COSTABONNE TUNGSTEN SKARN DEPOSIT (PYRENEES, FRANCE)

Bernard GUY

Département Géochimie École Nationale Supérieure des Mines 158 Cours Fauriel

42023 Saint-Étienne Cedex 2 France

Key words: Calcic, Magnesian Skarns. Scheelite. Zoning. Dolostone Costabonne. Pyrenees. France.

Abstract: At Costabonne (Pyrenees, France) skarns develop by metasomatic alteration of various metasedimentary rocks of Cambrian age, in the vicinity of the Costabonne Hercynian granitic stock. The transformation took place during a large temperature interval, from about 680° C for the early stages to about 250° C for the late stages. As a consequence the metasomatic minerals and zoning patterns developed at early stages differ from those developed at the end of skarn evolution. This is particularly conspicuous in the case of the transformation of dolostone. The first zoning pattern shows the development of calcite + forsterite, diopside and andradite, the intermediate patterns show the development of more grossular–rich garnet and more hedenbergitic pyroxene, and in the late zoning pattern, manganese-rich garnet and pyroxene, and calcic amphiboles develop. The various zoning patterns can be portrayed on a diagram where time is represented along the vertical axis and space along the horizontal axis. Chemical potential diagrams at different temperatures explain part of the changes observed in the zoning patterns.

Introduction

The Costabonne scheelite skarn deposit is located in the Eastern part of the French Pyrenees, near the Spanish border, 60 km west of Perpignan and 100 km North-West of Barcelona. Mineralized outcrops are known between altitudes of 1900 and 2465 m (Costabonne Pike). Several aspects of the transformation of various rocks are to be seen; the paper by Guitard and Laffitte, 1958, gives their first description. Since then, several pieces of work on the Costabonne deposit have been completed in Saint-Etienne School of Mines. Synthesis may be found in the works of Guy, 1979, 1980, 1988. At the contact and near the granitic stock, skarns develop by metasomatic alteration of calcitic and dolomitic marbles, calc-silicate hornfels, pelitic schists and granitic rocks. The present paper is mainly dedicated to the transformation of dolostones; it gives a brief account and discussion of the zoning patterns developed within these rocks.

Transformation of dolostones

Types and chronology of zoning patterns

The zoning patterns developed within dolomitic rocks may generally clearly be observed in the field; because of their moderate permeability and their abundance, the rocks are not completely transformed and one can always see the starting material and the first zones; the variety of the magnesian minerals (forsterite, diopside, tremolite, serpentine, talc, borates etc.) that may be stable under the physical and chemical conditions of skarn formation is another factor accounting for the clarity of the zoning patterns. Several types of zonings may be seen. According to Guy (1979), on the basis of the study of garnet generations, the different zonings may have developed at different times and the overall transformation has taken place under a large interval of conditions. A unique frame of interpretation for the succession of the zoning systems seems to be applicable at the scale of the deposit.

Let A, B, C and so on be the main zonings observed (Tab. 1).

Table 1

Inventory of the metasomatic zonings developed at Costabonne on dolomitic starting materials

A	(G2)/G1/DI/CC + FO/DOL
B	DI/TRE/CC + FO/DOL
C	G1/DI/CC + TREM/DOL
D	G2/G1/SA/DI/TRE/CC/DOL
E,F	G3/ACT/TREM/CC/DOL

Zonings have been ordered according to the observations. The phases indicated between brackets have not been seen in strict continuity with the others: these seem to follow in the context. The existence of a zoning with tremolite and andradite shows that andradite may last longer than forsterite. Quartz may precipitate in an early stage contemporaneously or a little after garnet; disappearance of andradite and appearance of salite, after forsterite has disappeared, are likely to be simultaneous, since these two transformations are linked to the behaviour of iron and to the oxygen fugacity (Guy, 1988). At the stage when garnet 3 develops, it is possible that pyroxene no longer does; amphibole labelled ACT may contain aluminium. Other types of zonings containing talc, serpentine, humite group minerals, magnetite, brucite have been observed; they are not incorporated in the present study (see Guy, 1988, Dubru, 1986).

ABBREVIATIONS: CC = calcite; FO = forsterite, DI = diopside, G1 = first type garnet, andradite, G2 = second type garnet of grandite type (average composition: Gro 65, And 25, Alm + Sp 10), TR = tremolite, ACT = actinolitic amphibole, SA = salite, Gr3 = late garnet (Gro + And $\approx$ 60 %, with And $\leq$ 10 %, Alm from to 15 % and Spess from 25 to 35 %).

The classification of zonings is described in Fig. 1 and is established on the basis of the field and microscopic observations. For instance, zoning B cross-cuts zoning A, and is later than zoning A. The ordering of zonings allows one to order the triple points numbered 1, 2, 3 and so on, in Fig. 1; these points correspond to the disappearance of a zone from the zoning system and to the appearance of a new one. For instance, point 2 is subsequent to point 1, these two points are separated by zoning B. The observations do not allow to order all the triple points and the figure presents the most likely ordering.

The salient features concerning the transformation of the dolomitic starting materials are as follows (Fig. 1). The earliest zoning shows the succession: dolomite/calcite+forsterite/diopside/andradite ("garnet 1")/grandite ("garnet 2"). In a second step, forsterite disappears and a tremolite zone appears at the contact with dolostone. Andradite then disappears and a salitic pyroxene takes its place between the diopside and the garnet. Then an iron-rich amphibole intercalates between salite and garnet, and this last mineral gets a higher Fe^{2+} + Mn content ("garnet 3"); eventually, salite and diopside disappear and zoning may be observed as

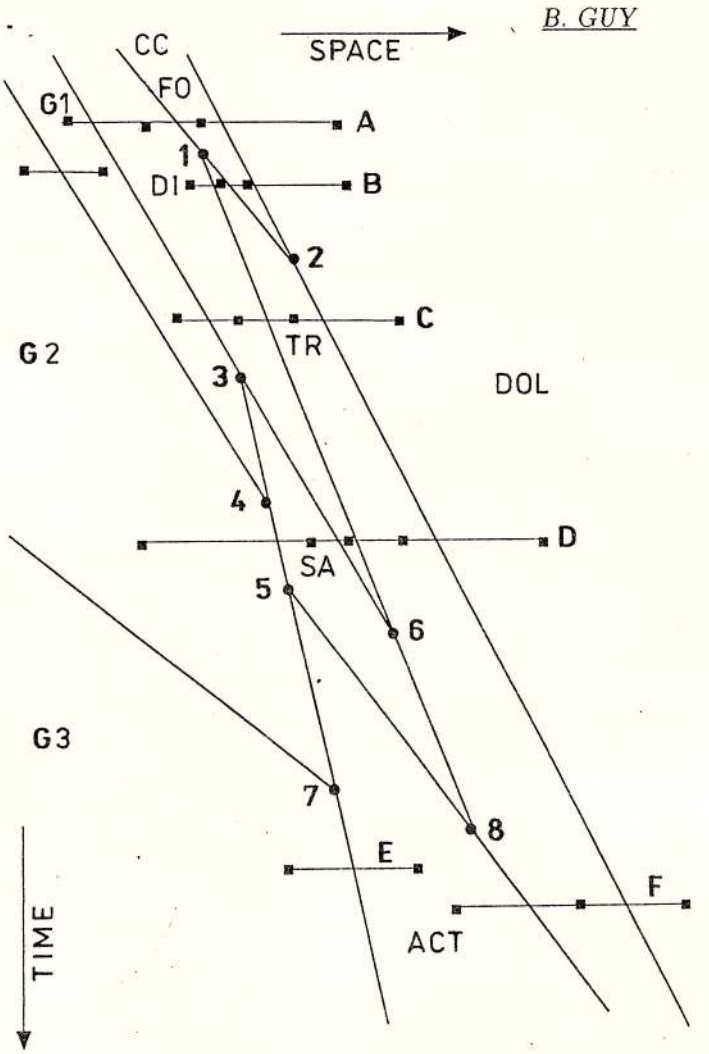

Fig. 1 – The several types of zonings on dolomitic starting materials and their temporal relationships. Space is indicated in abscissa, time in co-ordinate. The figure represents the sequence with time of the zonings that could be observed at a given locality: during the pervasion of the fluid at the same place, zoning is evolving and overprinting itself. The movement of the fluid is from the left (feeding vein) to the right (dolomite). The different zonings are not simultaneous: a zoning replaces the preceding as one progresses downward along the vertical axis. The correlative increase with time of thickness of the zones is indicated by the obliquity NW–SE of the different fronts (a front that ceases to progress would be indicated by a vertical limit). Spatial scale: the width of the drawing represents a few tens of centimeters to a few tens of meters. Temporal scale: it is difficult to give an estimate; according to what is known on advection velocities for the fluids and on the thermal evolution in perigranitic contexts (Guy, 1979) one can image that the length of the figure, starting with the early skarns at the top to the last stages at the bottom, represents a few hundreds of thousands of years. Zonings A, B etc. have been observed in the field (see Tab.1). Triple points corresponding to the temporal end or beginning of zonings are numbered 1, 2 etc. Typical compositions of minerals are given in Table 2.

ABBREVIATIONS: CC = calcite, FO = forsterite, DI = diopside, G1 = first type garnet, andradite, G2 = second type garnet of grandite type (average composition: Gro 65, And 25, Alm + Sp 10), TR = tremolite, ACT = actinolitic amphibole, SA = salite, Gr3 = late garnet, Grossular rich with Almandine + Spessartine from 30 to 50 %.

follows: dolomite/magnesian amphibole/iron-rich amphibole/garnet. Typical compositions for skarn minerals are given in Table 2.

tain ferruginous and magnesian silicates (andradite is present in the transformation of dolostone and salitic pyroxene in the case of calcitic marble, Guy, 1988).

Table 2
Selected compositions of skarn minerals

Sample no.	C43X7	C43-1-2	C43-1-2'	215	107	216	260
SiO_2	35.46	36.95	36.69	53.35	52.47	57.48	51.69
TiO_2	0.00	0.06	0.20	0.00	0.00	0.00	0.00
Al_2O_3	1.26	19.12	12.69	0.23	0.25	0.30	1.06
FeO	26.66	5.89	12.01	3.70	11.55	1.18	18.55
MnO	0.16	15.54	3.98	1.61	5.15	0.26	4.26
MgO	0.13	0.01	0.05	14.85	8.81	23.14	10.18
CaO	32.93	20.74	30.27	23.70	23.49	13.10	11.67
Na_2O	0.00	0.00	0.03	0.00	0.08	0.10	0.14
K_2O	0.00	0.04	0.00	0.00	0.00	0.05	0.09
Cr_2O_3	0.09	0.00	0.00	0.00	0.00	0.00	0.00
Total	96.69	98.35	95.92	97.44	101.80	95.61	97.64

GARNETS: C43X7: yellow andraditic core inside a garnetite of gallery 2033 ("garnet 1"); C43-1-2: rim of garnets inside garnetite, gallery 2033 ("garnet 3"); C43-1-2': garnet from garnetite, gallery 2033, (garnet 2).
PYROXENES: 215: diopside in veinlets inside the dolostone, sample CB48; 107: salitic pyroxene inside the garnetopyroxenite, sample C42.
AMPHIBOLES: 216: tremolite at the border of a skarn veinlet in dolostone, sample CB48; 260: actinolitic amphibole in garnet pyroxenite.

General evolution of zoning: first discussion

An evolution of zoning is revealed. To describe and explain it one must come out of the duality between "primary zoning" and "alteration of the primary zoning"; this is often the only rule for interpreting the parageneses in skarns, compelling one to change abruptly from a mobilist point of view (the fluid progresses, the zones develop) to a fixist point of view (the fluid ceases to percolate; the conditions change and the first formed minerals are transformed). In such dualistic frame of interpretation, once a "primary zoning system" has been defined, the only way to understand those minerals that do not belong to that system is imagining that they transform the minerals of the primary system. It is now necessary to have a more precise view and imagine that the conditions may have varied at the same time as the fluid was pervading; this leads the zoning system to evolve during its development. The "conditions" include the physical conditions (pressure and temperature), and the chemical conditions (the composition of the pervading fluid entering the system) as well. The appearance of oscillatory precipitations may be understood by a critical situation within this frame (Guy, 1988).

Systems of zones developed on dolostones are different from those developed on calcitic marbles, where no magnesian silicate is observed in external part, on the side of the starting material. But both systems do contain ferruginous and magnesian silicates (andradite is present in the transformation of dolostone and salitic pyroxene in the case of calcitic marble, Guy, 1988). The widespread classification between calcic skarns and magnesian skarns must then be used with caution.

Conditions of formation

Analysis of parageneses does not suffice by itself to determine a parameter such as temperature, since skarn assemblages have a low number of phases and low variance. The triple points such as those indicated in Figure 1 may, however, be more easily located on the diagrams; they correspond to the time when a phase disappears from the system of zones and is replaced by another (for instance, the end of forsterite and the beginning of tremolite occurs at T = 500^0 C, for P = 2 kb, according to Dubru, 1986). Conditions of formation may be estimated by gathering data issued from fluid inclusions and stable isotope studies, and phase analysis (Guy, 1988, Guy et al., 1988). Stable isotope analysis for the peak of amphibole development indicates a temperature of about 400^0 C. Pressure may be determined as that necessary to bring to this value the temperature of fluid inclusions corresponding to the amphibole stage (homogenisation temperature around 200^0 C; salinity of approximately 20 % eq. NaCl); estimated pressure was then of about 1.7 to 2 kb. This estimate fits with the information gained from the thickness of the sedimentary cover and the analysis of par-

ageneses. With the same pressure, the thermometric information given by the fluid inclusions of the early stages allows an estimate of the first temperatures, 650 to 700^0 C. These temperatures are close to that corresponding to the end of crystallization of granite at the same pressure; the early skarns closely follow the crystallization of granite. Pressure probably diminished from the early stages when the rocks underwent fracturing and when veins developed (pressure close to lithostatic) till the latest stages when hydrostatic regime was reached and allowed the incorporation of meteoritic waters in the system, as is suspected on the basis of hydrogen isotopes (Guy, op. cit.). Fluid pressure estimated above for the amphibole stage does not correspond to the lithostatic early stage and the value of 1.7 to 2 kb is thus a minimum estimate for the first stage. In contrast, the pressure during the last stages was probably lower than the above estimate. As a synthesis, Costabonne skarn formation began at high temperature (680^0 C; P$\approx$ 2kb) and a large temperature interval existed till the latest stages (end of evolution around 200^0 C, P $\leq$ 1.7 kb). The existence of periclase (Dubru, 1986) at a stage that may be supposed to predate by little skarn development, is also an indication of the high temperature of the early stages and in agreement with the temperature estimate for the early stage.

Effect of temperature on zoning evolution

The understanding of the zonings requires the knowledge of all chemical parameters of the pervading aqueous solution; because of the chemical gradients in this zonings, no parameter can presumably be held constant for an entire zonation. Zonings cannot be explained by temperature gradients; systems of zones are observed within small distances and with a complex geometry to which no likely T gradient may be adjusted. Reasonings may thus be done while keeping T constant in space, at least by steps. The discussion of the relationship between paragenesis, oxygen fugacity levels and temperature within the early skarns at Costabonne (Guy, 1988) indicates that the parameter fCO_2 is not constant along the whole zonation and that it has a gradient that can be connected to the decarbonization process. Its level within skarns remains low (XCO_2 around 0.05), confirmed by fluid inclusion study, (Guy, op. cit., Santarelli et al., 1988). The study of chemical potential (or of similar type) diagrams indicates that gradients for the chemical potential of SiO_2 prevailed within the skarns developed on dolostone (Dubru, 1986, Fig. 2), and that gradient for CaO potential was obtained in the skarns on granite, and schist (Van Marcke, 1983). Gradients are represented by the spatial positions of the different parageneses on the diagram.

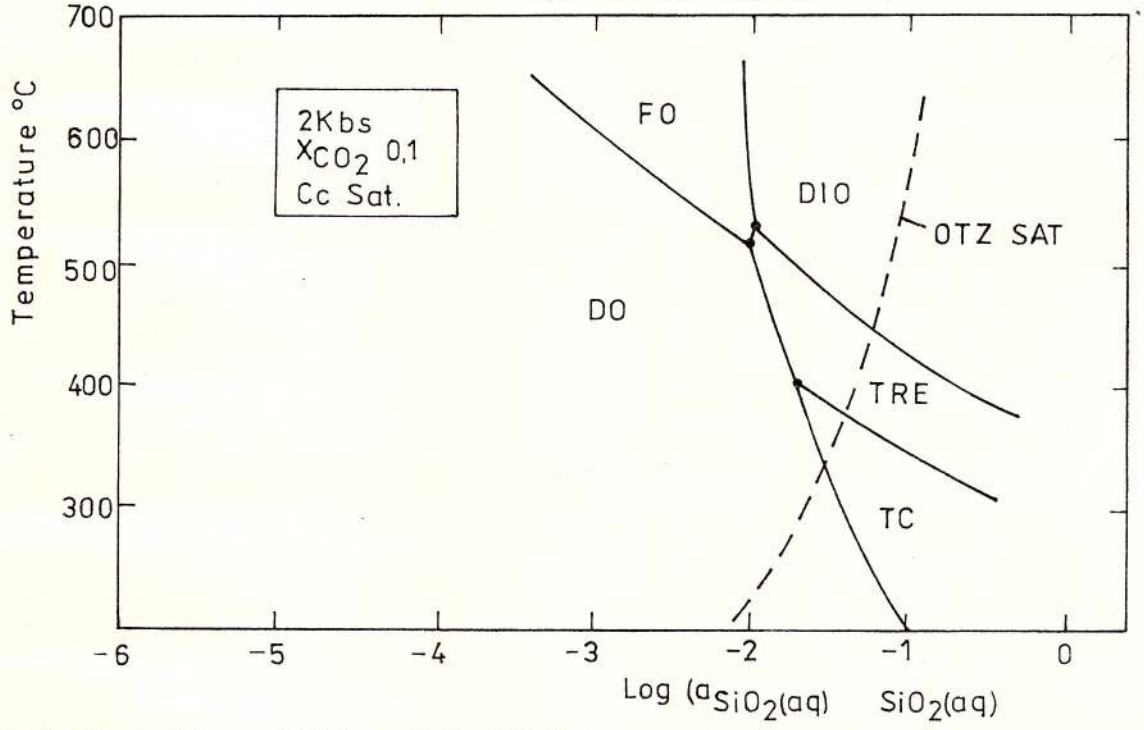

Fig. 2 – SiO_2 chemical potential/T diagram for P = 2 kb, XCO_2 = 0.01 and at calcite saturation; at high temperature T > 500^0 C, the minerals develop in increasing chemical potential of silica: dolomite, forsterite, diopside; for T < 500^0 C, tremolite develops between dolostone and diopside (Dubru, 1986).

On the other hand temperature is responsible for the evolution of zoning, as seen in the preceding section and in agreement with diagram studies; in summary, all these results may be represented on a μSiO_2–T diagram (Fig. 2), the first parameter describes the spatial zoning and the second the temporal evolution of the zoning; on the diagram, substitution of forsterite by tremolite is well explained by this temperature decrease (Fig. 2), in agreement with Bucher–Nurminen, 1981, Dubru, 1986.

Acknowledgements: the author thanks his colleagues from the Geological Institute of Romania, Bucharest, for welcoming him at the Romanian Mineralogical Congress and on field trip skarn occurrences; the stimulation of G. Udubaşa to write this paper is appreciated.

References

Bucher–Nurminen, K. (1981) The formation of metasomatic reaction veins in dolomitic marble roof pendants in the Bergell intrusion (Province Sandrio, Northern Italy). *Am. J. Sc.*, 281, p.1197–1222, Washington.

Dubru, M. (1986) Pétrologie et géochimie des marbres à brucite et des borates associés au gisement de tungstène de Costabonne (Pyrénées Orientales, France), thèse Doctorat Université Catholique de Louvain, 443 p.

Guitard, G., Laffitte, P. (1958) Les calcaires métamorphiques et les skarns du Pic de Costabonne (Pyrénées Orientales). *Sc. Terre Nancy*, VI, 1–2, p. 57–137.

Guy, B. (1979) Pétrologie et géochimie isotopique (S, C, O) des skarns à scheelite de Costabonne (Pyrénées Orientales, France), thèse Ing. Doct. École des Mines, Paris, 270 p.

— **(1980)** Étude géologique et pétrologique du gisement de Costabonne. *Mémoire du BRGM*, 99, 5, p. 236–250, Paris.

— **(1988)** Contribution à l'étude des skarns de Costabonne (Pyrénées Orientales, France) et à la théorie de la zonation métasomatique, thèse Doctorat d'État, Université Paris VI, 928 p.

— **, Sheppard, S., Fouillac, A. M., Le Guyader, R., Toulhoat, P., Fonteilles, M. (1988)** Geochemical and isotopic (H, C, O, S) studies of barren and tungsten bearing skarns of the French Pyrenees, in: Mineral Deposits within the European Community, J. Boissonas and P. Omenetto editors, Springer Verlag, p. 53–75, Berlin.

Santarelli, F., Alderton, D., Guy, B. (1988) Étude des fluides des skarns à tungstène de Costabonne (Pyrénées); analyses chimiques, minéraux fils: quelques résultats, *C. R. Acad. Sci.*, 307, II, p. 1231–1236.

Van Marcke, G. (1983) Pétrologie et géochimie des skarnoïdes du site tungstifère de Costabonne (Pyrénées Orientales), thèse Doct. Univ. Cath. Louvain, 293 p., annexes 150 p.

Received: June 1994
Accepted: September 1994

Rom. J. Mineralogy, 1995, 77, p. 57–60, Bucureşti

SULPHOSPINELS FROM BĂIŢA BIHOR: NEW OCCURRENCES IN ROMANIA

Mircea Ionuţ PETRESCU

Universitatea "Politehnica" Bucureşti, Facultatea de Ştiinţe şi Ingineria Materialelor, Laboratorul de Mineralogie.
Splaiul Independenţei nr. 313, 77206 Bucureşti

Key words: Sulphospinels. Carrollite. Fletcherite. EDAX. Băiţa Bihor.

Abstract: The cupriferous members of the sulphospinel group, namely carrollite and fletcherite (?) have been identified in the Băiţa Bihor ore deposit, in the massive copper mineralization in association with the chalcopyrite and the ferro–zinciferous tetrahedrite (horizon 580 m of the Baia Roşie zone). The identity of these two minerals was established by studying their optical properties and by carrying out quantitative and qualitative microprobe analyses both with a wavelength dispersive and an energy dispersive X ray microprobe analyzer. X ray distribution images and characteristic energy spectra for S, Co, Ni, Cu and Fe have been obtained. The chemical compositions have also been determined quantitatively by point EDAX analysis, and they were in a good agreement with the analysis of these minerals found elsewhere.

The Băiţa Bihor ore is located on the upper course of the Crişul Negru river in the Bihor Mountains of the Northern compartment of the Apuseni Mountains. It contains mainly Mo and Bi minerals associated with W, Cu and B minerals. The mineralization is hosted by skarns formed at the boundary between the Laramian magmatites on one side and the Norian limestones and the Carnian dolomites, belonging to the Codru nappe, on the other side. About 100 minerals have been cited in this ore deposit, some of them being discovered here: rezbanyite, szaibelyite, ascharite and kotoite (Cioflica, Vlad, 1971).

The sulphospinel minerals, with the general formula AB_2S_4, comprise linnaeite, polydymite, greigite and the intermediate members: siegenite, violarite, carrollite and fletcherite. The metallic elements (A and B) in the general formula are represented by Co, Ni, Fe or Cu. The carrollite represents an intermediate member between Co and Cu having the theoretical formula $CuCo_2S_4$ (Kostov, Minčeva–Stefanova, 1981). But most of the chemical analyses carried out on carrollite show also the presence of Ni (up to 10 at %) and of Fe (less than 2 at %). So, practically the following formula may be taken into consideration: $(Cu,Ni,Fe)(Co,Ni)_2S_4$ where Ni and Fe may substitute for Cu (up to 50 at %), while Ni substitutes for Co (up to 20 at %).

The carrollite presented here was found in samples from the Baia Roşie zone of the Băiţa Bihor ore deposit, namely from a massive copper mineralization occurring at the 580 m horizon.

The microscopic examination shows that carrollite consists of subhedral or even euhedral crystals, less than 1 mm in size, included in chalcopyrite compact aggregates together with tetrahedrite (Pl. I, Fig. 1,2). The mineral assemblage consists of chalcopyrite, ferrozinciferous tetrahedrite, carrollite and bornite. Optically the carrollite is isotropic, light gray coloured, having slight reddish hues. The reflectivity of carrollite is higher than that of the chalcopyrite that is in close contact to it, having a value of about 45 %.

The chemistry of carrollite was determined in a semiquantitative manner by means of the wavelength dispersive microprobe analysis. The X ray images obtained by this method (Pl. I, Fig. 3, 4, 5, 6) show the presence of Co, Ni, Cu and subordinately of iron. The semiquantitative information on the composition of the carrollite crystals was confirmed quantitatively by the characteristic energy spectra obtained in a given point of the crystal by means of an EDAX energy dispersive X ray analyzer (Fig. 1).

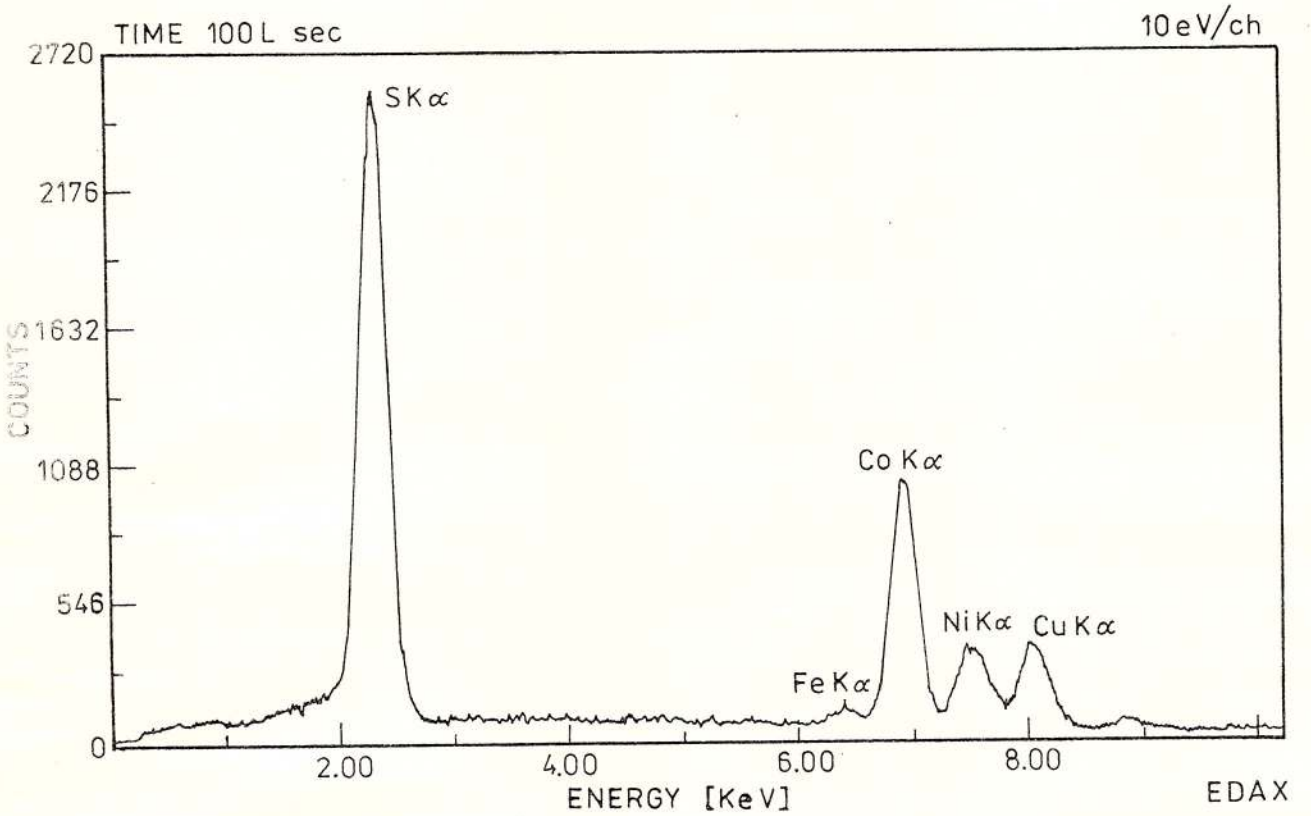

Fig. 1 – Characteristic energy spectra for carrollite.

Table 1
Point chemical composition (weight percent and atomic percent) of carrollite and fletcherite (?) determined by EDAX

	Co		Ni		Fe		Cu		S	
	wt%	at%	wt%	at%	wt%	at%	wt%	at%	wt%	at%
1.	38.06	28.57	0.00	0.00	0.00	0.00	20.53	14.29	41.41	57.13
2.	35.30	26.94	1.76	1.35	2.33	1.88	20.42	14.46	39.47	55.37
3.	35.79	26.96	3.66	2.77	0.93	0.74	18.98	13.26	40.64	56.27
4.	35.15	26.58	7.01	5.32	2.18	1.74	13.90	9.57	40.74	56.62
5.	36.08	27.25	7.65	5.80	2.25	1.79	9.98	6.99	41.89	58.16
6.	31.11	23.14	9.68	7.23	1.63	1.28	15.32	10.57	42.26	57.78

1. $CuCO_2S_4$ (Palache et al., 1966);
2. Carrollite – Gladhammar Sweden (Johansson 1924 fide Palache et al., 1966);
3. Carrollite – Siegen Germany (Laspeyres 1891 fide Palache et al., 1966);
4. Carollite – Gladhammar Sweden (Johansson 1924 fide Palache et al., 1966);
5. Carrollite – Mineral Hill mine, near Sykesville USA (Shannon 1926 fide Palache et al., 1966);
6. Carrollite – Băiţa Bihor, Romania.

The quantitative composition of the carrollite determined by EDAX is show in the Table 1 in comparison with the chemical compositions of the carrollite from Siegen–Germany, Gladhmmar–Sweden and Mineral Hill Sykesville–USA (Palache et al., 1966).

By comparing the chemistry of the carrollite from Băiţa Bihor with the data from the above–mentioned occurrences, it is likely that from a chemical point of view our carrollite is very close to the Gladhammar material (Tab. 1; line 4). Computation of the chemical data shows that the nickel atoms might appear both in a tetrahedral co-ordination, by substituting for copper (11 at %), and in an octahedral co-ordination, by substituting for cobalt (20

at %). The iron atoms are present uniquely in a tetrahedral co-ordination, by substituting for copper (10 at %). Therefore the empiric formula may be: $(Cu_{0.79},Ni_{0.11},Fe_{0.10})(Co_{0.8},Ni_{0.2})_2S_4$.

Small and rare grains of mineral resembling carrollite but having a lower reflectivity has been also found. The point X ray analyzer (EDAX), has pointed out the characteristic energy spectra for S, Co, Ni and Cu (Fig. 2); the chemical composition inferred from these spectra is given in Table 2.

in tetrahedral and octahedral co-ordination, while copper appears only in tetrahedral and nickel in octahedral co-ordination, the following empiric formula would result: $(Cu_{0.72},Co_{0.28})(Co_{0.57},Ni_{0.43})_2S_4$. This formula lies in the compositional limits given by most analyses for fletcherite: $Cu(Co_{0.5},Ni_{0.5})_2S_4$ and $(Cu_{0.5},Co_{0.5})Ni_2S_4$ (Craig, Carpenter, 1977 fide Kostov, Minčeva-Stefanova, 1981). Based on these considerations this mineral may be the fletcherite (?), the intermediate member (Ni,Co,Cu) of the sulphospinel group.

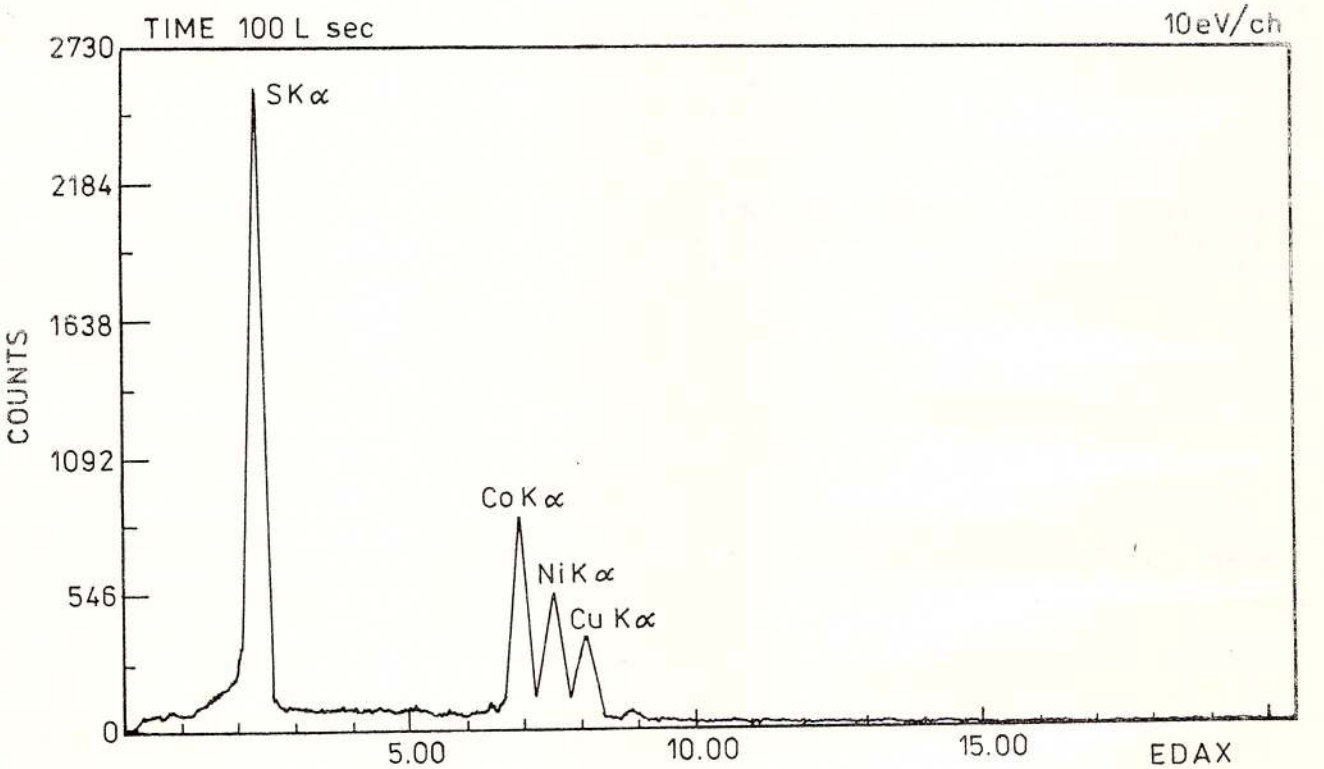

Fig. 2 – Characteristic energy spectra for fletcherite (?).

Table 2
Point chemical composition (weight percent and atomic percent) of fletcherite (?) determined by EDAX

	Co		Ni		Fe		Cu		S	
	wt %	at %	wt %	at %	wt %	at %	wt %	at %	wt %	at %
1.	26.38	19.60	15.96	11.90	0.00	0.00	15.14	10.43	42.52	58.07

1. Fletcherite (?) – Băiţa Bihor, Romania.

This chemical composition results in the following formula, $Cu_{0.72}Ni_{0.82}Co_{1.36}S_4$, that lies between the compositional limits for fletcherite expresed by $Cu_{1.13}Ni_{1.01}Co_{0.84}Fe_{0.06}S_4$ and $Cu_{0.67}Ni_{2.11}Co_{0.61}Fe_{0.01}S_4$ (Kostov, Minčeva-Stefanova, 1981). Supposing that cobalt appears both

This is the first occurrence of carrollite and fletcherite (?) joining the other members of the sulphospinel group: linnaeite and siegenite at Sasca Montană, greigite at Gilort and Jitia, violarite at Vâlsan (Udubaşa et al., 1992), as yet identified in Romania.

Acknowledgements. I am grateful to Dr. G. Udubaşa (Geological Institute of Romania) for valuable suggestions and critical review of the text.

References

Cioflica, G., Vlad, Ş. (1971) Répartition de la minéralisation dans les skarns de Băiţa Bihorului. *Rev. Roum. IGG, ser. Géologie*, 15, 1, p. 43–59, Bucureşti.

Palache, Ch., Berman, H., Frondel, C. (1966) The System of Mineralogy, I, John Wiley & Sons Inc., 834 p., New York.

Kostov, I., Minčeva-Stefanova, J. (1981) Sulphide Minerals-Crystal Chemistry Parageneses and Systematics, Publishing House of Bulgarian Academy of Sciences, 212 p., Sofia.

Udubaşa, G., Ilinca, Gh., Marincea, Şt., Săbău, G., Rădan, S. (1992) Minerals in Romania: the State of Art 1991. *Rom. J. Mineralogy*, 75, p. 1–51, Bucureşti.

Received: December 1993
Revised: March 1994
Accepted: April 1994

Plate

Fig. 1 – Optical micrograph of polished section, N ||, x 260. a) carrollite, b) ferro-zincian tetrahedrite, c) chalcopyrite.

Fig. 2 – Composition image (electron reflectivity contrast according to atomic number) recorded with a scanning electron microscope x 260. a) carrollite, b) ferro–zincian tetrahedrite, c) chalcopyrite.

Fig. 3 – X–ray distribution image for emitted Co – Kα x 260.

Fig. 4 – X–ray distribution image for emitted Ni – Kα x 260.

Fig. 5 – X–ray distribution image for emitted Cu – Kα x 260.

Fig. 6 – X–ray distribution image for emitted Fe – Kα x 260.

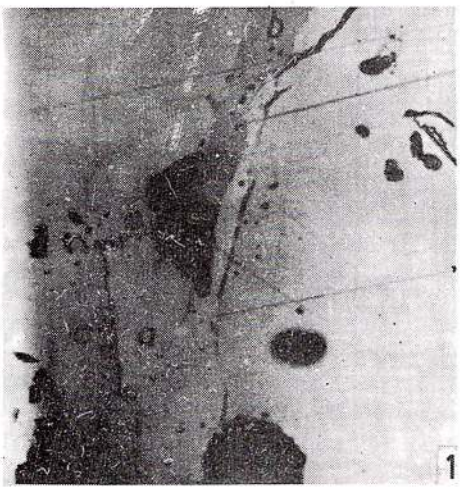

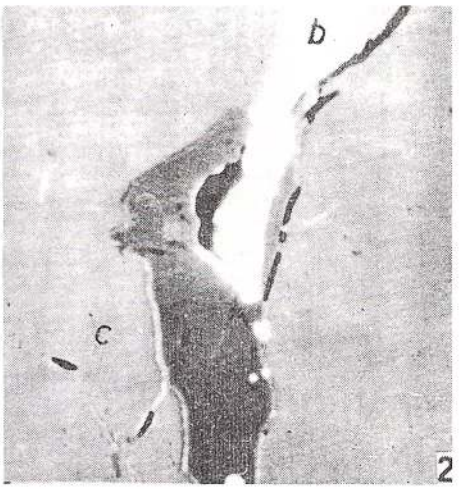

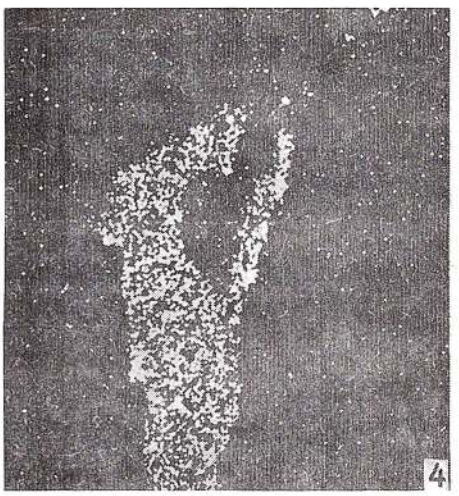

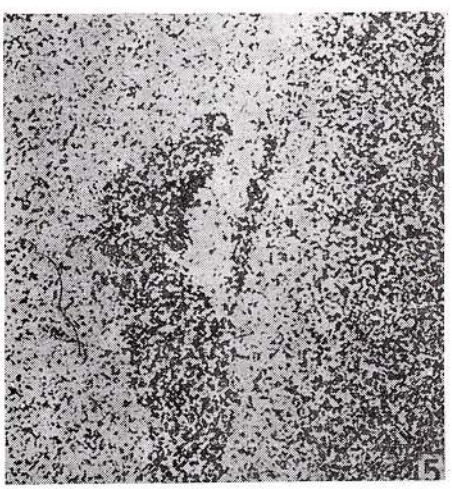

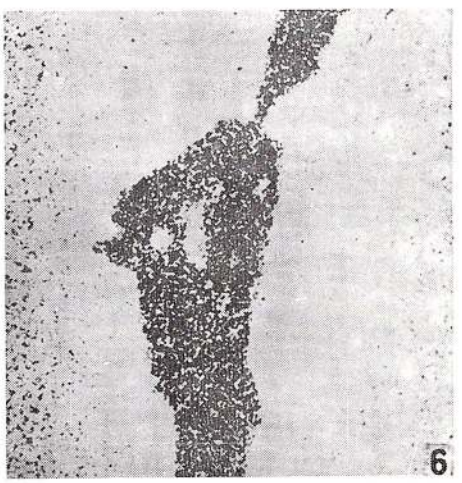

Rom. J. Mineralogy, 1995, 77, p. 61–66, Bucureşti

MINERALOGY OF SOME NEW ALPINE VEINS FROM THE SOUTH CARPATHIANS AND THE APUSENI MOUNTAINS, ROMANIA

Robert Octavian STRUSIEVICZ, Dana POP

Departamentul Mineralogie-Petrometalogenie, Universitatea "Babeş-Bolyai"

Str. M. Kogălniceanu nr. 1, RO-3400 Cluj-Napoca, România.

Key words: Alpine veins. Quartz. Feldspars. Chlorites. Epidote. Oxides. Crystal shape. X-ray data. South Carpathians. Apuseni Mountains. Romania.

Abstract: We describe here the mineralogy of some Alpine veins found in the Danubian Realm of the South Carpathians (Retezat, Godeanu and Vâlcan Mts), as well as in the NW part of the Apuseni Mountains, i.e. in the Plopiş (Rez) Mts. The investigated veins, ranging in width from 1 to 20 cm, are mostly filled up, but lenticular geodes within them exhibit perfectly shaped millimetric to centimetric crystals and very interesting assemblages of minerals. The following parageneses were identified: (1) quartz + albite + calcite in laminated granitoids of the Lainici-Păiuş Group (Retezat Mts); (2) quartz +epidote + chlorite in amphibolites of the Drăgşan Group (Vâlcan Mts); (3) quartz + albite + calcite + chlorite in anchimetamorphic sandstones of the Poiana Mărului Unit (Godeanu Mts.); (4) quartz + adularia + muscovite; (5) quartz + albite + muscovite + limonite (pseudomorphs after siderite) and (6) quartz + albite + feroan clinochlore + rutile, the latest ones in migmatized gneisses of the Someş Group (Plopiş Mts).

Introduction. Alpine veins are a particular type of veins which generally cross-cut the schistosity or the sedimentary stratification of the host rocks. They are more common in metamorphic rocks, the larger ones being described from the Swiss, German, French, Italian and Austrian Alps (Niggli, 1940; Poty, 1969; Weninger, 1974), but also from the Bohemian Massif (Koller et al., 1978), as well as from Ural (Grigoriev, 1960). The Alpine veins are a product of dissolution and recrystallisation of minerals from the wall rock by late hydrothermal metamorphic solutions, their walls being covered with very well crystallised minerals that are found also in the host rocks. Up to now Alpine veins were mentioned in Romania only in the paper of Constantinescu & Săbău (1984), which describe parageneses with feldspars, quartz, chlorites, actinolite, pyrophyllite, muscovite, paragonite, epidote, chloritoid, calcite and hematite in gneisses, amphibolites and pyrophyllitic schists of the Parâng and Făgăraş Mountains (South Carpathians).

This paper deals with the description of some new occurrences of Alpine veins found in the Retezat, Vâlcan and Godeanu Mts in the Central South Carpathians, as well as in the Plopiş (Rez) Mts in the NW part of the Apuseni Mts (Fig. 1).

Description of occurrences and parageneses. The investigated veins were grouped geographically and according to their parageneses in 6 types.

(1) The paragenesis quartz + albite + calcite was found in veins crossing mylonitised plagiogranitoids of the Lainici-Păiuş Group (Upper Precambrian) cropping out in the upper basin of the Sterminos Valley, a left tributary of the Jiul de Vest River, north of Uricani, in the Retezat Mts (Fig. 1a). The veins are usually very narrow and filled up with massive quartz, but in places they contain small crevices - up to 2 cm in width - filled with very nice quartz and albite crystals. Both mineral species are small in size (up to 1 cm).

The quartz crystals are very pure, colourless and perfectly transparent, of the Dauphiné-type habit (Rykart, 1989). They are built up of dominant $(10\bar{1}0)$ prism, intermediary $(10\bar{1}1)$ and $(01\bar{1}1)$ rhombohedron, as well as of subordinated and rare $(11\bar{2}1)$ and $(2\bar{1}\bar{1}1)$ trigonal bipyramid and $(51\bar{6}1)$ or $(6\bar{1}51)$ trapezohedron faces (Fig. 2a).

Albite appears as colourless, transparent, idiomorphic tabular crystals (albite type habit) having very well developed (010) brachypinacoid faces striated parallel to the c axis, and intermediary (001), $(10\bar{1})$, 110),

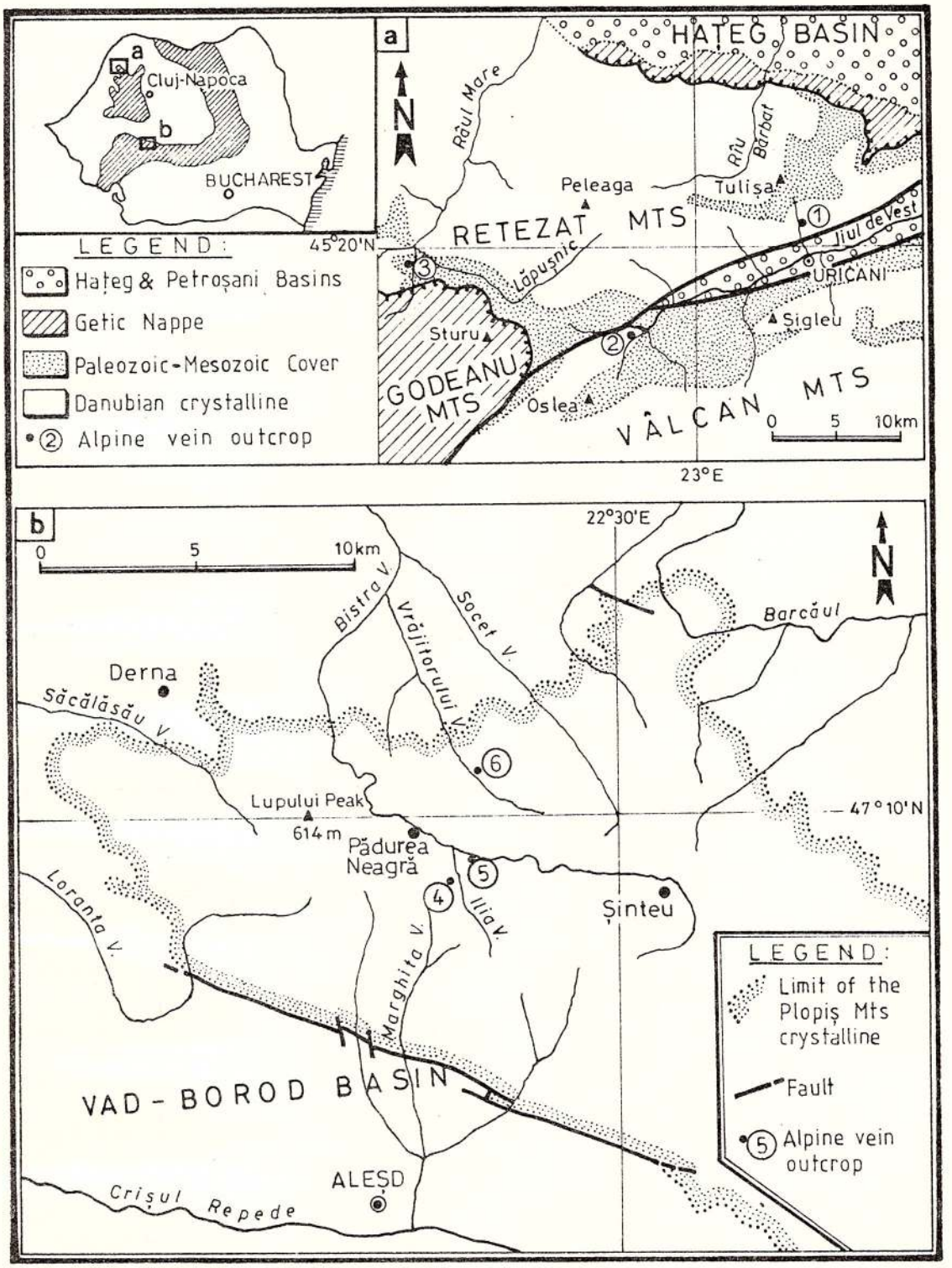

Fig. 1 – Localisation of the investigated Alpine veins.

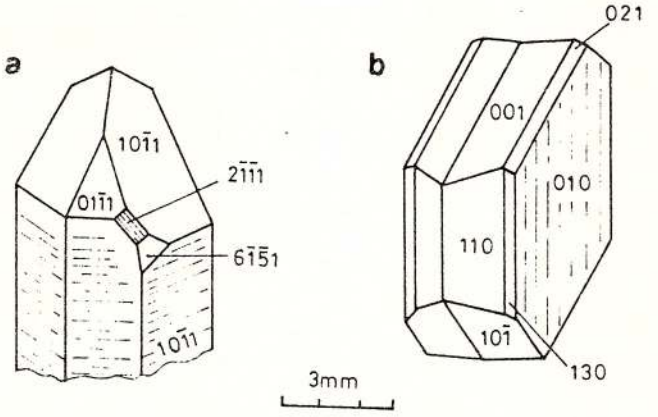

Fig. 2 - Crystal shape of minerals from the Alpine veins in Sterminos Valley: a, quartz with bipyramid and left trapezohedron faces; b, twinned albite with striated (010) face.

(130) and (021) faces, and is always twinned after the albite law (Fig. 2b and Plate, Fig. 1).

Quartz and albite crystallised simultaneously, both quartz overgrowing albite and the reverse situation being common. Calcite, when present, is always the latest phase, filling the spaces between albite and quartz. It is milky- white, xenomorphic with distinct cleavage.

(2) The paragenesis quartz + epidote + chlorite was found in a sole occurrence in retromorphosed amphibolites of the Drăgşan Group (Upper Precambrian) which crop out on the Valea Boului, a right tributary of the Jiul de Vest River, east of Uricani, in the Vâlcan Mts (Fig. 1a). The shape of the veins is sigmoidal, characteristic of the so-called "shear-veins" (= "Scherkluft", Mullis, 1991).

The quartz crystals are larger than those in the former occurrence (1 to 2.5 cm), have a short-prismatic habit, with equally developed prism and rhombohedron faces. They are asymmetrically developed and display a greenish- brownish colour. The colour is due to minute lamellar inclusions of chlorite which also diminish the crystals transparency. In thin sections one can see very nice helmintic aggregates of chlorite concentrated mainly in the outer zone of the quartz crystals.

Epidote is present as very thin grayish-green crystals (up to 6 mm long and 0.3 mm in diameter) arranged in drusy aggregates which cover the walls of the vein, and which are partly overgrown by the larger and younger quartz crystals. Due to the very small size of the crystals no clear faces could be identified. The X-ray diffraction lines of epidote are shown in Table 1.

(3) The paragenesis quartz + albite + chlorite + calcite was found in anchimetamorphic metagraywackes, of Jurassic age, in the Poiana Mărului Unit of the Danubian Realm (Fig. 1a). These metagraywackes

Table 1
X-ray data for epidote from Valea Boului, Vâlcan Mts

Refl. no.	Epidote, Valea Boului		Epidote, JCPDS file no. 9-438	
	d/n	I	d/n	I
1	7.060	14	7.020	3
2	5.020	22	5.018	40
3	4.020	22	3.997	40
4	3.485	30	3.492	40
5	3.206	6	3.197	15
6	2.897	100	2.900	100
7	2.812	14	2.809	50
8	2.687	27	2.677	60
9	2.599	18	2.593	55
10	2.531	9	2.525	10
11	2.454	5	2.449	7
12	2.401	90	2.396	70
13	2.291	9	2.289	25
14	2.165	9	2.161	25
15	2.127	11	2.110	40
16	1.880	14	1.869	60
17	1.636	36	1.635	65
18	1.588	9	1.590	11
19	1.577	14	1.574	13
20	1.541	14	1.539	13

are cross-cut in the Branu Valley, a left tributary of the Lăpuşnicu Mare River (Godeanu Mts), by up to 20 cm wide veins, most of them filled up with calcite. In some sectors of these veins where calcite is lacking, the walls are covered by millimetric (up to 1 cm) idiomorphic crystals of quartz and albite.

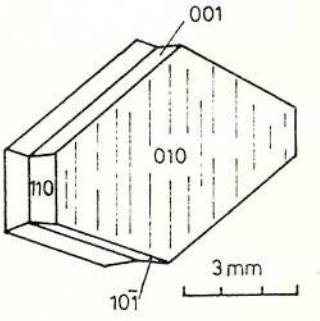

Fig. 3 - Shape of albite crystals from Branu Valley.

While quartz has the same characteristics as those mentioned for paragenesis (1), albite is colourless to milky-white and has a characteristic rhombic-truncated tabular habit due to the equal development of the intermediary (001) and (10$\bar{1}$) faces besides the dominant brachypinacoid (010) and the subordinated (110) faces (Fig. 3, and Plate, Fig. 2). As in paragenesis (1) all albite crystals appear as twins after the albite law made up of two individuals.

The X-ray diffraction data of albite from this occurrence are presented in Table 2.

Table 2
X-ray diffraction data for albites from Alpine veins in Romania

Refl. no.	Albite-type ab. Branu Valley, Godeanu Mts.		Pericline-type ab. Valea Vrăjitorului, Plopiş Mts.		Low-temp. albite ASTM 9-446	
	d/n	I	d/n	I	d/n	I
1	6.360	20	6.370	6	6.390	20
2	4.020	25	4.029	8	4.030	15
3	3.840	10	3.857	4	3.857	7
4	3.770	40	3.770	18	3.780	25
5			inflection		3.684	20
6	3.660	25	3.668	10	3.663	15
7	3.490	8	3.501	3	3.509	10
8	3.360	8	3.358	6	3.375	7
9	3.196	100	3.196	100	3.196	100
10	3.097	2			3.151	9
11	2.950	10	2.964	5	2.964	9
12	2.920	16	2.932	7	2.933	15
13	2.846	9	2.853	6	2.866	7
14	2.634	4	2.645	2	2.639	5
15	2.554	6	2.554	3	2.563	7
16	2.499	2			2.496	5
17	2.473	1			2.460	5
18	2.396	3			2.388	3
19	2.313	3	2.317	1	2.320	3
20	2.184	2	2.186	1	2.189	3
21	2.120	4	2.124	4	2.125	7
22	1.975	4	1.979	1	1.980	3

* lines with intensities of 1 and 2 omitted.

Quartz and albite are the first crystallised phases, while calcite (this time forming up to 1.5 cm rhombohedral crystals) and chlorite (found as centimetric nests made up of massive aggregates of light-green colour hosted in calcite) are the latest ones.

(4) The paragenesis quartz + adularia + muscovite was found in veins crossing migmatised gneisses of the Someş Group in the Plopiş Mts. The outcrops are situated in the scarps of the Aleşd-Pădurea Neagră road, on the left bank of the Ilia Valley, a left tributary of the Bistra River (Fig. 1b). A distinct feature of this zone is the intense limonitisation of the outcrops due to oxidation of disseminated pyrite in the wall rock.

Quartz was found in up to 7 cm long crystals, of the Tessin-type habit (Rykart, 1989), having rounded hexagonal prism faces, due to the presence of steep rhombohedrons. The crystals are translucent and always coated with limonite.

Adularia is present as minute (up to 1.5 mm in diameter) milky-white crystals grown over the larger quartz crystals. They exhibit their characteristic "pseudorhombohedral" habit, due to the equal development of the (110) prism and (10$\bar{1}$) pinacoid faces (Fig. 4 and Plate, Fig. 6).

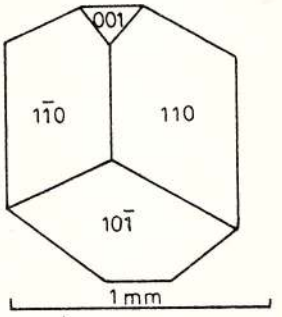

Fig. 4 – Shape of adularia crystals from Ilia Valley.

Muscovite forms scaly aggregates made up of pseudohexagonal lamellae up to 4 mm in diameter. The order of deposition of these minerals is muscovite-quartz-adularia, but they clearly form a paragenesis.

(5) The paragenesis quartz + albite + muscovite + hematite + limonite (pseudomorph after siderite) was found in the Bistra Valley, upstream of the confluence with the Ilia Valley, not far from the site of (4), in veins crossing paragneisses.

Quartz and albite in these veins are very small in size, and are always coated with limonite. By far the most interesting minerals in this paragenesis are the hematite rosettes and the limonite pseudomorphs after a carbonate mineral.

Hematite appears as specularite, i.e. as lamellar, iron-black crystals (up to 4 mm in diameter), which form scaly aggregates, or sometimes small (up to 1 cm in diameter) "iron roses" (Plate, Fig. 8). The crystals are very friable and have a splendent submetallic luster.

Pseudomorphs of amorphous limonite after a carbonate mineral are very nice appearances in these veins. The shapes of these pseudomorphs are typical curved (saddle-shaped) rhombohedrons, which even preserve the perfect rhombohedral cleavage lines on the faces (Plate, Fig. 7). They are up to 8 mm in diameter, have a reddish-brown colour, and a nearly adamantine luster. Considering all these morphological aspects as well as the Fe content of the pseudomorphosing mass, we assume that the initial mineral was siderite or ankerite.

(6) The paragenesis quartz + albite + feroan clinochlore + rutile was found in an alpine vein crossing amphibolites of the Someş Group, north of Pădurea Neagră, in the Vrăjitorului Brook (Fig. 1b). The vein, not wider than 4–15 cm, contained some small geodes with very good crystals.

Quartz appears as up 1 cm small crystals, milky-white, with no good terminal faces (Plate, Fig. 3 and 4).

Albite is of the pericline-type habitus, the up to 5 mm pearly- white, non-transparent crystals, elongated parallel to the b–axis showing the faces (001), (110), ($1\bar{1}0$), ($10\bar{1}$) and (010), the latter being subordinated and having striae parallel to the c–axis (Fig. 5 and Plate, Fig. 3). The X-ray diffraction lines of albite are shown in Table 2.

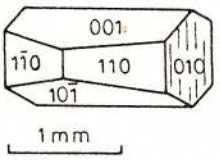

Fig. 5 - Pericline-type albite from Valea Vrăjitorului.

Clinochlore (the feroan variety ripidolite) forms 2 to 3 mm radial aggregates made up of very thin six-sided lamellae. These aggregates are partly included in the outer zone of the quartz crystals, but they are more often grown over albite (Plate, Fig. 3 and 4). Ripidolite is dark-green with pearly luster and perfect basal cleavage. The X-ray diffraction lines are shown in Table 3.

Table 3
X–ray diffraction data for ripidolite from Alpine veins in Romania

Refl. no.	V. Vrăjitorului, Plopiş Mts. (this paper)		Parâng Mts. (Constantinescu, Săbău, 1984)		ASTM card No. 7–76* (Isère, France)	
	d/n	I	d/n	I	d/n	I
1	14.100	20	14.10	40	14.100	80
2	7.070	70	7.08	100	7.070	100
3	4.741	30	4.71	10	4.724	30
4	3.553	100	3.54	20	3.537	50
5	2.832	25	2.82	10	2.827	10
6	2.600	1	2.59	10	2.599	20
7	2.560	1	2.54	10	2.556	30
8	2.450	1	2.45	15	2.450	30
9	2.390	1	2.38	10	2.389	20
10	2.260	1	2.25	10	2.265	10
11	2.022	6	2.00	15	2.009	20
12	1.877	1			1.888	10
13	1.568	2			1.566	10

* 6 reflexes between 4.620 and 1.665 with intensities 5 omitted.

Rutile is rare in the studied samples. The crystals are acicular, very thin (max. 0.4 mm), and up to 4 mm long. They appear as diverging aggregates, mostly included in quartz, but also as free crystals. In only one case a free tabular sagenite aggregate was encountered (Plate, Fig. 5). This might be interpreted as a rutile paramorph after brookite.

Comments. The mineral content of the investigated Alpine veins is clearly dependent of the mineral composition of the host rock, i.e., veins crossing gneisses or metagraywackes contain parageneses with quartz, albite, adularia, muscovite, while veins in basic rocks are characterised by the presence of epidote, chlorite, rutile besides quartz and feldspars. The genesis of Alpine veins implies two phases: (1) dissolution of minerals from the host rock by hydrothermal solutions and (2) crystallising of minerals in shear or tension fissures of the host rock, due to uplifting. It is presumed that quartz, one of the most common minerals in Alpine veins, is dissolved by late hydrothermal metamorphic solutions, at 4–500^0 C and pressures of 3–3.3 kbars, that is at depths of 12–14 km, in greenschist metamorphic conditions (Mullis, 1991). Fluid inclusion studies (Poty et al., 1974) demonstrated the existence of at least three temperature dependent parageneses in Alpine veins of the Alps:

(I) quartz + albite + chlorite + muscovite + epidote + (biotite + ilmenite + titanite) - formed at temperatures of 400 to 370^0 C;

(II) quartz + rutile + siderite + (phengite) - formed at temperatures of 300^0 C, and,

(III) quartz + calcite + goethite - formed at temperatures below 300^0 C.

According to these data the parageneses investigated by us are all of high temperature (I). A special case is represented by the paragenesis (5) where the presence of limonite pseudomorphs after siderite pleads for the existence of three superposed stages, siderite being characteristic of intermediary temperatures (II), while limonite which is replacing it is a typical low temperature product (III). In fact (5) is better defined as a "mineral association" (Udubaşa, 1993).

References

Constantinescu, E., Săbău, G. (1984) Mineralogy of alpine veins from the Romanian Carpathians. *An. I.G.G.*, LXIV, p. 33–43, Bucureşti.

Grigoriev, D. P. (1960) The origin of quartz as a fissure mineral of the Alpine type with special reference to occurrences in the U.S.S.R., *Curs. Conf. Inst. Lucas Mallada*, VII, p. 63–76.

Koller, Fr., Neumayer, R., Niedermayr, G. (1978) "Alpine Klüfte" im Kristallin der Böhmischen Masse. *Der Aufschluss*, 29/11, p. 373–378, Heidelberg.

Mullis, J. (1991) Bergkristall. *Schweiz. Strahler*, 9/3, p. 127–161, Zürich.

Niggli, P. (1940) Die Mineralien der Schweizer Alpen, vol. I and II, Wepf & Co., 661 p., Basel.

Poty, B. (1969) La croissance des cristaux de quartz dans les filons sur l'exemple du filon de la Gardette (Bourg d'Oisans et des filons de Mont Blanc). *Science de la Terre, Mém.*, 17, Nancy.

— **, Stalder, H.A., Weisbrod, A. (1974)** Fluid Inclusions Studies in Quartz from Fissures of Western and Central Alps. *Schweiz. mineral. petrogr. Mitt.*, 54, p. 717–752.

Rykart, R. (1989) Quartz - Monographie. Ott Verlag, Thun.

Udubaşa, G. (1993) PTS Constraints of Ore Paragenese with Some Case Studies. *Rom. J. Mineralogy.*, 76/1, p. 7–13., Bucureşti.

Weninger, H. (1974) Die alpinen Kluftmineralien der österreichischen Ostalpen. *Der Aufschluss*, 25, 165 p., Heidelberg.

Received: October 1994
Accepted: December 1994

Plate

Fig. 1 — Tabular albite from Sterminos Valley, Retezat Mts.

Fig. 2 — "Rhombic-truncated" tabular albite from Branu Valley, Godeanu Mts.

Fig. 3–4 — Pericline-type albite, quartz and feroan clinochlore (ripidolite) from Valea Vrăjitorului, Plopiş Mts.

Fig. 5 — Lamellar aggregate of rutile needles (sagenite) from Valea Vrăjitorului, Plopiş Mts.

Fig. 6 — Minute adularia crystals grown over quartz from Ilia Valley, Plopiş Mts.

Fig. 7 — Quartz associated with limonite pseudomorphs after siderite from Bistra Valley, Plopiş Mts.

Fig.8 — Hematite "iron rose" from Bistra Valley, Plopiş Mts.

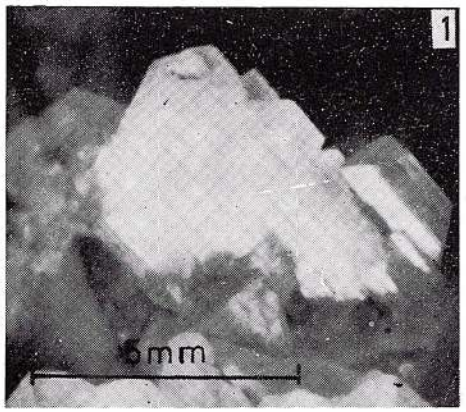

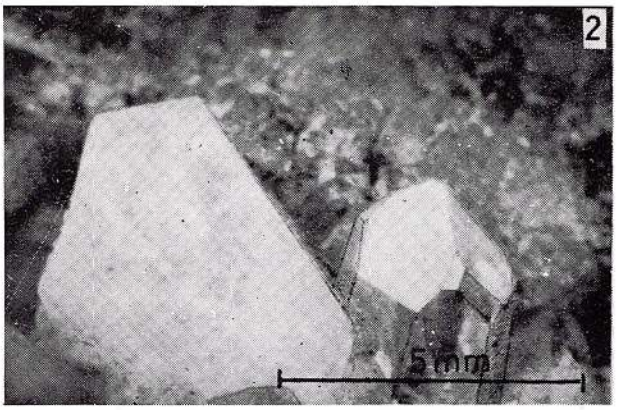

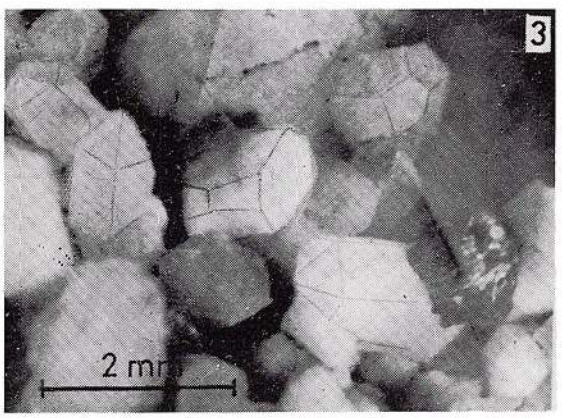

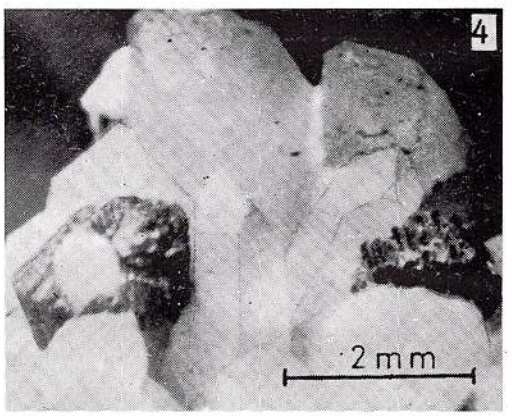

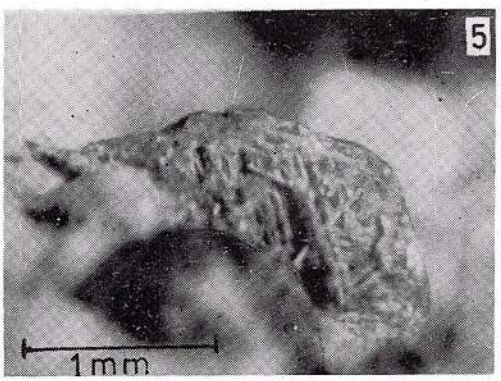

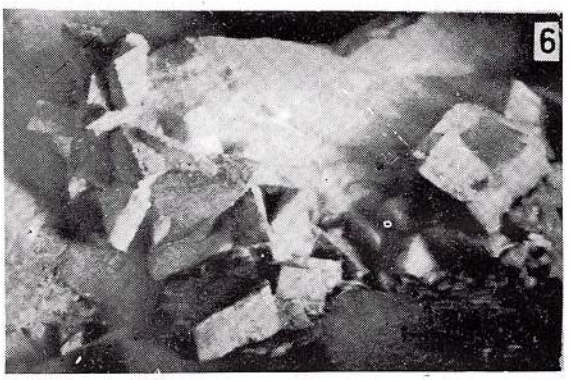

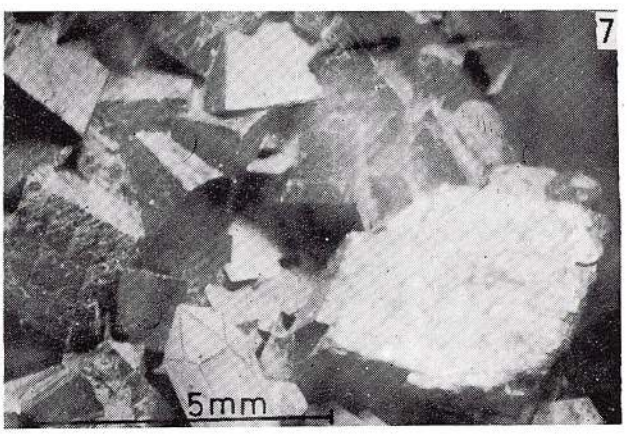

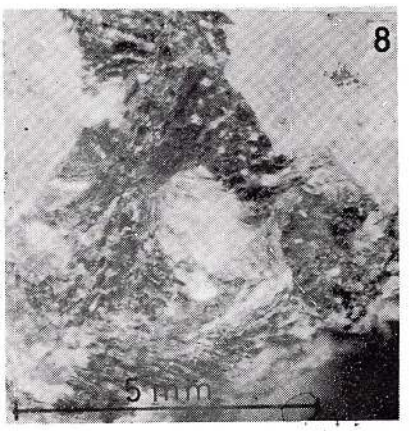

Rom. J. Mineralogy, 1995, 77, p. 67–70, Bucureşti

A BRIEF SURVEY OF THE DEVELOPMENT OF MINERALOGY IN NEW ZEALAND[1]

David SHELLEY
Geology Department, University of Canterbury, Christchurch, New Zealand

(Compiled in 1994)

1. Introduction

New Zealand was systematically settled by Europeans from about 1840 onwards, although first contacts between the indigenous Maori population and Europeans go back to 1642. Before this, the Maoris had occupied New Zealand for less than 1000 years, and not having developed a metal culture, made little use of minerals; however, some materials such as nephrite, serpentine, obsidian and chert, were particularly sought by them for use as stone implements and ornaments, and the minerals hematite and vivianite sought as pigments. Further information, including a list of Maori names for various rocks and minerals, is given in Fleming (1959) and also Keyes (1974).

Following European settlement, the need for systematic geological surveying was quickly appreciated. Already by 1850, Mantell had produced a geological sketch map of part of the South Island, and in 1861 James Hector was appointed by the Provincial Government of Otago to set up a Geological Survey. Hector arrived in April 1862 and undertook extensive exploratory expeditions and produced a large map. In 1863, Ferdinand van Hochstetter presented his "Geologie von Neu-Seeland" (translated by Fleming, 1959); this was the result of the first regional geological survey of New Zealand in 1858–59, and the work included some of the earliest geological maps of New Zealand. In 1865, Hector moved to Wellington to set up what became the NZ Geological Survey, and he took with him from Otago his rock and mineral analyst W. Skey. In its first century of existence, the Geological Survey produced geological maps of much of the country, and its work culminated in the production of the nation-wide 1:250,000 geological maps of the 1960's. This series is presently undergoing a major revision by the Survey's successor, the Institute of Geological and Nuclear Sciences. The Institute also publishes numerous 1:50,000 and 1:63,360 scale geological maps, but as yet the entire country has not been mapped in this detail.

Universities were established in the four principal New Zealand cities before the close of the century (Otago University, Dunedin, 1869; Canterbury University, Christchurch, 1873; Auckland University, 1882; Victoria University, Wellington, 1897). The needs of agriculture led to the early foundation of Lincoln College (1878) near Christchurch. Further developments include the establishment of Massey Agricultural College at Palmerston North in 1926 (which became Massey University of the Manawatu in 1964) and the University of Waikato in Hamilton in 1963.

At the present time, the principal centers of mineralogical research and/or teaching in New Zealand (see appended map for localities) are as follows:

– Institute of Geological and Nuclear Sciences, P.O. Box 30368, Lower Hutt.

– N.Z. Oceanographic Institute, P.O. Box 14901, Wellington.

– Landcare Research New Zealand, P.O. Box 40, Lincoln.

– Department of Geology, University of Auckland, Private Bag 92019, Auckland.

– Department of Earth Sciences, University of Waikato, Private Bag 3105, Hamilton.

– Department of Soil Science, Massey University, Private Bag 11222, Palmerston North.

– Department of Geology, Victoria University, P.O. Box 600, Wellington.

– Department of Geology, Canterbury University,

[1]Publication of the International Mineralogical Association (IMA), Commission on History and Teaching.

Private Bag 4800, Christchurch.

– Department of Soil Science, Lincoln University, P.O. Box 94, Lincoln, Canterbury.

– Department of Geology, Otago University, P.O. Box 56, Dunedin.

2. Number of workers in mineralogy in New Zealand

Most New Zealand workers in mineralogy think of themselves as petrologist, geologists, soil-scientists, geochemists, etc., rather than as mineralogists. The national organisation of mineralogists is the Mineralogical Society of New Zealand which succeeds the loosely structured "New Zealand Mineralogical Group". One principal aim is to maintain contact with the IMA. There is no separate department of mineralogy in any of the universities or in the Institute of Geological and Nuclear Sciences and a precise count of workers is virtually impossible.

For the first hundred years following systematic European settlement, mineralogists at any one time numbered less than 10. At present there are 40-50 scientists who in the course of their work are seriously involved in mineralogy.

Important events leading to an expansion in mineralogical studies include (a) formation of a separate petrology section in the N.Z. Geological Survey in 1938, (b) clay mineral studies expanded at Massey, Lincoln, and in the Soil Bureau from about 1950 onwards, (c) geothermal power exploration and development from the 1950's onwards, (d) a general expansion of the universities in the 1960's, (e) renewed interest in exploration for and utilisation of indigenous minerals, especially from the late 1960's, (f) recognition of the potential economic importance of the seas around New Zealand leading to increased oceanographic studies, especially from the 1960's onwards.

3. Training programmes in New Zealand

The universities in Auckland, Hamilton, Palmerston North, Wellington, Christchurch and Dunedin, provide substantial mineralogical training as part of undergraduate courses in geology and the earth-sciences. Clay mineral studies form a part of soil-science courses at Massey University and Lincoln University. All these institutions offer research opportunities in mineralogical fields leading to the Ph.D. degree. It can be noted again, however, that most N.Z. mineralogists teach or engage in research in the subject in the broader context of geology, soil-science, etc.

Universities and Research Institutes in New Zealand operate or have ready access to a wide range of modern microscopic, chemical, X-ray, and other analytical equipment. Electron microprobes are operational in the universities in Auckland Wellington and Dunedin. Scanning electron microscopes, some with energy dispersive attachments, are housed in the universities in Auckland, Hamilton, Wellington, Christchurch and Dunedin, and also in the Institute of Geological & Nuclear Sciences. Although transmission electron microprobes are available, equipment to study dislocations in ultra-thin silicate sections is not.

Three mineralogy texts for students have been written by New Zealanders: Battey (1972 and 1981); Berry, Mason, and Deitrich (1959 and 1983); and Shelley (1975 and 1985). Mason is domiciled in the USA but in retirement spends the Northern Hemisphere winters in New Zealand.

4. Minerals and rocks first described from New Zealand

Localities referred to below are marked on the appended map of New Zealand.

Taranakite

$K_x[Al_{2-y}(H_3)_y](OH)_2[Al_xP_{4-x-z}(H_3)_xO_{10}]$

First described by Hector and Skey (1866) in thin seams in andesite in Taranaki, and ascribed to the action of solutions on guano.

Awaruite Ni_3Fe

First described by Skey (1886 and 1867), first found in alluvial sands of the Gorge River (not Awarua Bay as commonly believed), and later in parent serpentinite rock. Confusion over the original locality for this mineral has been discussed recently by Rodgers and Hey (1980).

Tuhualite $(Na,K)_2(Fe^{3+})_2Si_{12}O_{30}H_2O$

First described by Marshall (1932 and 1936), and found in comendite (peralkaline rhyolite) from Mayor Island (Maori name - Tuhua).

Hydrogrossular $Ca_3Al_2Si_2O_8(SiO_4)_{1-m}(OH)_{4m}$

First described by Hutton (1943), and found as a prominent constituent of rodingite, a rock also first named from New Zealand.

Huttonite $ThSiO_4$

First described by Pabst (1950) and Pabst and Hutton (1951), and found in beach sands in South Westland.

Wairakite $CaAl_2Si_4O_{12}2H_2O$

First described by Steiner (1955), and found in pores, cavities, and veinlets, and replacing feldspar in hydrothermally altered volcanics from Wairakei geothermal development cores.

Wairauite CoFe

First named by Challis and Long (1964), and found as grains in serpentinite in the Wairau Valley.

Akatoreite $(Mn,Fe,Mg,Ca)_9Si_{7.75}Al_{2.09}O_{23.2}(OH)_{8.8}$

First named by Read and Reay (1971), and found in low-grade metacherts on the coast of the South Island 32 km south-west of Dunedin. Named from the locality.

Motukoreaite

$NaMg_{19}Al_{12}(CO_3)_{6.5}(SO_4)_4(OH)_{54}28H_2O$

First named by Rodgers, Chisholm, Davis and Nelson (1977), and found as a cement in beach-rock and basaltic tuffs on Brown's Island (Maori name - Motukorea), Auckland.

Feruvite $CaFe_3(Al,Mg)_6(BO_3)_3Si_6O_{18}(OH)_4$

First named by Grice and Robinson (1989), and found in pegmatitic tourmalinized rocks on Cuvier Island, near the Coromandel Peninsula. The name derives from the fact the mineral is the Fe analogue of uvite.

Coombsite $K(Mn,Mg)_{13}(Si,Al)_{18}O_{42}(OH)_{14}$

First named by Sameshima and Kawachi (1991), and found in Mn-rich siliceous rocks within the prehnite-pumpellyite facies Caples Terrane rocks at Watsons Beach, S. of Dunedin. The name is for Douglas S. Coombs, Emeritus Professor of Geology at Otago University.

The best known rock names originating in New Zealand are dunite, ignimbrite and rodingite.

References

Battey, M.H. (1972) (1st Ed) and 1981 (2nd Ed): *Mineralogy for Students.* Longman, U.K.

Beery, L.G., Mason, B. (1959) (1st Ed) and with Dietrich, R.V. 1982 (2nd Ed) *Mineralogy.* Freeman, San Francisco.

Challis, G.A., Long, J.V.P. (1964) Wairauite - a new cobalt-iron mineral. *Min. Mag.*, 33, p. 942-948.

Fleming, C.A. (1959) Translation of F. von Hochstetter's "Geology of New Zealand (1863)". Government Printer, Wellington.

Grice, J.D., Robinson, G.W.(1989) Feruvite, a new member of the tourmaline group, and its crystal structure. *Can. Min.*, 27, p. 199-203.

Hector, J., Skey, W. (1866) Supplementary report on Class 1. "N.Z. Exhibition 1865: report and awards of the jurors", Mills, Dick, Dunedin. Appendix A: p. 371-452.

Hutton, C.A. (1943) Hydrogrossular, a new mineral. *Trans. Roy. Soc. N.Z.*, 73, p. 174-180.

Keyes, I.W. (1974) Appendix 3 (p. 35) in G.J. Williams: D.S.I.R. Bulletin 212: Cenozoic Geology of the Lower Nevis Basin.

Mantell, W. (1850) Notice of the remains of the DINORNIS and other birds, and of fossils and rock-specimens. *Quart. J. Geol. Soc.*, 6, p. 319-342.

Marshall, P. (1932) Volcanic rocks of the North Island. *N.Z. Journ. Sci. Tech.*, 13, p. 198-202.

– **(1936)** The mineral tuhualite. *Trans. Roy. Soc. N.Z.*, 66, p. 330-336.

Pabst, A. (1950) Monoclinic Thorium Silicate. *Nature*, 166, p. 157.

– **, Hutton, C.O. (1951)** Huttonite, a new monoclinic thorium silicate. *Amer. Min.*, 36, p. 60-69.

Read, P.B., Reay, A. (1971) Akatoreite, a new manganese silicate from eastern Otago, New Zealand. *Amer. Min.*, 56, p. 416-426.

Rodgers, K.A., Chisholm, J.E., Davis, R.J., Nelson, C.S. (1977) Motukoreaite, a new hydrated, carbonate, sulphate, and hydroxide of Mg and Al from Auckland, New Zealand. *Min. Mag.*, 41, p. 389-390.

– **, Hey, M.H. (1980)** On the type locality and other occurrences of awaruite ($FeNi_3$) in Westland, New Zealand. *Min. Mag.*, 43, p. 647-650.

Sameshima, T., Kawachi, Y. (1991) Coombsite, Mn analogue of Zussmanite, and associated Mn-silicates, parsettensite and caryopilite, from southeast Otago, New Zealand. *N.Z. Journ. Geol. Geophys.*, 34, p. 329-335.

Shelley, D. (1975) *Manual of Optical Mineralogy.* Elsevier, Amsterdam and New York.

– **(1985)** *Optical Mineralogy.* Elsevier, New York.

Skey, W. (1886) On a new mineral (awaruite) from Barn Bay. *Trans. N.Z. Inst.*, 18, p. 401-402.

– **(1887)** Minerals. *N.Z. Colonial Museum Lab. Ann. Report No 22:* p. 46.

Steiner, A. (1955) Wairakite, the Ca analogue of analcime, a new zeolite mineral. *Min. Mag.*, 30, p. 691-698.

Other References

Useful general sources of information on N.Z. mineralogy are:

– Bulletin No. 32 (New Series) of the N.Z. Geological Survey (by P.G. Morgan), which is a complete catalogue of mineral occurrences in New Zealand as known at the time of publication in 1927.

– Railton, G.T., Watters, W.A. (1990) Minerals of New Zealand, NZ Geol. Surv. Bulletin 104, is an alphabetical check list of minerals recorded from New Zealand up to 1990.

– N.Z. Journal of Geology and Geophysics, 1965, volume 8, no. 6, which is a special issue to celebrate and record the centenary of the N.Z. Geological Survey. Of particular interest is the article (p. 999-1087) by J.J. Reed: "Mineralogy and Petrology in the N.Z. Geological Survey, 1865-1965"

– The book by G.J. Williams "Economic Geology of New Zealand" 2nd Edition, 1974, published by the Australasian Institute of Mining and Metallurgy, which is a comprehensive account of the occurrence and utilisation of economic minerals in New Zealand, and contains much interesting historical information.

– Volume 4 of the UN Atlas of Mineral Resources of the ESCAP Region provides a summary of the distribution of mineral deposits in New Zealand.

– B.N. Brothers (ed.). 1983. University of Auckland. History of Geology 1883-1983. Kingsland Maxwell Printing Auckland.

– The Geological Society of NZ Newsletters (from no. 55 1982 to the present) contain various obituaries, reminiscences, and a series of articles on the development of ideas in NZ geology with miscellaneous snippets of mineralogical interest.

– The Historical Studies Special Interest Group of the Geological Society also publishes a separate series of newsletters on the development of geology in NZ.

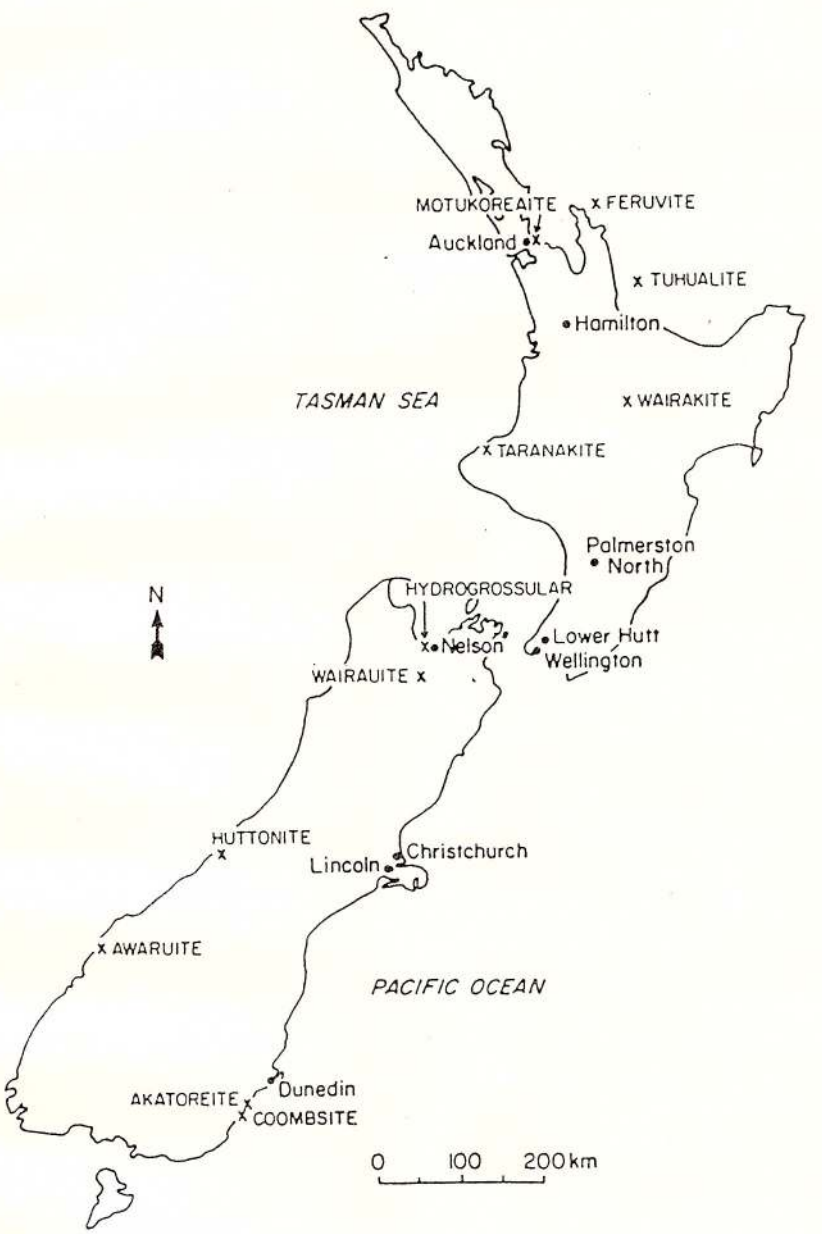

Rom. J. Mineralogy, 1995, 77, p. 71–74, Bucureşti

IN MEMORIAM:

Dr. ing. CAIUS I. SUPERCEANU
1925–1985

Dr. ing. Caius I. Superceanu s-a născut la data de 10 aprilie 1925 în municipiul Timişoara, ca fiu al lui Ioan Superceanu, profesor de limba română şi al Mariei Superceanu. Şcoala primară şi liceul le-a absolvit în perioada 1931–1943 la actualul Colegiu Diaconovici Loga din Timişoara.

Pasiunea pentru ştiinţele geologice, şi în special pentru cele chimico-mineralogice a apărut încă din perioada liceului, când tînărul elev Caius Superceanu a materializat această pasiune, de care şi-a legat toată viaţa, prin înfiinţarea unui laborator de chimie în casa bunicilor de la Sasca Montană.

În perioada care a urmat de la terminarea liceului, a fost student între anii 1943–1948 la Şcoala Politehnică din Bucureşti, Facultatea de Chimie. Încă din anul III de facultate a fost remarcat de Academicianul Alexandru Codarcea pentru activitatea ştiinţifică şi cunoştinţele pe care le avea dobîndite despre geologia şi mineralogia Banatului. În anul 1946 a fost numit preparator la catedra de mineralogie, care era condusă de distinsul academician. Diploma de inginer cu menţiunea "Magna Cum Laude" a fost obţinută la 14 decembrie 1948.

Între anii 1948–1952 a funcţionat ca asistent la catedra de cristalografie - mineralogie a Facultăţii de Chimie Industrială din Timişoara şi apoi ca şef de lucrări în cadrul Facultăţii de Mine şi Metalurgie din Timişoara.

Din anul 1952 şi până în 1962 a fost şeful laboratorului de analize chimice şi mineralogice din cadrul Institutului de Cercetări Miniere din Bucureşti şi apoi a lucrat o perioadă scurtă la Trustul de Prospecţiuni şi Explorări Miniere din Bucureşti. Activitatea ştiinţifică prodigioasă pe care a efectuat-o în această perioadă Caius Superceanu a fost materializată prin elaborarea unor studii şi cercetări despre unele zăcăminte din România. De asemenea, a pus în evidenţă noi ocurenţe mineralogice de columbit, beril, montebrasit, spodumen, molibdenit (în zăcămintele pegmatitice din Carpaţii de Sud), vezuvian, beril, wollastonit, epidot, scheelit, tungstit (in zăcămintele de skarn asociate magmatismului banatitic), safforit, breithauptit, nichelină (în mineralizaţiile cobaltifere legate de complexul de roci ultrabazice din Banatul de Sud).

Din anul 1962 revine la Timişoara ca lector la disciplina de geologie de la Facultatea de Ştiinţele Naturii din cadrul Institutului Pedagogic, ulterior Universitatea din Timişoara.

Cu gândul de a crea o colecţie mineralogică în cadrul Universităţii din Timişoara, în mai puţin de 8 ani de la venirea sa la Facultatea de Ştiinţele Naturii a pus în valoare o numeroasă colecţie mineralogică şi petrografică cu eşantioane din zona Banatului şi a Munţilor Apuseni.

În anul 1970 editează sub egida Universităţii primul album color cu minerale din Banat. Tot în anul 1970 susţine teza de doctorat intitulată "Studiul chimico-mineralogic al zăcămintelor de Cu-Mo-Re din România", teză susţinută în cadrul Facultăţii de Chimie Industrială din Timişoara.

Din anul 1982, odată cu desfiinţarea Facultăţii de Ştiinţele Naturii, a trecut la Centrul de Seismologie al Universităţii din Timişoara, unde a lucrat ca cercetător ştiinţific până în anul 1984.

La 1 ianuarie 1985 s-a stins din viaţă un om de excepţie, dr. ing Caius Superceanu. Seriozitatea, loialitatea şi respectul faţă de ştiinţă au fost unicele sale îndemnuri şi calităţi, care l-au susţinut în întreaga activitate ştiinţifică şi didactică. A murit cu gândul regretului etern că toată această activitate şi experienţă ştiinţifică nu a avut şansa să fie moştenită şi valorificată de urmaşi.

LUCRĂRI ŞTIINŢIFICE PUBLICATE

1. Superceanu, C. (1955) Asupra unei noi mineralizaţii cobaltifere din Banatul de Sud. *Revista Minelor*, VI, 10. p. 341–371.

2. – (1955) Asupra chimismului scheelitelor. *Rev.de Chimie*, 9, p. 483–486, Bucureşti.

3. – (1955) Minereurile de fier cu scheelit din Banatul de Est. *Rev.Minelor*, VI, 11, p. 349–352, Bucureşti.

4. – (1956) Asupra chimismului montebrasitelor. *Rev. de Chimie*, 12, p. 694–697, Bucureşti.

5. – (1956) Studiul microscopic al zgurilor cuprifere din Banat. *Studii şi Cercetări de Metalurgie*, Tom. I, 2, p. 353–368, Bucureşti.

6. – (1956) Noi apariţiuni de scheelit în zăcămintele de contact din provincia geochimică a banatitelor, Partea I, Zăcămintele Băiţa Bihor. *Rev. Minelor*, 4, p. 170–182.

7. – (1956) Noi apariţiuni de scheelit în zăcămintele de contact din provincia geochimică a banatitelor, Partea II-a, Zăcămintele din Poiana Ruscă (Tincova). *Rev. Minelor*, 5, p. 230–242.

8. – (1956)` Noi apariţiuni de scheelit în zăcămintele de contact din provincia geochimică a banatitelor, Partea a III-a, Zăcămintele Oraviţa, Ciclova şi Sasca Montană. *Rev. Minelor*, 6, p. 298–302.

9. – (1956) Mineralizaţii cupro-nichelifere cu conţinut de platin în piroxenitele din Banatul de Sud. *Rev. Minelor*, 2, p. 80–90.

10. – , Maieru, O. (1956) Aluviunî cu ilmenit şi zircon, noi surse de materii prime pentru industria titanului. *Rev. de Chimie*, 3, p. 145–148, Bucureşti.

11. – (1956) Tehnica nouă în domeniul analizei electrono-microscopice a minereurilor şi cărbunilor. *Rev. Minelor*, 12, p. 635–640.

12. – (1957) Uber das Kobalterzvorkommen von Eibenthal im südlichen Banat. *N.Jb. Miner, Mh*, p. 149–156, Stuttgart.

13. – (1957) Neue Scheelitvorkommen in der Erzlagerstätte von Baia Mare (Felsobanya), Nordsiebenburgen. *N. J. Miner. Mh*, p. 165–173, 7/8 Stuttgart.

14. – (1957) Minerale rare în pegmatitele granitice din Banat. *Rev. Minelor*, 3, p. 140–155, Bucureşti.

15. – (1957) Contribuţiuni la paragenezele scheelitului şi wolframitului din zăcămintele de minereuri complexe de la Baia Mare. *Rev. Minelor*, 9, p. 399–404, Bucureşti.

16. – (1957) Valorificarea complexă a nisipurilor aluvionare din România. I. Baza de materii prime. *Rev. de chimie*, 4, p. 221–227.

17. – (1957) Erzmikroskopische Untersuchungen über der Banater Kupferschlacken. *Rev. de Metalurgie*, II, p. 159–172, Bucharest.

18. – (1958) Skarne vezuvianice şi granatice cu conţinut de beriliu în zăcămîntul de contact de la Ciclova. *Rev. Minelor*, IX/12, p. 552–568, Bucureşti.

19. – (1958) Studiul calcografic asupra mineralizaţiilor cuprifere de la Deva. *Rev. Minelor*, IX/3, p. 112–125.

20. – , Botnarencu, A., Maieru, O., Scripăţ, V. (1958) Aluviuni cu rutil provenite din Cristalinul Getic al Carpaţilor Meridionali. *Rev. Minelor*, IX/12, p. 536–542, Bucureşti.

21. – (1958) Zăcăminte aluvionare de titan, zircon şi titanomagnetit vanadifer din zona izvoarelor Mureşului (Carpaţii Orientali). *Rev. de Chimie*, 7/8, p. 373–380, Bucureşti.

22. – , Socolescu, M., Vlaicu, C.Z. (1958) Asupra mineralizaţiei de la Cobăşel Rodna veche, *Rev. Minelor*, IX/12, p. 542–548, Bucureşti.

23. – (1958) Zăcămintele de disten din Carpaţii Meridionali ca bază de materii prime refractare silico-aluminoase, *Rev. Minelor*, IX, p. 410–414, Bucureşti.

24. – (1958) Aluviuni cu rutil provenite din cristalinul getic al Carpaţilor Meridionali. *Rev. Minelor*,12, p. 536–543, Bucureşti.

25. – (1960) Noi mineralizaţii cuprifere cu domeykit şi algodonit în Munţii Metaliferi. *Rev. Minelor*, XI/10, p. 430–448, Bucureşti.

26. – (1960) Noi iviri de minereuri de fier în Carpaţii Meridionali. *Rev. Min.*, XI/6, p. 267–271, Bucureşti.

27. – (1961) Noi apariţiuni de scheelit în mineralizaţiile complexe de la Tibleş Măgura Neagră. *Rev. Minelor* XII/11, p. 507–510, Bucureşti.

28. – (1962) Noi mineralizaţii nichelifere în Carpaţii Meridionali. *Rev. Minelor*, XIII/11, p. 515–518.

29. – (1967) Metallogenetische Provinzen Rumaniens. *Zeit. für angew. Geologie*, 13, 2/67, p. 57–65, Berlin.

30. – (1967) Neue silberhaltige Bleierzvorkommen mit Flüsspat Schwerspat im Poiana Ruscă Gebirge (Banat). *Geologie*, 16, 10, p. 1136–1144, Berlin.

31. – (1967) Die Geosynklinal Lagerstättenprovinzen Rumäniens. *Geol.Rundsch*, 56, 3, p. 848–972, Stuttgart.

32. Maieru, O., Superceanu, C., Apostoloiu, A. (1968) Neue Spodumene und Beryllpegmatite im mittleren südkarpatischen Schiefergebirge (Rumänien). *Geologie*, 17, 4, p. 388–397, Berlin.

33. Superceanu, C. (1969) Die Kupfererzlagerstätte von Sasca Montană im SW Banat und ihre Stellung in dem alpidischen ostmittelmeerischen Kupfer-Molybdän-Erzgürtel. *Geol. Rundsch*, 58, 3, p.798–861, Stuttgart.

34. – (1970) Pyrometasomatic copper ore deposits (Kamaishi type) of Sasca Montană Stinăpari (Banat). IMA IAGOD Meetings, Collected Abstracts, p. 278 , Tokyo.

35. – (1970) The Eastern Mediterranean - Iranian alpine copper-molybdenum Belt. IMA - IAGOD Meetings, Collected Abstracts, p. 279, Tokyo.

36. – (1970) Minerale din Banat (album), Litogr. Univ. din Timişoara.

37. – (1972) Typomorphe Mineralparagenesen und Zonierung in den laramischen Kontaktlagerstatten der Banater Metall Provinz, *Freiberger Forschungshefte*, 288, p. 37–72, Freiberg.

38. – (1975) Die Kupfer- Molybdänvererzungen der Clementis-Grube im Kontaktgebiet von Oravitza/Banat. *Miner Deposita*, 10, 4, p. 305–314, Berlin.

39. – (1983) Metallogenetic province of Banat and its plate - tectonic position in the Balkan Peninsula. *Acta Mineralog.-Petrograph.*, XXVI-1, p. 99–108, Szeged.

40. – (1984) Die Metallogenese im Almascher Grundgebirge (Sud Banat, Rumanien). *Zbl. Geol. Paleont.*. I, 7/8, p.1068–1100, Stuttgart.

Iuliu Bobos
Universitatea Tehnică
Timişoara

Rom. J. Mineralogy, 1995, 77, p. 75–80, Bucureşti

NEW MINERALS RECENTLY APPROVED

(1992)

BY THE COMMISSION ON NEW MINERALS AND MINERAL NAMES

International Mineralogical Association

The information given here is provided by the Commission on New Minerals and Mineral Names, I. M. A. for comparative purposes and as a service to mineralogists working on new species. Each mineral is described in the following format:

Chemical Formula

IMA No. (any relationship to other minerals)
Crystal system, space group unit cell parameters
Color; luster; diaphaneity.
Optical properties.
Strongest lines in the X-ray powder diffraction pattern.

The names of these approved species are considered confidential information until the authors have published their descriptions or released information themselves.

NO OTHER INFORMATION WILL BE RELEASED BY THE COMMISSION

J. A. Mandarino, Chairman
Commision on New Minerals and Mineral Names
International Mineralogical Association

1992 PROPOSALS

$FeZr(PO_4)_2 \cdot 4H_2O$
IMA No. 92-001
Monoclinic: $P2_1/c$
a 9.12 b 5.42 c 19.17 Å β 94.8^0
Pale yellowish white; vitreous to dull; transparent.
Biaxial (+), α 1.644, β 1.652, γ 1.652, 2V(meas.) 0^0, 2V(calc.)0^0
9.58(75), 4.572(65), 4.382(80), 4.092(60), 3.160(100), 2.640(70).

$Bi_2O(OH)_2SO_4$
IMA No. 92-002
Monoclinic: $P2_1/c$
a 7.700 b 13.839 c 5.686 Å β 109.11^0
Colorless; adamantine; transparent.
Biaxial, indices of refraction calculated from reflectance data at 589nm: R_1 1.91, R_2 1.99. 3.644(60), 3.466(60), 3206(100), 2.924(70), 2.782(50), 1.984(90).

Sb_2Se_3
IMA No. 92-003 The selenium analog of stibnite.
Orthorhombic: Pbnm
a 11.593 b 11.747 c 3.984 E
Black; metallic; opaque.
In reflected light: white, distinct anisotropism, distinct bireflectance, pleochroic white to grayish white. R_{max} & R_{min}: (42.62, 40.55 %) 470 nm, (41.95, 39.02 %) 546 nm, (41.23, 39.42 %) 589 nm, (44.39, 41.56 %) 650 nm.
3.70(70), 3.17(50), 2.870(100), 2.625(60), 1.930(30), 1.764(35).

$Mg[UO_2(AsO_3)_x(AsO_4)_{1-x}]_2 \cdot 7H_2O$ x about 2/3
IMA No. 92-005
Monoclinic: C2/m
a 18.194 b 7.071 c 6.670 Å β 99.70^0
Bright yellow to straw-yellow; vitreous; transparent.
Biaxial (-), α 1.610, β 1.730, γ 1.740, 2V(meas.) 34^0, 2V(calc.) 30^0. 9.02(100), 4.90(40), 4.48(80), 4.00(40), 3.53(40), 3.28(50), 3.01(60), 2.849(60).

$Ni_5(CO_3)_4(OH)_2 \cdot 4 - 5H_2O$
IMA No. 92-006 The nickel-analog of hydromagnesite.
Monoclinic: $P2_1/c$
a 10.06 b 8.75 c 8.32 Å β 114.3^0

Bluish green; silky; transparent.
Biaxial (sign unknown), α' 1.630, γ' 1.640, 2V unknown.
6.30(5), 5.75(10), 4.36(4), 4.14(3), 2.871(4b), 2.458(2b), 2.120(3).

$NaH(CO_3)H_3(BO_3)\cdot 2H_2O$
IMA No. 92-008
Monoclinic: C2
a 16.119 b 6.928 c 6.730 Å β 100.46^0
Colorless; vitreous; transparent.
Biaxial (-), α 1.351 (calc.), β 1.459, γ 1.486, 2V(meas.) 50^0.
6.36(25), 4.203(6), 3.464(100), 3.173(59), 2.608(5), 1.731(19).

$Ca_9B_{26}O_{34}(OH)_{24}Cl_4\cdot 13H_2O$
IMA No. 92-010 A triclinic polymorph of 92-011.
Triclinic: P1
a 12.759 b 13.060 c 9.733 Å α 102.14^0 β 103.03^0 γ 85.68^0
Colorless to very pale yellow; vitreous; translucent to transparent. Biaxial (+), α 1.537, β 1.548, γ 1.570, 2V(meas.) 77^0, 2V(calc.) 71^0.
9.21 (70), 7.69(100), 5.74 (60), 4.63 (40), 3.845 (35), 2.199 (30b), 3.768(30), 3.493(30).

$Ca_9B_{26}O_{34}(OH)_{24}Cl_4\cdot 13H_2O$
IMA No. 92-011 A monoclinic polymorph of 92-010.
Triclinic: $P2_1$
a 19.88 b 9.715 c 17.551 Å β 114.85^0
Colorless to very pale yellow; vitreous; translucent to transparent. Biaxial (+), α 1.542, β 1.545, γ 1.565, 2V(meas.) 47^0, 2V(calc.) 43^0.
9.03(60), 8.56(100), 6.62(70), 6.14(30b), 5.12(30), 4.09(30), 3.768(30), 3.493(30).

$Ca_2(CaMn)(SiO_3OH)_2(OH)_2$
IMA No. 92-012
Orthorhombic: Pbca
a 9.398 b 9.139 c 10.535 Å
Colorless; vitreous; transparent.
Biaxial (+), α 1.634, β 1.640, γ 1.656, 2V(meas.) 65^0, 2V(calc.) 63^0.
4.18(45), 3.231(100), 2.846(42), 2.789(35), 2.391(42), 2.042(28).

$Bi_3O(OH)(PO_4)_2$
IMA No. 92-013 The phosphate analog of preisingerite and schumacherite.
Triclinic: P
a 9.798 b 7.250 c 6.866 Å α 88.28^0 β 115.27^0 γ 110.70^0
White to pale pink, sometimes brown; vitreous; transparent to translucent.
Mean index of refraction estimated from reflectance data: 2.01 at 589 nm.
4.437(46), 3.247(87), 3.188(100), 3.135(95), 3.026(75), 2.953(47), 2.165(41).

$Na_xCa_yCu_z(Mg,Fe^{3+},Al)_3(AsO_4)_3$
x $\sim$ 0.76, y $\sim$ 0.42, z $\sim$ 0.39
IMA No. 92-014
Monoclinic: C2/c
a 11.882 b 12.760 c 6.647 Å β 112.81^0
Light blue; vitreous; translucent.
Biaxial (+), α 1.714, β 1.744, γ 1.783, 2V(meas.) 60^0, 2V(calc.) 84^0.
4.35(40), 4.06(50), 3.56(40), 3.053(40), 3.495(60), 3.066(40), 2.744(140), 2.605(40).

$(Fe,Al)_2(SO_4)_3$
IMA No. 92-015 The ferric analog of millosevichite.
Hexagonal: R3
a 8.14 c 21.99 Å
White to light brown; dull; transparent.
Uniaxial (sign unknown), n is between 1.555 and 1.625.
5.99(28), 4.35(23), 3.56(100), 2.97(20), 2.72(20), 2.64(11).

$Mn_5(PO_4)_2(OH)_4$
IMA No. 92-016 The phosphate analog of arsenoclasite.
Orthorhombic: $P2_12_12_1$
a 9.097 b 5.693 c 18.00 Å
Pale yellow, yellow, pale burnt orange; adamantine; transparent.
Biaxial (sing unknown), α' 1.74, γ' 1.76, 2V unknown.
2.900(100), 2.853(70), 2.802(50), 2.702(80), 2.022(15), 1.608(15).

$Ca_3(Ti,Fe^{2+}Fe^{3+})_2(Si,Fe^{3+})_3O_{12}$
IMA No. 92-017 A member of the garnet group.
Cubic: Ia3d
a 12.162 Å
Black; adamantine; opaque.
Isotropic, ω 1.955.
3.039(72), 2.720(100), 2.483(51), 2.385(21), 1.973(24), 1.687(26), 1.626(56).

$Ca_2Y(AsO_4)(WO_4)_2$
IMA No. 92-018
Tetragonal: $I4_1/a$
a 5.135 c 33.882 Å
Creamy yellow; vitreous to adamantine; translucent.
Uniaxial (+). ω 1.874, ε 1.918.
4.674(18), 3.059(100), 2.571(19), 1.901(32), 1.818(16), 1.674(17), 1.562(32).

$C_{14}H_{10}$
IMA No. 92-019
Monoclinic: $P2_1$
a 8.392 b 6.181 c 9.558 Å β 98.48^0
Colorless to grayish-white; vitreous to waxy; transparent.
Biaxial (+), n_{min}, 1.75n_{max}, 1.95, 2V(meas.) 90^0.
9.434(100), 4.941(11), 4.724(11), 4.546(5), 4.028(13), 3.371(10).

$(Na,K)(Ca,Na)_2(Mg,Fe^{3+},Fe^{2+})_5Si_8O_{22}(F,OH,O)_2$
IMA No. 92-020 A member of the amphibole group.
Monoclinic: C2/m
a 9.762 b 17.888 c 5.122 Å β 102.25^0
Blue green and green; vitreous; transparent.
Biaxial (-), α 1.618, β 1.624, γ 1.627, 2V(meas.) 71^0, 2V(calc.) 70^0.
9.9(70), 3.69(60), 3.34(100), 3.18(60), 3.13(90), 2.82(70), 1.98(90), 1.439(60).

$CuBi_2O_4$
IMA No. 92-024
Tetragonal: P4/ncc
a 8.511 c 5.823 Å
Black; metallic; opaque.
In reflected light: gray, weak anisotropism, weak but distinct bireflectance, pleochroic gray with a faint bluish tint and brownish gray. R_{max} & R_{min}: (21.1, 19.0 %) 482 nm, (20.2, 18.0 %) 545 nm, (19.7, 17.6 %) 589 nm, (19.5, 17.3 %) 659 nm.
4.26(17), 3.191 (100), 2.913 (16), 2.695 (18), 1.947 (18).

$Cu_3TeO_6 \cdot H_2O$
IMA No. 92-025
Cubic: P-lattice, space group unknown
a 9.555 Å
Emerald green; adamantine; transparent to translucent.
Isotropic, ω 2.01 calculated from reflectance values at 589 nm.
4.26(40). 2.763(100), 2.384(70), 1.873(40). 1.689(80), 1.440(60).

$Mn_4Al_2(OH)_{12}CO_3 \cdot 3H_2O$
IMA No. 92-026 The -2H polytype of 92-027.
Hexagonal: $P6_322$
a 10.985 c 15.10 Å
Orange-brown, pale brown, pale blue, colorless; vitreous; transparent.
Uniaxial (-), ω 1.587, ε 1.547.
7.53(100), 3.768(60), 2.578(50), 2.221(40), 1.856(40), 1.552(40).

$Mn_4Al_2(OH)_{12}CO_3 \cdot 3H_2O$
IMA No. 92-027 The -3T polytype of 92-026.
Hexagonal (trigonal): $P3_112$ or $P3_212$
a 10.985 c 22.63 E
Orange-brown, pale brown; vitreous; transparent.
Uniaxial (-), ω 1.587, ε could not be measured.
7.55(100), 3.770(90), 2.670(70), 2.346(70), 1.973(60), 1.586(30), 1.662(30).

$Mg_4Al_2(OH)_{12}CO_3 \cdot 3H_2O$
IMA No. 92-028 The -2H polytype of 92-029.
Hexagonal: $P6_322$
a 10.571 c 15.139 Å
Orange-brown, pale brown; vitreous; transparent.
Uniaxial (+), ω 1.533, ε 1.533.
7.63(100), 3.785(100), 2.603(15), 2.496(15), 2.341(15), 2.166(15), 1.991(15), 1.825(20), 1.495(15).

$Mg_4Al_2(OH)_{12}CO_3 \cdot 3H_2O$
IMA No. 92-029 The -3T polytype of 92-028.
Hexagonal (trigonal): $P3_112$ or $P3_212$
a 10.558 c 22.71 Å
Yellow to pale yellow; vitreous; transparent.
Uniaxial (+ or -), ω 1.533, ε 1.533.
7.57(100), 3.778(90), 2.570(40), 2.281(40), 1.932(40), 1.524(20), 1.493(20).

$Fe_4Al_2(OH)_{12}CO_3 \cdot 3H_2O$
IMA No. 92-030
Hexagonal (trigonal): $P3_112$ or $P3_212$
a 10.805 c 22.48 Å
Green-brown with black coating; vitreous; transparent.
Uniaxial (-), ω 1.599, ε 1.570.
7.49(100), 3.746(50), 2.625(40), 2.314(50), 1.948(40), 1.558(15), 1.526(20).

$Na_5YZrSi_6O_{18} \cdot 6H_2O$
IMA No. 92-031
Hexagonal (trigonal): R32
a 10.825c 15.809 E
Light green to yellow-green; vitreous; transparent to translucent.
Uniaxial (-), ω 1.585, ε 1.578.
6.03(32), 5.40(63), 3.236(84), 3.127(88), 3.030(100), 1.805(21).

$(K,Na)(Na,Li)_2(Mg,Mn^{3+},Fe^{3+}Li)_5Si_8O_{22}(OH)_2$
IMA No. 92-032 A member of the amphibole group.
Monoclinic: $P2_1/m$
a 9.94 b 17.80 c 5.302 Å β 105.5 Å
Dark red to brownish lilac; vitreous; transparent.
Biaxial (-), α 1.654, β 1.675 (calculated), γ 1.696, 2V(meas.) 88-92^0.
8.890(M), 8.427(M), 5.077(M), 4.442(M), 3.357(M), 3.257(S), 3.132(S), 2.812(S), 2.553(S), plus seven other of intensity (M).

$SrMn_2^{3+}[Si_2O_7](OH)_2H_2O$
IMA No. 92-033
Orthorhombic: Cmcm
a 6.245 b 9.031 c 13.404 Å
Orange-brown; vitreous; translucent.
Biaxial (+), n's > 1.82, 2V(meas.) 63^0.
4.804(86), 3.373(66), 2.833(100), 2.807(82), 2.695(98), 2.401(68).

$\square(Fe_2^{2+}Al)Al_6Si_6O_{18}(BO_3)_3(OH)_4$
IMA No. 92-034 A member of the tourmaline group.
Hexagonal (trigonal): R3m
a 15.967 c 7.126 Å

Bluish black; vitreous; transparent.
Uniaxial (–), ω, 1.664, ε 1.642.
6.338(84), 4.212(48), 3.989(38), 3.452(91), 2.944(71), 2.573(100).

$(Mg, Li, Fe, \square)_4 Al_{18} Si_8 O_{44}(OH)_4$
IMA No. 92-035 The magnesium-analog of staurolite.
Monoclinic: C2/m
a 7.872 b 16.55 c 5.634 Åβ 90.00^0
Colorless in thin section; vitreous to resinous; transparent.
Biaxial (sign unknown), mean n 1.709, 2V unknown.
4.139(24), 2.678(38), 2.390(50), 2.370(33), 2.356(24), 1.968(100).

$(Zn, Li, Fe, Mg, \square)_4 Al_{18} Si_8 O_{44}(OH)_4$
IMA No. 92-036 The zinc-analog of staurolite.
Monoclinic: C2/m
a 7.853 b 16.54 c 5.639 Åβ 90.00^0
Colorless in thin section: vitreous to resinous; transparent.
Biaxial (sign unknown), α 1.722, β unknown, γ 1.734, 2V unknown.
3.001(61), 2.678(70), 2.390(87), 2.363(46), 2.349(45), 1.968(61), 1.964(48),
1.391(100).

$NaPbCu_5(AsO_4)_4Cl \cdot 5H_2O$
IMA No. 92-037 The tetragonal, lead-analog of lavendulan.
Tetragonal: $P4_122$ or $P4_322$
Tetragonal: $P4_122$ or $P4_322$
a 10.066 c 39.39 Å
Intense blue: vitreous; translucent.
Uniaxial (–), ω 1.770, ε 1.710.
9.83(100), 4.925(60), 4.482(50), 3.132(90), 2.772(40), 2.515(50), 1.778(40).

$Cu_{20}(Fe, Cu, Zn)_6 Mo_2 Ge_6 S_{32}$
IMA No. 92-038
Cubic: space group unknown
a 10.64 Å
Megascopic color unknown; metallic; opaque.
In reflected light: pale yellow to grayish yellow, no anisotropism, no bireflectance, nonpleochroic. R: (23.7 %) 470 nm, (25.5%) 546nm, (25.7 %) 589 nm, (25.6 %) 650 nm.
3.07(10), 2.66(2), 1.884(8), 1.603(4), 1.536(), 1.331(1), 1.220(2), 1.190(1).

$Cu_{20}(Fe, Zn, Cu)_6 W_2 Ge_6 S_{32}$
IMA No. 92-039
Cubic: space group unknown
a 10.675 Å
Megascopic color unknown; metallic; opaque.
In reflected light: pale yellowish pink, no anisotropism, no bireflectance, nonpleochroic. R: (23.2 %) 470 nm, (23.7 %) 546 nm, (24,0 %) 589 nm, (23,8 %) 650 nm.
4.36(1), 3.38(1), 3.08(10), 2.67(2), 1.887(7), 1.612(5), 1.543(1), 1.333(1), 1.225(1), 1.192( ).

$Na_4 Zn_2 Si_7 O_{18} \cdot 5H_2O$
IMA No. 92-040
Orthorhombic: F2dd
a 10.211 b 39.88 c 10.304 Å
Colorless to light mauve; vitreous; transparent.
Biaxial (+), α 1.520, β 1.521, γ 1.524, 2V(meas.) 61^0.
2V(calc) 60^0. 6.346(10), 4.959(3), 3.240(6), 3.167(4), 2.821(3).

$(Tl, K)Fe_3(SO_4)_2(OH)_6$
IMA No. 92-041 The thallium-analog of jarosite.
Hexagonal (trigonal): R3m
a 7.3301 c 17.6631 Å
Gold-yellow; adamantine; transparent.
Uniaxial (–), ω 1.822, ε 1.768.
5.974(87), 3.666(34), 3.112(100), 2.9877(22), 2.5773(21), 1.9912(29), 1.8329(23).

$Ca(UO_2)_4(SO_4)_2(OH)_6 \cdot 6H_2O$
IMA No. 92-043
Orthorhombic: P-lattice, space group unknown
a 8.73 b 17.09 c 15.72 Å
Sulphur-yellow; vitreous; translucent.
Biaxial (–), α 1.617 (calculated), β 1.710, γ 1.758, 2V(meas.) 68^0.
7.90(100), 4.17(30), 3.98(40), 3.49(80), 3.38(70), 2.844(30b).

$PbFe_3^{3+}(PO_4)_2(OH, H_2O)_6$
IMA No. 92-045 The phosphate-analog of segnitite.
Hexagonal (trigonal): R3m
a 7.325 c 16.900 Å
Cream to brownish yellow to yellowish green; adamantine; translucent.
Uniaxial (–), ω 1.955, ε 1.935.
5.96(90), 3.67(60), 3.07(100), 2.538(50), 2.257(50), 1.979(50).

$AlF_3 \cdot 3H_2O$
IMA No. 92-046
Tetragonal: P4/n
a 7.715 c 3.648 Å
Colorless; vitreous; transparent.
Uniaxial (–), ω 1.427, ε 1.403.
5.47(100), 2.439(72), 2.027(70), 1.775(78), 1.725(85), 1.306(70).

$Na_4 REE_2(CO_3)_5$ with Ce the dominant REE
IMA No. 92-048
Monoclinic: $P2_1$
a 20.84 b 6.374 c 10.578 Åβ 120.45^0
Gray with slight pinkish tint; vitreous; translucent.
Biaxial (+ or –), α 1.623, β 1.636, γ 1.649, 2V(meas.) 90^0, 2V(calc.) 89^0. 9.13 (3), 5.22 (5), 4.13 (3), 3.70 (4), 2.607 (10), 2.148 (3), 1.921 (3).

$(Mg, Ti\square)(Al, Mg)_2 Al_4 Si_3 O_{18-x}(OH)_x B$ x $\approx$ 3
IMA No. 92-050 The magnesium-analog of dumortierite.
Orthorhombic: Pmcn
a 12.02 b 20.22 c 4.732 Å
Pink to red; vitreous; transparent.
Biaxial (–), α 1.678, β 1.700, γ 1.701, 2V(meas.) 38^0, 2V(calc.) 24^0.
6.01(59), 5.88(100), 3.489(60), 3.255(82), 3.074(53), 2.927(74), 2.131(50), 2.090(48).

NOTE:

The following three minerals from previous years also have been approved.

$Fe_{16}O_{16}(OH)_y(SO_4)_z$ where 16 - y = 2z and $2.0 \leq z \leq 3.5$
IMA No. 90-006
Tetragonal: probably P4/m
a 10.66 c 6.04 Å
Brownish yellow; dull; translucent.
Optical properties unknown.
4.86(37), 3.38(46), 2.55(100), 2.28(23), 1.66(21), 1.51(24), 1.46(18).

$(U,Y)(Ti,Nb,Ta)_2O_8$
IMA No. 90-046 The uranium-analog of polycrase-(Y).
Orthorhombic: Pbcn
a 14.48 b 5.5559 c 5.223 Å
Brown-red; adamantine; opaque.
In reflected light: pale gray with bluish tones; no anisotropism, bireflectance, or pleochroism. R: (23.6 %) 470 nm, (21.5 %) 546 nm, (22.3 %) 589 nm, (25.1 %) 650 nm.
3.73(W), 3.21(W), 2.99(S), 2.78(W), 1.90(MS), 1.86(W), 1.77(MW), 1.48(M).

$Fe_2(OH)_3Cl$
IMA No. 91-036
Orthorhombic: Pnam
a 6.31 b 9.20 c 7.10 Å
Megascopic color unknown; luster probably dull; transparent.
Index of refraction: 1.6 to 1.7.
Electron diffraction pattern: 5.86, 5.07, 2.93, 2.37, 2.14, 1.65.

Rom. J. Mineralogy, 1995, 77, p. 81-82, Bucureşti

SOCIETATEA MINERALOGICĂ A ROMÂNIEI

78344 Str. Caransebeş nr. 1, Bucureşti - 32, Telefon: 665.75.30, Fax: 312.84.44

STATUTUL SOCIETĂŢII MINERALOGICE A ROMÂNIEI (SMR)

Capitolul I – Dispoziţii generale

Art. 1. Societatea Mineralogică a României (SMR) este organizată şi funcţionează ca persoană juridică în conformitate cu legislaţia în vigoare şi cu prevederile prezentului statut.

Art. 2. SMR are drept scop dezvoltarea mineralogiei (în sens larg, incluzând cristalografia, petrologia, gitologia, geochimia etc.)' în România, în strânsă legătură şi cooperare cu societăţi similare din lume şi pe principiile generale ale Asociaţiei Internaţionale de Mineralogie (IMA).

Art. 3. Durata societăţii este nelimitată; data înfiinţării sale (18 octombrie 1992) a fost consemnată de participanţii la Primul Simpozion Naţional de Mineralogie (Cluj-Napoca, 15–20 octombrie 1992). SMR continuă activitatea secţiei de mineralogie a Societăţii Geologice a Romaniei.

Art. 4. Sediul SMR este la sediul Institutului Geologic al României din Bucureşti, Str. Caransebeş, nr.1. Societatea are siglă şi ştampilă proprii.

Capitolul II – Activitatea societăţii

Art. 5. SMR este o asociaţie nelucrativă, non-profit, având ca obiectiv principal stimularea cercetărilor mineralogice în sens larg în toate instituţiile cu activitate geologică din ţară, precum şi în cele în care există preocupări de petrurgie, mineralurgie, biomineralogie, petrofizică, etc. SMR îşi propune să colaboreze cu fizicieni şi chimişti, care lucrează în domeniul creşterii cristalelor, cristalografiei, spectrometriei de masă şi de rezonanţă etc., cu metalurgi şi specialişti în domeniul fizicii corpului solid, cu ecologi şi naturalişti în general.

Art. 6. În colaborare cu Institutul Geologic al României din Bucureşti, SMR va edita "Romanian Journal of Mineralogy", care va deveni şi Buletinul SMR. În contul cotizaţiei anuale, membrii SMR vor primi Rom. J. Mineralogy sau, la alegere, Rom. J. Petrology, sau Rom. J. Mineral Deposits.

Art. 7. SMR va organiza periodic, din 2 în 2 ani , sau ocazional simpozioane generale sau tematice la nivelul întregii ţări, la care vor fi invitaţi şi specialişti din străinătate.

Art. 8. SMR va colabora cu societăţi mineralogice din Europa şi din alte ţări, cu care va iniţia forme de colaborare (simpozioane, aplicaţii pe teren), cu IMA, în special prin comisiile acesteia şi cu EMU (Uniunea Europeană de Mineralogie).

Art. 9. Titlul de membru al IMA, conferit secţiei de mineralogie a Societăţii Geologice a României prin votul Consiliului IMA (Kyoto, August, 1992), se transferă asupra SMR.

Art. 10. SMR va acorda, în măsura fondurilor disponibile, premii tinerilor cercetători (sub 35 ani), pentru lucrări deosebite în domeniile menţionate la art. 2 şi 5, care vor fi decernate cu ocazia simpozioanelor.

Capitolul III – Structura şi conducerea societăţii

Art. 11. SMR funcţionează sub forma grupurilor de specialişti, constituite în instituţii în care se desfăşoară activitate geologică sau există preocupări de tipul celor enunţate în art. 5. Fiecare grup are un reprezentant, care ţine legătura cu conducerea SMR.

Art. 12. Conducerea societăţii este asigurată de un preşedinte, 2 vicepreşedinţi, 3 membri şi un secretar, care vor fi aleşi la fiecare 4 ani; realegerea lor în funcţiile deţinute se hotărăşte la fiecare Adunare Generală de alegeri. Legătura cu IMA, EMU şi EUCr (Uniunea Europeană de Cristalografie) se asigură prin "reprezentanţi naţionali", aleşi simultan cu conducerea societăţii; aceştia pot fi preşedintele, respectiv vicepreşedinţii sau alte persoane reprezentative, membri SMR.

Art. 13. Activitatea SMR se desfăşoară pe comisii, structurate după modelul IMA, la care se pot adăuga şi alte comisii sau grupuri de lucru, în funcţie de opţiunile membrilor SMR. Coordonatorii fiecărei comisii sau ai fiecărui grup de lucru naţional (şi ei eligibili) vor ţine direct legătura cu omologii lor din alte societăţi mineralogice sau IMA.

Capitolul IV – Membrii societăţii

Art. 14. Pot fi membri ai SMR persoane fizice (membri ordinari) sau juridice (membri susţinători), care desfăşoară activităţi de tipul celor amintite în art. 2 şi 5, în instituţiile de cercetare, învăţământ, proiectare, producţie, etc., precum şi studenţi.

Art. 15. Titlul de "Membru de onoare al SMR" se poate acorda unor personalităţi române sau străine, active în domeniile enunţate în art.2 şi 5, recunoscute pe plan intern şi internaţional, ataşate dezvoltării mineralogiei în România. Acordarea titlului se face la propunerea conducerii SMR.

Art. 16. Primirea ca membru ordinar se face la cerere, prin completarea formularului de adeziune. Pentru studenţi este necesară cel puţin o recomandare din partea profesorului de specialitate.

Capitolul V – Fondurile societăţii

Art. 17. Fondurile SMR se constituie din (a) taxe de înscriere, (b) cotizaţii, (c) subvenţii şi sponsorizări, (d) taxe de participare la simpozioane, (e) donaţii. Cotizaţia anuală a membrilor ordinari se stabileşte conform preţului de vânzare al Rom. J. Mineralogy, plus 50 %, iar pentru studenţi la 1/3; taxa de inscriere este, de asemenea, 1/3 din cotizaţie. Pentru persoanele juridice /membrii susţinători, cotizaţia anuală este de minimum 10 ori cotizaţia pentru membrii ordinari.

Art. 18. Gestionarea fondurilor SMR se face de către un trezorier, numit de conducerea societăţii. Pentru activitatea sa, trezorierul va fi recompensat printr-o modalitate legală de către conducerea societăţii.

Art. 19. Activitatea financiară a societăţii va fi verificată de o Comisie de Cenzori, formată din 3 membri, eligibili la 4 ani. Cel puţin la încheierea legislaturii sale, Comisia de Cenzori va prezenta raportul privind gestionarea fondurilor.

Capitolul VI – Dispoziţii finale

Art. 20. Statutul SMR poate fi modificat de către Adunarea Generală a societăţii, pe baza votului a cel puţin 2/3 din numărul delegaţilor prezenţi.

Art. 21. În cazul dizolvării SMR, o adunare extraordinară va hotări destinaţia patrimoniului societăţii, în condiţiile arătate la art. 20.

Notă. Anexa 1 (comisiile şi grupurile de lucru ale SMR) şi Anexa 2 (procesul verbal de constituire a SMR) fac parte din statut.

INSTRUCŢIUNI PENTRU AUTORI

ROMANIAN JOURNAL OF MYNERALOGY publică contribuţii ştiinţifice originale referitoare la acest domeniu.

Vor fi acceptate numai lucrările care prezintă concis şi clar informaţii noi. Manuscrisul va fi supus lecturii critice a unuia sau mai multor specialişti; după a doua revizie nesatisfăcătoare din partea autorilor va fi respins definitiv şi nu va fi înapoiat.

Manuscrisele trebuie prezentate, de regulă, în engleză sau franceză; cele prezentate în limba română trebuie să fie însoţite de un rezumat, în engleză sau franceză, de maximum 10 % din volumul manuscrisului.

Lucrările trebuie depuse, în două exemplare, la secretariatul Comitetului de redacţie, inclusiv ilustraţiile în original. Manuscrisul trebuie să cuprindă: textul (cu o pagină de titlu, care este şi prima pagină a lucrării), bibliografie, cuvinte cheie, abstract, ilustraţii, explicaţii ale figurilor şi planşelor, şi un sumar cu scop tehnic.

Se va adăuga o filă separată cu un colontitlu de maximum 60 semne şi un sumar, în care se va indica ierarhia titlurilor din text în clasificarea zecimală (1; 1.1; 1.1.1), care nu trebuie să depăşească patru categorii.

Textul va fi dactilografiat la două rînduri (31 rînduri/pagină şi 64 semne/rînd), pe o singură parte a colii, cu un spaţiu liber de 3–4 cm în partea stîngă a paginii şi nu trebuie să depăşească 20 pagini dactilografiate (inclusiv bibliografia şi figurile).

Prima pagină a textului va cuprinde: a) titlul lucrării (concis, dar informativ), cu un spaţiu de 8 cm deasupra; b) numele întreg al autorului (autorilor); c) instituţia (instituţiile) şi adresa (adresele) pentru fiecare autor sau grup de autori; d) text.

Notele de subsol se vor numerota consecutiv.

Citările din text trebuie să includă numele autorului şi anul publicării. Exemplu: Ionescu (1970) sau (Ionescu, 1970). Pentru doi autori: Ionescu, Popescu (1969) sau (Ionescu, Popescu, 1969). Pentru mai mult de doi autori: Ionescu et al. (1980) sau (Ionescu et al., 1980). Pentru lucrările care se află sub tipar, anul publicării va fi înlocuit cu "in press". Lucrările nepublicate şi rapoartele vor fi citate în text ca şi cele publicate.

Abstractul, maximum 20 rînduri (pe filă separată), trebuie să fie în limba engleză şi să prezinte pe scurt principalele rezultate şi concluzii (nu o simplă listă cu subiecte abordate).

Cuvintele cheie (maximum 10) trebuie să fie în limba engleză sau franceză, corespunzător limbii în care este lucrarea (sau abstractul, dacă textul este în română), prezentate în succesiune de la general la specific şi dactilografiate pe pagina cu abstractul.

Bibliografia se va dactilografia la două rînduri, în ordine alfabetică şi cronologică pentru autorii cu mai mult de o lucrare. Abrevierile titlului jurnalului sau ale editurii trebuie să fie conforme cu recomandările respectivelor publicaţii sau cu standardele internaţionale.

Exemple:

a) jurnale:

Giuşcă, D. (1952) Contributions à l'étude cristallochimique des niobates. *An. Com. Geol.*, XXIII, p. 259–268, Bucureşti.

– , Pavelescu, L. (1954) Contribuţii la studiul mineralogic al zăcămîntului de la Muşca. *Comm. Acad. Rom.*, IV, 11–12, p. 658–991, Bucureşti.

b) publicaţii speciale:

Strand, T. (1972) The Norwegian Caledonides. p. 1–20. In: Kulling, O., Strand, T. (eds.) Scandinavian Caledonides, 560 p., Interscience Publishers.

c) cărţi:

Bălan, M. (1976) Zăcămintele manganifere de la Iacobeni. Ed. Acad. Rom., 132 p., Bucureşti.

d) hărţi:

Ionescu, I., Popescu, P., Georgescu, G. (1990) Geological Map of Romania, scale 1:50,000, sheet Cîmpulung. Inst. Geol. Geofiz., Bucureşti.

e) lucrări nepublicate sau rapoarte:

Dumitrescu, D., Ionescu, I., Moldoveanu, M. (1987) Report. Arch. Inst. Geol. Geofiz., Bucureşti.

Lucrările sau cărţile publicate în rusă, bulgară, sârbă etc. trebuie menţionate în bibliografie transliterînd numele şi titlurile. Exemplu:

Krasheninnikov, V. A., Basov, I. A. (1968) Stratigrafiya kainozoia. Trudy GIN, 410, 208 p., Nauka, Moskow.

Ilustraţiile (figuri şi planşe) trebuie numerotate şi prezentate în original, pe coli separate (hîrtie de calc), bune pentru reprodus. Dimensiunea liniilor, a literelor şi a simbolurilor pe figuri trebuie să fie suficient de mare pentru a putea fi citite cu uşurinţă după ce au fost reduse. Dimensiunea originalului nu trebuie să depăşească suprafaţa tipografică a paginii: lăţimea coloanei 8 cm, lăţimea paginii 16,5 cm, lungimea paginii 23 cm, pentru figuri, iar pentru planşele liniare nu trebuie să depăşească dimensiunile unei pagini simple (16,5/23 cm) sau duble (23/33 cm) şi trebuie să fie autoexplicativă (să includă titlul, autori, explicaţie etc.). Scară grafică obligatorie.

Ilustraţiile fotografice (numai alb-negru) trebuie să fie clare, cu contrast bun şi grupate pe planşe de 16/23 cm. In cadrul fiecărei planşe numărătoarea fotografiilor se repetă (de. ex. Pl. I, fig. 1, Pl. II, fig. 1).

Tabelele vor fi numerotate şi vor avea un titlu. Dimensiunea originală a tabelelor trebuie să corespundă dimensiunilor tipografice menţionate mai sus (8/16,5 sau 16,5/23).

Autorii vor primi un singur set de corectură, pe care trebuie să-l înapoieze, cu corecturile corespunzătoare, după 10 zile de la primire. Numai greşelile de tipar trebuie corectate; nu sînt acceptate modificări.

Autorii vor primi gratuit 30 de extrase pentru fiecare lucrare.

Comitetul de redacţie

INSTRUCTIONS TO AUTHORS

ROMANIAN JOURNAL OF MYNERALOGFY publishes original scientific contributions dealing with any subject of this field.

Only papers presenting concisely and clearly new information will be accepted. The manuscript will be submitted for critical lecture to one or several advisers. Papers will be definitely rejected after a second unsatisfactory revision by the authors. The manuscripts will not be returned to the authors even if rejected.

Manuscripts are prefered in English or French. Manuscripts submitted in Romanian will be accompanied by an abstract in English or French (maximum 10 per cent of the manuscript volume).

Papers should be submitted in duplicate to the secretary of the Editorial Board, including the reproduction ready original figures. The manuscript should comprise: text (with a title page which is the first page of it), references, key words, abstract, illustrations, captions and a summary for technical purposes.

Author(s) should add a separate sheet with a short title (colontitle) of maximum 60 strokes and a summary indicating the hierarchy of headings from the text listed in decimal classification (1; 1.1; 1.1.1) but not exceeding four categories.

Text should be double-spaced typed (31 lines/page with 64 strokes each line) on one side of the paper only, holding an empty place of 3–4 cm on the left side of the page. The text cannot exceed 20 typewritten pages (including references and figures).

Front page (first page of the text) should comprise: a) title of the paper (concise but informative) with an empty space of 8 cm above it; b) full name(s) of the author(s); c) institution(s) and address(es) for each author or group of authors; d) text.

Footnotes should be numbered consequtively.

Citations in the text should include the name of the author and the publication year. Example: Ionescu (1970) or (Ionescu, 1970). For two authors: Ionescu, Popescu (1969) or (Ionescu, Popescu, 1969). For more than two authors: Ionescu et al. (1980) or (Ionescu et al., 1980). For papers which are in course of print the publication year will be replaced by "in press". Unpublished papers or reports will be cited in the text like the published ones.

Abstract, of maximum 20 lines (on separate sheet), must be in English, summarizing the main results and conclusions (not a simple listing of topics).

Key words (max. 10 items), in English or French, following the language used in the text (or the Resumé if the text is in Romanian), given in succession from general to specific, should be typed on the abstract page.

References should be typed in double-line spacing, listed in alphabetical order and chronological order for authors with more than one reference. Abbreviations of journals or publishing houses should be in accordance with the recommendations of the respective publications or with the international practice.

Examples:

a) journals:

Giuşcă, D. (1952) Contributions à l'étude cristallochimique des niobates. *An. Com. Geol.*, XXIII, p. 259–268, Bucureşti.

– , Pavelescu, L. (1954) Contribuţii la studiul mineralogic al zăcămîntului de la Muşca. *Comm. Acad. Rom.*, IV, 11–12, p. 658–991, Bucureşti.

b) special issues:

Strand, T. (1972) The Norwegian Caledonides. p. 1–20. In: Kulling, O., Strand, T. (eds.) Scandinavian Caledonides, 560 p., Interscience Publishers.

c) books:

Bălan, M. (1976) Zăcămintele manganifere de la Iacobeni. Ed. Acad. Rom., 132 p., Bucureşti.

d) maps:

Ionescu, I., Popescu, P., Georgescu, G. (1990) Geological Map of Romania, scale 1:50,000, sheet Cîmpulung. Inst. Geol. Geofiz., Bucureşti.

e) unpublished papers or reports:

Dumitrescu, D., Ionescu, I., Moldoveanu, M. (1987) Report. Arch. Inst. Geol. Geofiz., Bucureşti.

Papers or books published in Russian, Bulgarian or Serbian etc. should be mentioned in the references transliterating the name and titles. Example:

Krasheninnikov, V. A., Basov, I. A. (1968) Stratigrafiya kainozoia. Trudy GIN, 410, 208 p., Nauka, Moskow.

Illustrations (figures and plates) must be numbered and submitted as originals on separate sheets (tracing papers), ready for reproduction. The thickness of the lines, lettering and symbols on figures should be large enough to be easily read after size-reduction. The original size should not extend beyond the print area of the page: column width 8 cm, page width 16.5 cm, page length 23 cm for figures; the width of line drawings should not extend over a single (16.5/23) or double (23/33 cm) page area and must be selfexplanatory (including title, authors, legend etc.). The graphic scale is obligatory.

Photographic illustrations (black-and-white only) must be of high quality and should be grouped into plates 16/23 cm in size. Each plate should have the photos numbered, i.e. Pl. I, Fig. 1; Pl. II, Fig. 1.

Tables should be numbered and entitled. Original size of the tables should correspond to the above mentioned (8/16.5 or 16.5/23) dimensions of the printing area.

Author(s) will receive only one set of preprint proofs which must be returned, with corrections, 10 days after receiving them. Only printing errors should be corrected, no changes in the text can be accepted.

Thirty offprints of each paper are supplied to the author(s) free of charge.

Editorial Board

Translation and language review by:
Adriana Năstase, Adriana Băjenaru, Mariana Borcoş

Editorial Staff:
Petruţa Cuciureanu, Anca Andăr

Illustration:
Paraschiv Toader